JGERI
Journal of Green Energy Research and Innovation
ISSN: 3041-9018

Journal of Green Energy Research and Innovation

Volume 1, Issue 1, Winter 2024

PUBLISHER
Arak University

Journal of Green Energy Research and Innovation (JGERI)

Publisher: **Arak University**

Director-in-Charge: **Dr. Ali Asghar Ghadimi**

Editor-in-Chief: **Prof. Gevork B. Gharehpetian**

Deputy Editor: **Dr. Abolghasem Daeichian**

Executive Editor**: Dr. Mahyar Abasi**

Coverage area: **International**

Journal Type: **Scientific and technical**

Language: **English**

Frequency: **Quarterly**

Review Time: **4-8 Weeks**

Publication Type: **Electronic, Print**

Open Access: **Yes**

Policy: **Peer-Reviewed**

DOI**: 10.61186/jgeri**

E-mails: **jgeri@araku.ac.ir**

Website: **https://jgeri.araku.ac.ir/**

Address: **Department of Electrical Engineering, Faculty of Engineering, Arak University, Arak, Iran.**

P.O. Box: **38156-8-8349**

Tel: **086-32625099**

Editorial Board

About Journal

JGERI is interested in the results of research in the field of green and renewable energies. The scope of publications of this journal in the field of green energy is extensive and it welcomes novel and innovative studies. Due to the increasing influence of renewable energy in power systems, studies, research, and reports resulting from scientific achievements in this specific area have risen compared to previous decades. This journal is ready to publish specialized articles in all fields related to green energy and interdisciplinary topics related to this scientific branch in the form of open access, which is published annually in four issues as free and open access by Arak University, Iran. **JGERI** is ready to receive the latest research results ranging from analytical methods, numerical simulation, experimental research, and development studies concerning the knowledge and application of green energy.

The following articles are acceptable:

- **Research articles** are expected to present innovative solutions, new concepts, or creative ideas that can help solve existing or emerging technical challenges in the field of green and renewable energy.
- **Review articles** are expected to provide enlightening and specialized reviews, trainings, or case studies on an important topic, timely and widely in the field of green and renewable energies.
- **Applied articles** are expected to share the results of the industry's valuable experiences in dealing with challenging technical issues, developing/adopting new standards, applying new technologies or solving complex problems in the field of green and renewable energies. These articles can have a significant impact on the strategic plans of the industry in the coming years.

Aims and Scope

JGERI is interested on the qualified international multidisciplinary research results related to all aspects of green energy. The scope of **JGERI** is very broad, and welcomes original, novel fundamental and engineering research. We also publish reviews and industrial reports of green energy and its impact on the eco-environment.

We welcome research papers that focus on, but are not limited to, the following areas:

- Policies and Strategies for Green Energy Systems
- Fundamental And Industrial Applications for Green Energy Systems
- Energy Conversion, Control Techniques, and Grid Interactive Systems for Green Energy Systems
- Environmental Impacts of Energy Technologies and Pollution Control
- Materials And Catalysis for Green Energy Systems
- Green Energy Consumption
- Artificial Intelligence, Machine Learning, and Computational Methods in Green Energy Systems
- Public Awareness and Education for Green Energy Systems
- Solar Energy and Photovoltaic
- Wind Energy
- Hydrogen Energy and Energy Storage
- Biofuel and Bioenergy

Each manuscript will go through a rigors peer-review process. you can visit our Instructions for Authors page for information on preparing your manuscript.

Guide for Authors

1. Important points and rules for manuscript submission and publication

-Submitting a manuscript to a journal means that the manuscript is not under review or has not been published anywhere in any other language before.
-The submission of the manuscript for publication by the author, implicitly or explicitly, implies the approval of the organization or body where the author works and has used its affiliation.
-By submitting the manuscript, all authors officially declare their agreement to grant the copyright of the manuscript in case of acceptance to Arak University and **JGERI**. However, the authors are responsible for all the contents published in the manuscript, and the journal is only a reviewer and publisher.
- All authors are required to declare any actual or potential conflicts of interest, including financial, personal, or relationships with individuals or organizations that could affect their work.
- Each of the authors must declare their contribution and role in the manuscript on the Title Page to the journal. The statement of approval of all authors and their role in the manuscript is the responsibility of the corresponding author.
- Authors should note that all manuscripts sent to **JGERI** are checked with Authenticate's CrossCheck software to analyze the authenticity of the content. In this analysis, the overlap and similar texts presented in the submitted manuscripts will be determined.
- **JGERI** makes its manuscripts open to access after publication and there is no charge (APC) for reviewing and publication of manuscripts, and readers can download and use the articles for free.
- All authors, if they had financial support in conducting research related to this manuscript, should briefly state their role. If financial source(s) have no role in the results of the research published by the article, this should also be mentioned by the authors.
- Acknowledgments to individuals and institutions can be mentioned in a separate section at the end of the manuscript before References, and they must not be included as footnotes or in any other form. In this section, it is recommended to mention the names of those who have collaborated during the research (such as those helping in the language correctness aspect of the manuscript, assisting in writing the manuscript or proofreading it, and other cases).
- Non-commercial use of the manuscript will be governed by the Creative Commons Attribution-NonCommercial 4.0 International License, which is currently available at the link (https://creativecommons.org/licenses/by-nc/4.0/). This certificate allows others to use the authors' work in a non-commercial way and utilize it in their research work, although in the new work, they need to acknowledge the authors and mention its non-commercial nature.

2. Initial submission of the manuscript

Submission to this journal is online and you will be accompanied in all the steps of creating a user account and uploading files. All correspondence, including notification of the editor's decision and request for revision, will be made via email. To submit your manuscript, just click on the **Submit Manuscript** option on the journal page. Then, click on **Register** to create an author account. A message will be sent to your email containing your username and password. Then, log in to the manuscript submission system on the Users login page, where you need to enter the username and password and submit your new manuscript. Once you are logged in, you can change your password by clicking on My Home in the top menu. For the next time, just log in to your account. Please include the names, addresses, and email addresses of at least three potential academic reviewers with the paper. Please include reviewers' names and their academic rank, affiliation, and contact information (mail address is mandatory). However, only the editor has the right to decide on the use of suggested reviewers. All the submitted manuscripts undergo the process of plagiarism check with IThenticate software and the review process begins. According to the journal policy, there is a difference between the requirements for initial and revised submission files. Required files for initial submission include three files: **JGERI_Main_Manuscript**, **JGERI_Form_for_Copyright_Transfer_Statement and Conflict_ of_ Interest_ Disclosure** and **JGERI_Cover_Letter**, all three of which must be sent to the journal in PDF format. You can use the links below to download the requirements and suggestions files of these three files.

- JGERI_Guideline_for_Main_Manuscript
- JGERI_Guideline_for_Cover_Letter
- JGERI_Form_for_Copyright_Transfer_Statement and Conflict_ of_ Interest_ Disclosure

3. Submission of the revised manuscript

If the submitted manuscript, after going through the initial review process, is evaluated by the officials and reviewers of the journal and a decision is made to make corrections and revisions in the form of minor or major, the authors are obliged to make the corrections and prepare the response letter to the reviewers within the time specified by the journal. Three files must be sent to the journal at this stage: WORD and PDF files of the revised manuscript (changes should be highlighted), PDF file of the response to the reviewers (including the comments and responses of each of the reviewers separately), Title Page and Authorship file in WORD format (containing two main forms: Title Page and Authorship). The link to download the necessary files along with their requirements and instructions is given below. Points raised in the file **JGERI_Revised_Manuscript** must be followed for compiling the revised manuscript. The authors are obliged to submit the revised file in PDF and WORD format to the journal. Also, different parts of the file **JGERI_Form_for_Title_Page_ and_ Authorship** needs to be completed and signed by the corresponding author, but **JGERI_Response_to_the_Reviewers_Comments** is suggested by the journal and it is not necessary to follow all the points of that file. It should be noted that all the stages of page layout and editing in the form of final publication are the responsibility of the journal. In the completion stages of this process, the cooperation of the authors is needed, and we will inform you at each stage. Thus, the minimum requirements for file compilation are provided in the template file.

- JGERI_Guideline_for_Revised_Manuscript
- JGERI_Form_for_Title_Page_ and_ Authorship
- JGERI_Guideline_for_Response_to_the_Reviewers_Comments

4. **After the final acceptance of the manuscript**

After announcing the final acceptance of the manuscript (reviews may happen several times), the files **JGERI_Revised_Manuscript** and **JGERI_Form_for_Title_Page_ and_ Authorship** will be sent to the paging unit for page layout and final editing. After the final acceptance announcement, the authors will be asked to send a graphic abstract included in a single file. Then, the process of compilation of the manuscript will be completed by the journal and finally, the proof version of the manuscript will be sent to the authors. The authors are obliged to check the proof file completely and report to the journal if they find any ambiguity or error in the final file. In some cases, along with the final proof file of the manuscript, there may be a series of errors and ambiguities in the manuscript, which are sent to the author in the form of comments along with the proof version of the manuscript. The corresponding author is obliged to clarify and resolve these problems and ambiguities in the specified time.

5. **After publication on the journal's website**

After announcing the initial acceptance, the information of the article without its content will be indexed in the Articles in the Press section of the website. After including the article in the issue selected by the journal, the desired article will be indexed in the Current Issue unit along with Vol, No, and pp. Also, the electronic file of the article can be introduced in all scientific references through the DOI link. The important point is that, after acceptance and indexing, the names of the authors cannot be changed, that is, it will not be possible to add, delete, or change the order of the names of the authors and their organizational affiliations.

Cooperative Publication Organization

Renewable Energy Research Institute of Arak University
http://araku.ac.ir/web/riren

Iranian Wind Energy Association
https://www.irwea.org/fa/

Indexing Databases and Social Networks

Google Scholar: https://scholar.google.com/citations?user=47bsJFoAAAAJ&hl=en

Linkedin: https://www.linkedin.com/in/jgeri-arak-university-0818872b9

Academia:https://independent.academia.edu/JournalofGreenEnergyResearchandInnovationJGERI

PaperHive: https://paperhive.org/users/jgeri

GrowKudos: https://www.growkudos.com/profile/j._green_energy_res._innov._jgeri

MyScineceWork: https://www.mysciencework.com/profile/j.green.energy.res.innov.jgeri

SciExplore: https://sciexplore.ir/profiles/author/987-081-740

Magiran: https://www.magiran.com/magazine/8484

Contents

Journal of Green Energy Research and Innovation

Design of a Power Management Strategy in Smart Distribution Networks with Wind Turbines and EV Charging Stations to Reduce Loss, Improve Voltage Profile, and Increase the Hosting Capacity of the Network

Javad Ebrahimi, Mahyar Abasi

Highlight

- Increasing hosting capacity by utilizing green energy sources
- Uncertainty analysis using the Monte Carlo method
- Optimal design of smart grids based on the IGWO method

Graphical Abstract

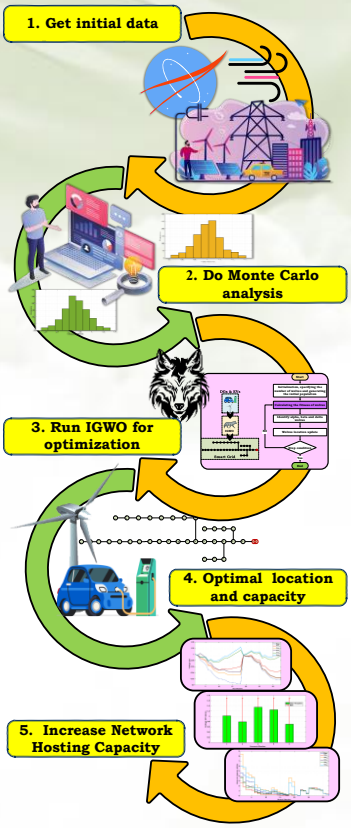

Use your device to scan and read the article online

Citation

J. Ebrahimi, and M. Abasi, "Design of a Power Management Strategy in Smart Distribution Networks with Wind Turbines and EV Charging Stations to Reduce Loss, Improve Voltage Profile, and Increase Hosting Capacity of the Network," *Journal of Green Energy Research and Innovation*, vol. 1, no. 1, pp. 1-15, 2024.

https://doi.org/10.61186/jgeri.1.1.1

JGERI Journal of Green Energy Research and Innovation

Online ISSN: 3041-9018

Journal of Green Energy Research and Innovation

Journal Homepage: www.jgeri.araku.ac.ir

Design of a Power Management Strategy in Smart Distribution Networks with Wind Turbines and EV Charging Stations to Reduce Loss, Improve Voltage Profile, and Increase the Hosting Capacity of the Network

Javad Ebrahimi [1], Mahyar Abasi [2,3]*

[1] *Department of Education and Training of Isfahan Province, District 4 Management, Isfahan, 81458-13331, Iran.*
[2] *Department of Electrical Engineering, Faculty of Engineering, Arak University, Arak 38156-8-8349, Iran.*
[3] *Research Institute of Renewable Energy, Arak University, Arak 38156-8-8349, Iran.*

* ***Corresponding Author:*** *m-abasi@araku.ac.ir*

ARTICLE INFO

Keywords:
Wind turbine,
Renewable energy,
Grey wolf algorithm,
Electric vehicles,
Distributed generation.

Article history:
Received: 04 November 2023;
Revised: 10 December 2023;
Accepted:02 January 2024;

Article type:
Research Article

ABSTRACT

Today, due to environmental and political reasons, countries around the world are required to use green energies, such as wind and solar energy. Also, most countries have switched to using electric vehicles (EVs) to reduce environmental pollution. Since smart distribution systems' distributed generation (DG) power output is limited, this paper addresses this issue by planning charging parking lots of EVs. The problem was formulated as a nonlinear optimization model. The objective function was to increase the power output, reduce the loss cost, and reduce the bus voltage deviations. Also, technical and economic limitations were considered in solving the planning problem. The uncertainty of consumption load, the behavior of EVs, and the output power of wind DGs were modeled using a combination of Monte Carlo and k-means methods. The improved gray wolf optimization (IGWO) algorithm was adopted to optimize the objective function. A standard IEEE 33-bus smart distribution system was studied to show the efficacy of the suggested solution. The results demonstrated the proposed solutions' high performance in improving the wind DG power output of the distribution system (PODS).

1. Introduction

Owing to technological advances, increasing environmental concerns, and efforts to reduce electricity costs, distributed generation (DG) in smart distribution systems is increasing. However, the DG power output of the distribution system (PODS) is limited. The growing use of solar and wind power plants, which are renewable energy sources, has highlighted the issue of their limited reliability compared to fossil fuel-powered generators. Consequently, there is a demand for energy storage devices. The power grid relies heavily on primarily producing electricity from thermal power plants, which, in turn, depend upon fossil fuels. This reliance is mostly due to the consistent and reliable energy generation they offer throughout each hour of the day. Unluckily, this reliability level is not yet achievable with clean wind and solar power plants.

The issue of poor reliability in solar and wind power plants can be mitigated by including electric vehicles (EVs). However, technological and economic constraints hinder the widespread adoption of these vehicles. This study demonstrates the impact of effectively integrating and managing renewable resources and EVs to enhance the system's power quality. The present study aimed to employ an emerging technology in the field of smart distribution systems that includes EV charging parking lots to enhance the DG power output of the smart distribution system. So far, many scholars have focused on increasing the DG power output of smart distribution systems.

Ref. [1] adopted an improved meta-heuristic optimization algorithm to optimally size and allocate DGs in a distribution system to finally enhance the power output of the smart distribution system. The results showed that resource planning could increase the power output of the 33-bus system by up to 4.5 MW. Ref. [2] improved the power output of a smart distribution system of solar cells by controlling the active and reactive power of solar cells and transformer tap changers.

Refs [3,4] analyzed a set of solutions for modeling the problem of improving PODS. They focused on three methods: stochastic planning, deterministic planning, and planning based on fuzzy logic and feasibility. The second and third methods were used to strengthen the PODS and protect the smart system by reversing the direction of the power flow through the main feeder. Refs. [5,6] determined the optimal DG power output of a smart distribution system based on the reactive power compensation approach by flexible AC transmission system (FACTS) devices in the distribution system. In the planning phase, they determined the optimal place and capacity of DG and reactive power compensators in the distribution system. Then, the optimal operation of DGs was addressed by considering the technical limitations of the distribution system in the operation phase.

Refs. [7,8] considered the challenges of the distribution system to accept DGs, including the constraints on the power flow in the feeders, the limitation of the bus voltage, the limitations of the power quality, such as the system's harmonics level, and also the limitations of the time coordination of the protective relays. These references considered the demand-side management programs, the utilization of electric energy storage devices, transformer tap-changer control, and reactive power control in the distribution system to be effective for improving DG PODS.

Refs. [9-11] evaluated distribution system reconfiguration methods to be economical and effective in improving PODS. However, solving this model was complicated due to the non-linearity of the optimization problem and the large size of real distribution systems. Therefore, they sought to design an innovative method to solve the problem.

Refs. [12-16] considered the presence of inverter-based DG as the cause of injecting harmonics in the system and sought to locate active filters in the distribution system with high DG penetration. In [17,18], two robust and smart methods were used for optimal management of the load in smart grids to enhance the voltage profile and shed the peak load. Both methods improved the system's load factor and the smart grid's performance and planning.

Refs. [19,20] studied methods for calculating the power output of the low-voltage distribution system. The authors considered that the power output evaluation methods included deterministic, probabilistic, and time-domain methods. These methods differed in accuracy, input type, time, and burden of calculations. Probabilistic methods were more optimal in uncertainties than conventional methods. Also, Ref. [21] dealt with locating and increasing the capacity of fast charging stations for EVs and DG in smart systems, taking urban traffic issues into account.

As is evident in the literature review, there are various techniques to improve DG PODS, such as DG planning, reactive power compensation, energy storage locating, reconfiguration planning [22], the application of FACTS devices [23], and voltage control and power factor control of resources and demand side load management. The present research proposed planning EV charging parking lots as a technique to boost the DG PODS. The goal was to evaluate the potential of planning EV charging parking lots to improve the wind DG PODS. Based on the literature review, some unresolved issues have not yet been explored by scholars and require additional investigation as a research concern.

This article delves into a few of these issues. The following are the research gaps:

- The concurrent integration of electric car capacity into the system alongside wind sources has been neglected.
- The ramifications and challenges it poses in the process of planning have not been acknowledged.
- The majority of the articles reviewed in this field are single-purposed.

Thus, based on the drawbacks identified in previous research, the present work has the following contributions and innovations:

- Taking the unpredictability of power demand, the availability of wind energy, and the presence of electric vehicles into account
- Employing the Monte Carlo approach to perform uncertainty calculations
- Utilizing the enhanced gray wolf algorithm

Section 2 discusses the formulation suggested for planning wind DG and EV charging parking lots. Also, the algorithm for solving the research problem, the method of modeling the uncertainties of the system load, the loading coefficient of the charging parking lots, and the wind speed are presented. Section 3 describes the studied distribution system and presents and analyzes the results. In the end, conclusions are provided in Section 4.

2. Materials and Approaches

Here, the problem of planning the presence of EV charging stations in smart distribution systems is discussed to enhance the power output and electrical parameters of the distribution system.

2.1. Objective function

Equation (1) shows the objective function.

$$MinF = -\sum_{i=1}^{N_b} C_1 \times Pdg_i + \sum_{i=1}^{N_b} C_2 \times \Delta V_i + \sum_{j=1}^{N_f} C_3 \times loss_j \quad (1)$$

where P_{dgi} represents the capacity of DG in bus I, i represents the bus number, N_b represents the total number of buses, j represents the index of branch counter, N_f represents the total number of feeders, $C_{1,2,3}$ represents the cost coefficients in the calculation of objective function terms, $loss_j$ represents the loss of feeder j, and ΔV_i represents the voltage deviation of bus i. As can be seen, the objective function in the optimization problem includes maximizing the total capacity of renewable DG installed in the distribution system buses, reducing the cost of losses, and reducing the voltage deviations of the system buses.

2.2. Constraints

To optimize the objective function, a set of economic and technical constraints are considered in the distribution system's operation, described below.

2.2.1. Consistency of active power in the entire system

According to Equation (2), the total active power generated in the system minus the total active loads must equal the system's total active losses.

$$P_{Generation} - P_{Load} = P_{Loss} \quad (2)$$

2.2.2. Consistency of reactive power in the entire system

According to Equation (3), the total reactive power produced in the system minus the total reactive loads has to equal the system's total reactive losses.

$$Q_{Generation} - Q_{Load} = Q_{Loss} \quad (3)$$

2.2.3. Active power balance in each bus

According to Equation (4), the total active power produced in the i-th bus (P_{Gi}) minus the total active power consumed in the i-th bus (P_{Di}) equals the total active power transferred from the i-th bus to the j-buses connected to this bus.

$$P_{G_i} - P_{D_i} = \sum P_{i\ to\ j} \quad (4)$$

2.2.4. Reactive power balance in each bus

According to Equation (5), the total reactive power produced in the i-th bus (Q_{Gi}) minus the total reactive power consumed in the i-th bus (Q_{Di}) equals the total reactive power transferred from the i-th bus to the j-buses connected to this bus.

$$Q_{G_i} - Q_{D_i} = \sum Q_{i\ to\ j} \quad (5)$$

2.2.5. Bus voltage limitation

According to Equation (6), the bus voltage (V_i) must be limited between V_{min} and V_{max}. According to IEEE standards, the bus voltage limit is set at 5% in this paper.

$$V_{imin} \leq V_i \leq V_{imax} \quad (6)$$

2.2.6. Limitation of heat capacity of the feeder

According to Equation (7), the power flow through the feeder should observe the thermal limit of the feeder.

$$fc_b < FC_{max} \quad (7)$$

This paper examines the thermal limit of the lines based on the highest apparent power flowing through them. The value of this limit is set at 1000 MVA for the lines.

2.2.7. Constraint of the total number of EV charging stations

According to Equation (8), the total number of EV charging stations that can be installed in the system buses (Nev) is limited to $N_{ev,max}$.

$$\sum_{ev=1}^{B_{ev}} N_{ev} \leq N_{ev,max} \quad (8)$$

2.2.8. Constraint of the maximum capacity of EV charging parking lots

Equation (9) states that the capacity of EV charging parking lots installed in the distribution system (CAP_{ev}) is limited to $CAP_{ev,\,max.}$

$$CAP_{ev} \leq CAP_{ev,max} \quad (9)$$

2.2.9. Limitation of candidate busses for installing EV charging parking lots

According to Equation (10), in all buses of the system (B) except for the buses that were candidates for installing charging parking lots (B_{ev}), the number of charging parking lots for EVs is considered equal to zero.

$$N_{ev} = 0 \;\; \forall ev \in B - B_{ev} \quad (10)$$

2.2.10. Constraint of the total number of DGs

According to Equation (11), the total number of DGs used in system buses (N_{dg}) is limited to $N_{dg,\,max.}$

$$dg{=}1 BdgNdg \leq Ndg, max \quad (11)$$

2.2.11. Constraint of the maximum capacity of DGs

Equation (12) states that the total DG capacity installed in the distribution system is limited to $CAP_{dg,max}$.

$$CAPdg \leq CAPdg,max \quad (12)$$

2.2.12. Limitation of the number of candidate buses for installing DGs

According to Equation (13), the number of DGs is considered equal to zero in all the buses of the system (B) except for the buses that were candidates for the installation of DG (B_{dg}).

$$N_{dg} = 0 \;\; \forall dg \;\; \in B - B_{dg} \quad (13)$$

2.3. IGWO Algorithm

The improved gray wolf (IGWO) algorithm was introduced in 2018 [24]. This algorithm is a mathematical model derived from gray wolves' social behavior and hunting technique. The IGWO algorithm is a metaheuristic algorithm that mimics the social behavior of gray wolves during hunting by utilizing a hierarchical structure. The

technique relies on demographic data, follows a straightforward procedure, and can be applied to more complex issues. The process consists of three primary stages:

- Observing, tracking, and pursuing the prey
- Approaching the prey closely, surrounding it, and deceiving it until it ceases its movement
- Attacking

The top three solutions in the IGWO algorithm are distinguished by α, β, and δ, respectively. ω characterizes the rest of the solutions. The GWO algorithm is guided by α, β, and δ, with ω subsequently following them. As previously stated, gray wolves besiege the prey. Equations (14) and (15) provide a mathematical representation of its action.

$$\vec{D} = \left|\vec{C}.\overrightarrow{X_p}(t) - \vec{X}(t)\right| \quad (14)$$

$$\vec{X}(t+1) = \overrightarrow{X_p}(t) - \vec{A}.\vec{D} \quad (15)$$

in which t is the current iteration, D is the track and direction vector, A and C are coefficient vectors, X_p is the prey position vector, and X is the position vector of a gray wolf. A and C vectors are calculated using Equation (16) and (17):

Here, t represents the current iteration, D denotes the track and direction vector, A and C represent coefficient vectors, X_p shows the prey position vector, and X represents the position vector of a gray wolf. The vectors A and C are computed using Equations (16) and (17).

$$\vec{A} = 2\vec{a}.\overrightarrow{a_1} - \vec{a} \quad (16)$$

$$\vec{C} = 2.\overrightarrow{r_2} \quad (17)$$

In Equation (16), a is decreased linearly from 2 to 0 during iterations, and r_1 and r_2 represent random vectors in the range of 0 and 1. As shown in Figure 1, a gray wolf's location is updated based on the prey's location.

The present position of various agents can be achieved by modifying the dimensions of vectors A and C. Consequently, a gray wolf can adjust its location within the vicinity of its prey by employing Equations (16) and (17) at random positions. The IGWO algorithm was presented to improve the original gray wolf algorithm. The basic algorithm has two flaws that could be enhanced [24].

The initial issue was related to the convergence factor, whereas the subsequent problem arose from a novel approach to determining the position of a wolf. This approach involved calculating the average of the motions of three specific wolves, namely alpha, beta, and delta. Enhancements were made to the two components of the GWO algorithm.

The convergence factor "a" exhibits a linear variation from 2 to 0 in the GWO algorithm. Nevertheless, the equation for the convergence factor was modified to Equation (18) to enhance detection and operation:

$$a = 2\left(1 - \left(\frac{t-1}{t_{max}}\right)^{1.5}\right) \quad (18)$$

where t represents the current iteration and t_{max} denotes the maximum number of iterations.

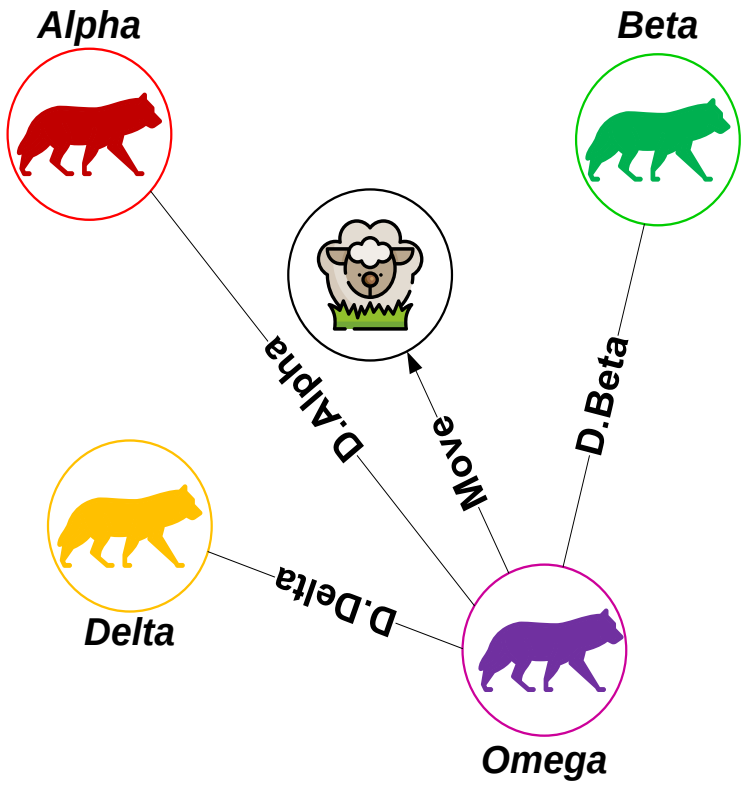

Figure 1. The IGWO position update [24].

The selection of the omega wolf's place in the hierarchy pyramid in the IGWO algorithm, as indicated by Equation (19), is mostly determined by the relative ranking of the three wolves.

$$X = X_{\alpha}.\left[\frac{Q(\alpha)}{Q(\alpha)} + Q(\beta) + Q(\delta)\right] + X_{\beta}.\left[\frac{Q(\beta)}{Q(\alpha)} + Q(\beta) + Q(\delta)\right] + X_{\delta}.\left[\frac{Q(\delta)}{Q(\alpha)} + Q(\beta) + Q(\delta)\right] \quad (19)$$

The new position of the gray wolf is calculated based on hierarchal weight, where the alpha wolf has more weight than the two other wolves. Q is wolf fitness in. Therefore, the omega wolf gets different weights from the three wolves according to their hierarchy. The gray wolf's new position is determined through hierarchical weighting, with the alpha wolf carrying greater weight than the other two wolves. The variable Q represents the fitness of the wolf in Equation (19). Consequently, the omega wolf receives distinct weights from the three wolves based on their order.

2.4. Uncertainty modeling

Uncertainties in the desired planning model include system consumption load, loading factor of the charging parking, and output power of wind DG. To model the uncertainty of the consumption load of the distribution system and the loading coefficient of the EV charging parking lot, the normal probability distribution function with the mean (μ) and standard deviation (σ) is used according to Equation (20):

$$f_{pd}(P_d) = \frac{1}{\sqrt{2\pi}\sigma_d} exp(-\frac{(P_d - \mu_d)^2}{2\sigma_d^2}) \quad (20)$$

Also, the Weibull probability distribution function is used to model the wind speed according to Equation (21) with parameters of shape factor c and scale factor k [25].

$$f_w(v) = \frac{k}{c}\left(\frac{v}{c}\right)^{k-1}.exp\left[-\left(\frac{v}{c}\right)^{k}\right] \quad (21)$$

The enhanced gray wolf method is a recent meta-heuristic algorithm that effectively solves multi-objective optimization problems. It has been extensively tested on many basic and complex functions in reference [24], yielding favorable results. Hence, in this study, given that our objective function is a three-objective function with numerous restrictions, it is advisable to employ this approach for its resolution.

3. Case Study and Results

3.1. Case Study

To show the effectiveness of the proposed solution, the standard IEEE 33-bus smart system with a single-line diagram was studied according to Figure 2. The backward-forward-sweep load flow approach is commonly employed for radial distribution systems. We employed this technique in the present work to execute load distribution [25].

To implement the simultaneous planning of wind DG and EV charging parking, it was assumed that all system busses, except for the primary substation, were candidates for installing DG and parking lots. The goal was to determine five buses in the system to install EV charging parking and five buses to install wind DG. The maximum capacity of EV charging parking lots in the entire system was considered 3.5 MVA. Also, the DG installation capacity in each bus was set at 2.5 MW. The study was carried out for one year, equivalent to 8760 hours. The expression of the objective function included the weighted sum of the cost of losses and the voltage deviations of the system buses minus the installed capacity of wind DG.

In evaluating the objective function expression, the cost of each kWh of losses was 4000 IRR, and the violation cost of each per-unit of system bus voltage deviations was 400 thousand IRR/h. If the power flow through the system feeders exceeded the thermal limit of the feeder (6.6 MVA), the objective function would be penalized 100 billion IRR. Uncertainties considered in solving the planning problem included the uncertainty in the system load, the load of EV charging parking lots, and the output power of wind turbines. To model the uncertainty of distribution system consumption, the normal distribution function was used with the mean and standard deviation values of 100% and 10%, respectively. Wind speed uncertainty was also modeled by the Weibull distribution function with shape and scale factor equal to 7 and 2, respectively.

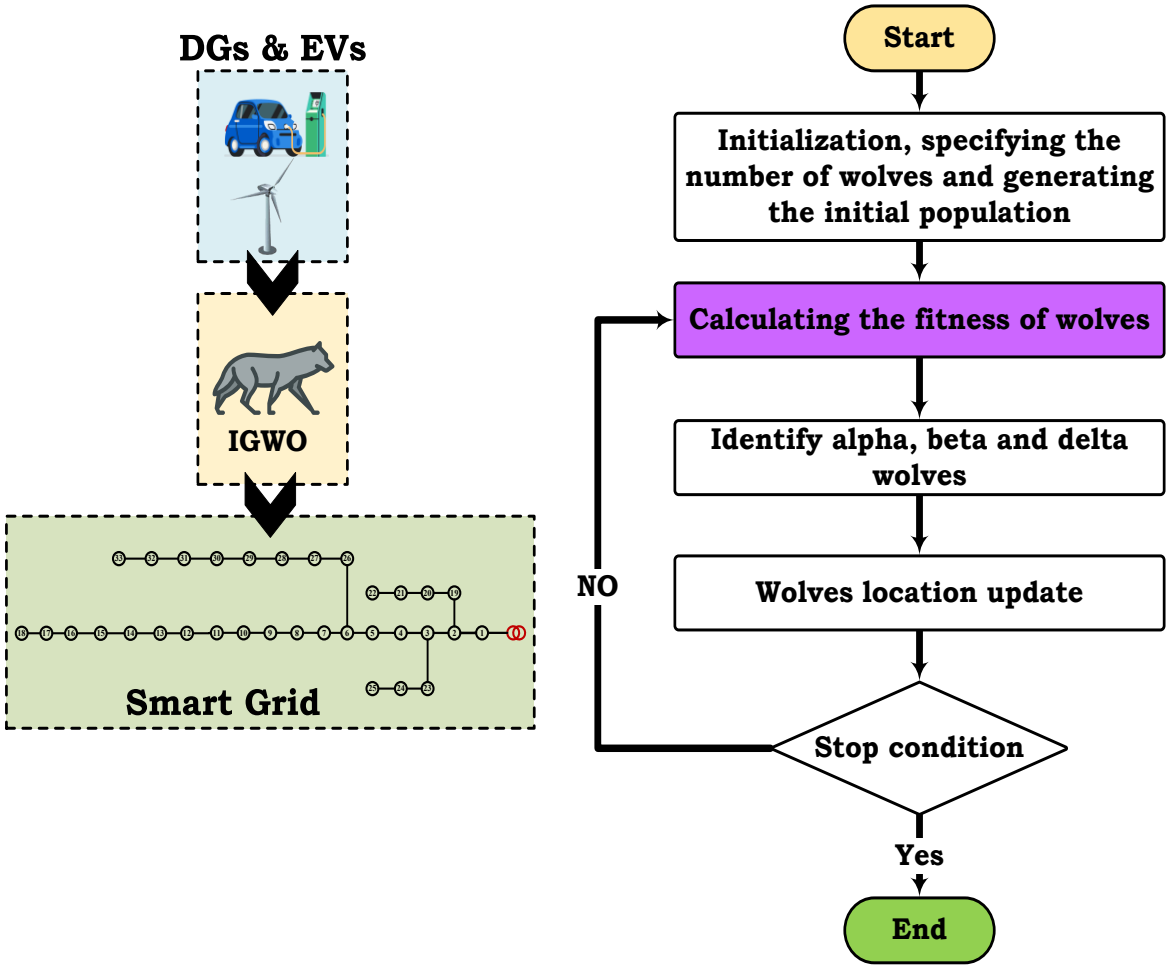

Figure 2. The standard IEEE 33-bus smart system and IGWO flowchart.

Also, the uncertainty of the charging profile of EVs was modeled with a normal distribution function with a mean and standard deviation of 70% and 20%, respectively. After designing the probability distribution functions with the mentioned parameters, a thousand samples were taken from each probability distribution function simultaneously with the *random* command. In this way, a 1000 × 3 matrix was built, in which the first to third columns show the system load factor, the EV charging parking lot load factor, and the wind turbine output power, respectively. Normally, it is unnecessary to study a thousand operation scenarios in a planning problem. To reduce the volume of calculations, the thousand scenarios generated from each variable with uncertainty were reduced to five scenarios using the data mining method. Figure 3-Figure 6 show the histogram curve of the system loading factor, charging parking loading factor, wind speed, and output power of the 500 kW (0.5 MW) wind turbine obtained by taking a thousand samples from specific probability distribution functions, respectively. By applying the *k*-means algorithm to 1000 samples, 5 scenarios of system load factor, charging parking load factor, and wind turbine output power of 500 kW were obtained according to Figure 7-Figure 9. Also, the probability of the occurrence of each scenario is shown in Figure 10.

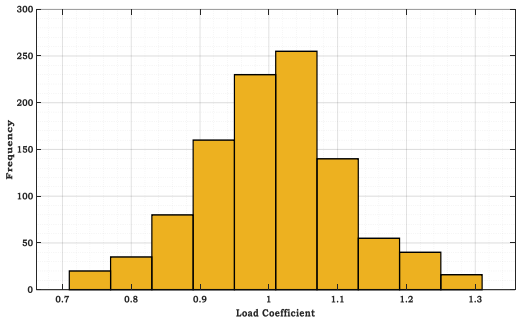

Figure 3. The system's load factor.

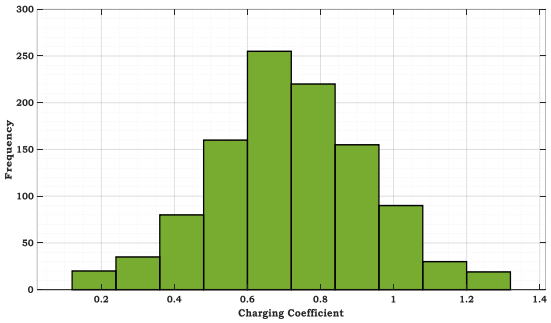

Figure 4. The loading coefficient of the parking lot.

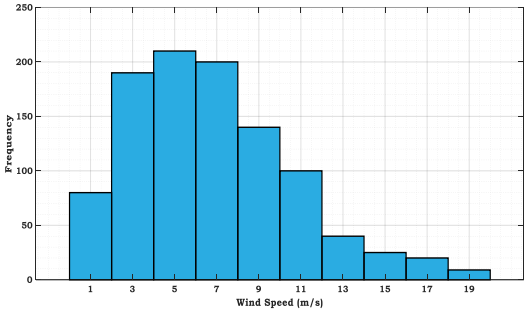

Figure 5. Wind speed.

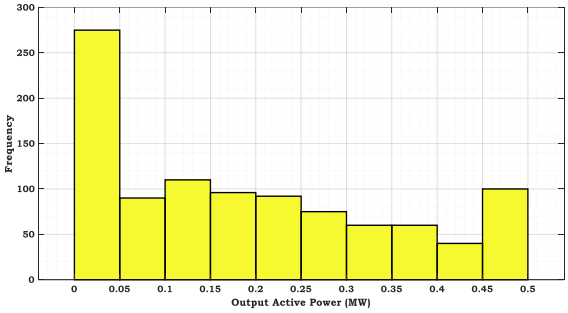

Figure 6. Wind turbine output power.

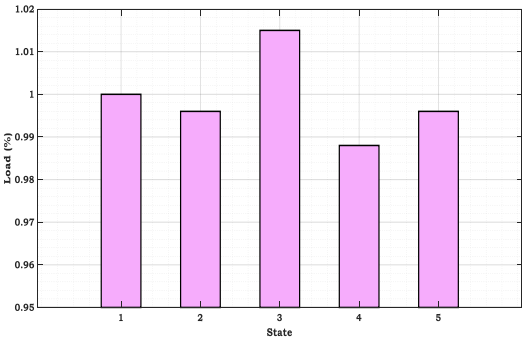

Figure 7. The system's load profile.

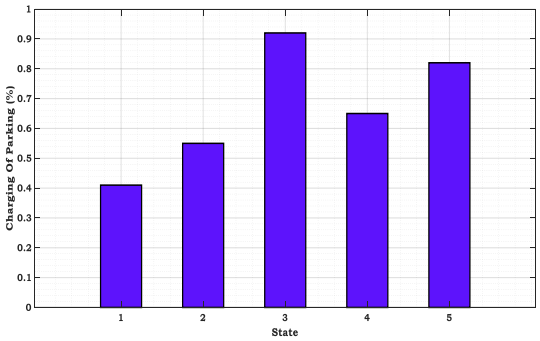

Figure 8. Charging profile of charging parking lots.

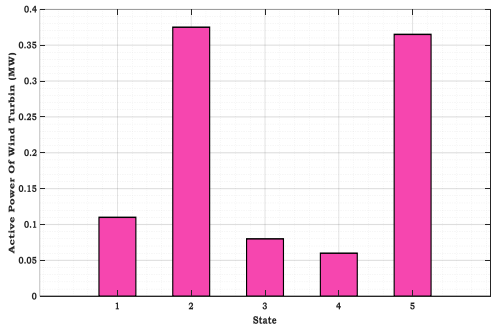

Figure 9. Active output power profile of the 500-kW wind turbine.

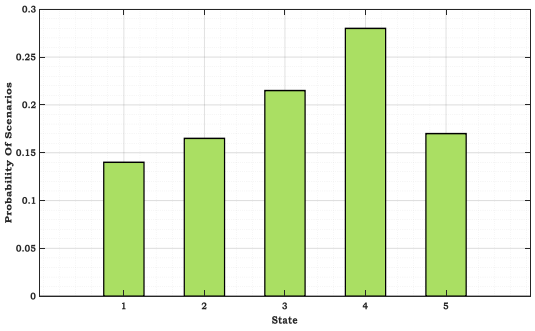

Figure 10. The probability of the occurrence of scenarios.

Table 1 provides a summary of the implementation considerations of the proposed solution. The proposed solution is simulated below by considering five possible scenarios. To perform the optimization, the gray wolf algorithm whose settings are presented in Table 1 and Table 2 was used.

3.2. Analysis of results

This section discusses the simulation of the suggested solution. The aim was to find the place and size of EV charging lots and wind DG optimally to improve the DG PODS and reduce operating costs. Figure 11 shows the improvement process of the objective function. In this curve, the horizontal and vertical axes represent the number of iterations and the objective function, respectively. Also, Table 3 and Table 4 show the optimal solution, including the place and size of the charging parking and wind DG. The optimal capacities were set as the maximum installation capacity of DG, which was used according to uncertainty coefficients in operating conditions. The distribution system's performance was evaluated after applying the optimal solution to the distribution system. Figure 12 to Figure 15 show the bus voltage curve, the power flow through the feeders of the distribution system, the losses of the feeders of the distribution system, and the voltage deviations of the system buses in the optimal state compared to the normal state, respectively.

Table 1. Technical and economic data of the hybrid energy system component.

Parameter	Value
Candidate buses for charging parking	Buses 2 to 33
Candidate buses of wind turbines	Buses 2 to 33
Maximum capacity of the charging parking lot	3.5 MWA
The total capacity of wind turbines in the bus	2.5 MW
C_1 coefficient	1000
C_2 coefficient	400 thousand IRR/per-unit hour
C_3 coefficient	10 billion IRR
The cost of losses	4000 IRR/kWh

Table 2. Optimization algorithm settings.

Variable	Value
The number of iterations	50
Population size	100
r_1 coefficient	Rand [0,1]
r_2 coefficient	Rand [0,1]

Table 3. Optimal location and installation capacity of charging parking lots.

Bus number	21	20	9	19	25
Capacity (kW)	490	830	370	590	180

Table 4. Optimum location and installation capacity of wind DGs.

Bus number	18	3	19	9	20
Capacity (MW)	1.7	3.9	2.9	2.5	4.05

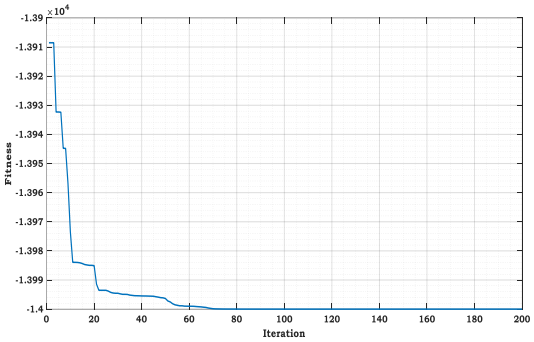

Figure 11. The process of improving the objective function.

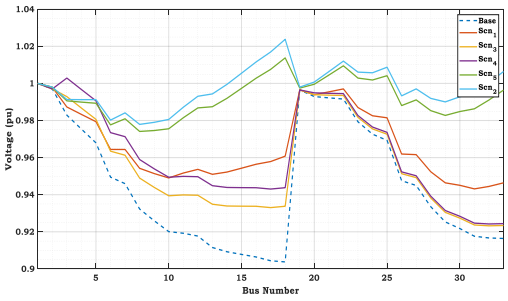

Figure 12. Voltage curves of distribution system buses in five uncertainty events.

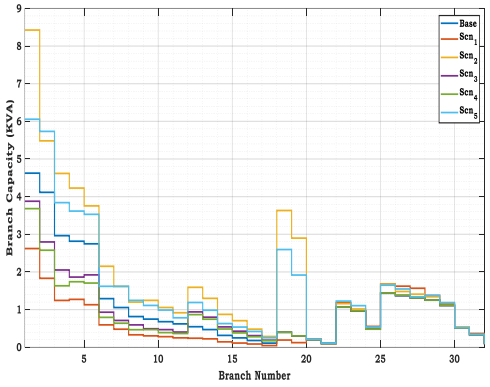

Figure 13. Power flow through distribution system feeders in five uncertainty events.

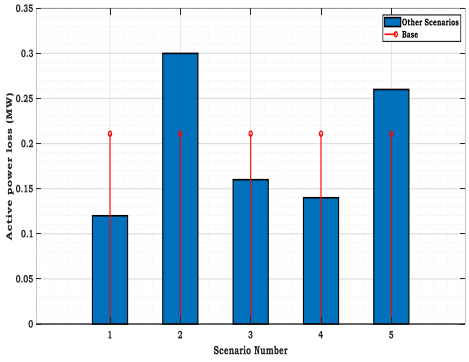

Figure 14. Comparison of losses of distribution system feeders in different states of uncertainty.

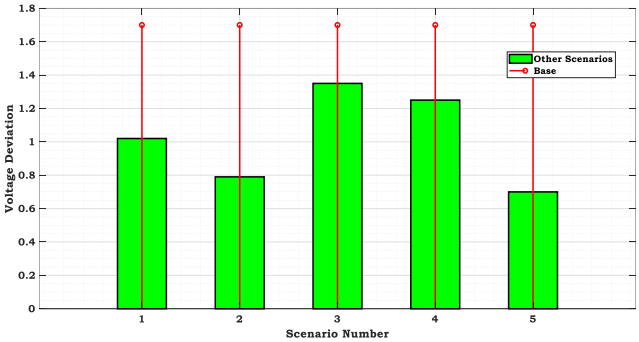

Figure 15. Comparison of voltage deviations of distribution system buses in different states of uncertainty

Accordingly, the voltage curve of the system buses improved considerably. Also, the power flow through the system feeders was such that it followed the thermal restrictions of the system feeders, which was 6.6 MVA. According to the results, the losses of system feeders in the second and fifth scenarios increased compared to the primary distribution system. Nonetheless, the loss of the whole system was improved compared to the initial state. It should be noted that in the process of evaluating DG PODS, system losses should not increase from the initial value.

4. Conclusions

The research aimed to plan EV charging parking lots to improve the electrical parameters of the smart distribution system and increase the wind DG PODS. The problem was formulated as a nonlinear optimization model. The objective function included reducing losses, reducing voltage deviations, and increasing the power output of the smart system. In solving the optimization problem, a set of technical and economic constraints were considered. To achieve robust optimal solutions, the uncertainties of charging parking lots, smart grid consumption, and wind speed were modeled by combining Monte Carlo and *k*-means methods. The gray wolf algorithm was adopted to address the optimization problem. Studies were done on the standard IEEE 33-bus smart system to demonstrate the effectiveness of the proposed solution. The results showed the high efficiency of the proposed solution.

In summary, the following outcomes were achieved:

- Employing the enhanced gray wolf algorithm for solving the multi-objective problem
- Taking several uncertainties related to wind resources, load, and cars into account
- Evaluating the outcomes with the clustering technique

Prospective projects and concepts:

- Utilizing alternative meta-heuristic techniques to address the problem and subsequently comparing the outcomes
- Taking the availability of solar resources in the power grid into account
- Implementing an electric spring in the system to enhance electrical flexibility

References

[1] K. H. Truong, P. Nallagownden, I. Elamvazuthi, and D. N.Vo, "An Improved Meta-Heuristic Method to Maximize the Penetration of Distributed Generation in Radial Distribution Networks," *Neural Computing and Applications*, vol. 32, pp. 10159-10181, 2020.

[2] M.S.S. Abad, and J. Ma, "Photovoltaic Hosting Capacity Sensitivity to Active Distribution Network Management," *IEEE Transactions on Power Systems*, vol. 36, no. 1, pp. 107-117, 2020.

[3] M. Zain ul Abideen, O. Ellabban, and L. Al-Fagih, "A Review of the Tools and Methods for Distribution Networks Hosting Capacity Calculation," *Energies*, vol. 13, no. 11, 2758, 2020.

[4] M. Abasi, A.T. Farsani, A. Rohani, and A. Beigzadeh, "A Novel Fuzzy Theory-Based Differential Protection Scheme for Transmission Lines," *International Journal of Integrated Engineering*, vol. 12, no. 8, pp.149-160, 2020.

[5] X. Xua, J. Lia, X. Zhao, Z. Jian, and C. Lai, "Enhancing Photovoltaic Power Output—A Stochastic Approach to Optimal Planning of Static Var Compensator Devices in Distribution Networks," *Applied Energy*, vol. 238, pp. 952–962, 2019.

[6] J. Ebrahimi, M. Abedini, M.M. Rezaie, and M. Nasri, "A Two-Step Approach to Energy Management in Smart Micro-Grids Aimed at Improving Social Welfare Levels and the Demand Side Management Effect," *Iranian Electric Industry Journal of Quality and Productivity*, vol. 9, no. 3, pp. 56-67, 2020.

[7] M. Abasi, A. Saffarian, M. Joorabian, and S.G. Seifossadat, "Location of Double-Circuit Grounded Cross-Country Faults in Gupfc-Compensated Transmission Lines Based on Current and Voltage Phasors Analysis," *Electric Power Systems Research*, vol. 195, 107124, 2021.

[8] S.M. Ismael, S.H.A, Aleem, A.Y. Abdelaziz, and A.F. Zobaa, "State-Of-The-Art of Hosting Capacity in Modern Power Systems with Distributed Generation," *Renewable Energy*, vol. 130, pp. 1002-1020, 2019.

[9] S.M. Sadeghi, M. Daryalal, and M. Abasi, "Two-Stage Planning of Synchronous Distributed Generations in Distribution Network Considering Protection Coordination Index and Optimal Operation Situation," *IET Renewable Power Generation*, vol. 16, no. 11, pp. 2338-2356, 2022.

[10] Y. Takenobu, N. Yasuda, S.I. Minato, and Y. Hayashi, "Scalable Enumeration Approach for Maximizing Hosting Capacity of Distributed Generation," *International Journal of Electrical Power & Energy Systems*, vol. 105, pp. 867-876, 2019.

[11] M. Abasi, N. Heydarzadeh, and A. Rohani, "Broken Conductor Fault Location in Power Transmission Lines Using GMDH Function and Single-Terminal Data Independent of Line Parameters," *Journal of Applied Research in Electrical Engineering*, vol. 1, no. 1, pp.22-32, 2021.

[12] M. Abasi, M. Joorabian, A. Saffarian, and S.G. Seifossadat, "A Comprehensive Review of Various Fault Location Methods for Transmission Lines Compensated by FACTS devices and Series Capacitors," *Journal of Operation and Automation in Power Engineering*, vol. 9, no.3, pp. 213-225, 2021.

[13] A. Lakum, and V. Mahajan, "Optimal Placement and Sizing of Multiple Active Power Filters in Radial Distribution System Using Grey Wolf Optimizer in Presence of Nonlinear Distributed Generation," *Electric Power Systems Research*, vol. 173, pp.281-290, 2019.

[14] M. Abasi, A. Torabi Farsani, A. Rohani, and M. Aghazadeh Shiran, "Improving Differential Relay Performance during Cross-Country Fault Using a Fuzzy Logic-based Control Algorithm," *5th Conference on Knowledge-Based Engineering and Innovation*, Iran, 2019.

[15] M. Abasi, A. Rohani, F. Hatami, M. Joorabian, and G.B. Gharehpetian, "Fault Location Determination in Three-Terminal Transmission Lines Connected to Industrial Microgrids Without Requiring Fault Classification Data and Independent of Line Parameters," *International Journal of Electrical Power & Energy Systems*, vol.131, 107044, 2021.

[16] A. Rohani, M. Abasi, A. Beigzadeh, M. Joorabian, and G.B. Gharehpetian, "Bi-Level Power Management Strategy in Harmonic-Polluted Active Distribution Network Including Virtual Power Plants," *IET Renewable Power Generation*, vol. 15, no. 2, pp. 462-476, 2021.

[17] J. Ebrahimi, and M. Abedini, "A Two-Stage Framework for Demand-Side Management and Energy Savings of Various Buildings in Multi Smart Grid Using Robust Optimization Algorithms," *Journal of Building Engineering*, vol. 53, 104486, 2022.

[18] M. Abasi, M. Joorabian, A. Saffarian, and S.G. Seifossadat, "An Algorithm Scheme for Detecting Single-Circuit, Inter-Circuit, and Grounded Double-Circuit Cross-Country Faults in GUPFC-Compensated Double-Circuit Transmission Lines," *Electrical Engineering*, vol. 104, pp. 2021-2024, 2022.

[19] E. Mulenga, M.H. Bollen, and N. Etherden, "A Review of Hosting Capacity Quantification Methods for Photovoltaics in Low-Voltage Distribution Grids," *International Journal of Electrical Power & Energy Systems,* vol. 115, 105445, 2020.

[20] M. Sadeghi, and M. Abasi, "Optimal Placement and Sizing of Hybrid Superconducting Fault Current Limiter to Protection Coordination Restoration of the Distribution Networks in the Presence of Simultaneous Distributed Generation," *Electric Power Systems Research*, vol. 201, 107541, 2021.

[21] J. Ebrahimi, M. Abedini, M.M. Rezaei, and M. Nasri, "Optimum Design of a Multi-Form Energy in The Presence of Electric Vehicle Charging Station and Renewable Resources Considering Uncertainty," *Sustainable Energy, Grids and Systems*, vol. 23, 100375, 2020.

[22] M. Abasi, A. Torabi Farsani, A. Rohani, and A. Beigzadeh, "A New Fuzzy Theory-Based Differential Protection Scheme for Transmission Lines," *International Journal of Integrated Engineering*, vol. 12, no. 8, pp. 149-160. 2020.

[23] H. Makvandi, M. Joorabian, and H. Barati, "A New Optimal Design of ACD-Based UPFC Supplementary Controller for Interconnected Power Systems," *Measurement*, vol. 182, 09670, 2021.

[24] BN.Gohil, and DR.Patel, "An Improved Grey Wolf Optimizer (IGWO) for Load Balancing in Cloud Computing Environment," *In Algorithms and Architectures for Parallel Processing: ICA3PP 2018 International Workshops*, Guangzhou, China, November 15-17, pp. 3-9, 2018.

[25] M. Abasi, H. Bahmani, M. Joorabian, J. Ebrahimi, and M. Razavi, "Designing an Energy Managing System for Distributed Dispersion in Smart Microgrids Based on Environmental Constraints," *In 12th Smart Grid Conference (SGC)*, pp. 1-6, 2023.

Declaration of Competing Interest

The authors declare that they have no known competing financial interests or personal relationships that could have appeared to influence the work reported in this paper. The ethical issues, including plagiarism, informed consent, misconduct, data fabrication and/or falsification, double publication and/or submission, redundancy, have been completely observed by the authors.

Credit Authorship Contribution Statement

Javad Ebrahimi: Conceptualization, Formal analysis, Project administration, Supervision, Validation, Roles/Writing - original draft. **Mahyar Abasi:** Conceptualization, Investigation, Methodology, Resources, Visualization, Writing - review & editing.

Bibliography

Javad Ebrahimi was born in Iran in 1988**.** He received his Ph.D. degree in Electrical Engineering (Power system) from Khomeinishahr Branch, Islamic Azad University, Khomeinishahr /Isfahan, Iran, in 2020. He currently works as a technical teacher in the Technical and Vocational Academy of Isfahan province. Also, he has taught for ten years at Borujerd Islamic Azad University and Ayatollah Borujerd University. He has published ten research papers, eight conference papers, and one industrial research project. His research interests include power quality, smart grids, demand-side management, and microgrids.

Mahyar Abasi was born in Iran in 1989. He graduated with a Ph.D. in Electrical Power Engineering from the Shahid Chamran University of Ahvaz, Ahvaz, Iran, in 2021. His research background is more than 60 published journal and conference papers, more than 10 authored books, 11 industrial research projects, and a patent in power systems. In 2021, he was introduced as the top researcher of Khuzestan province, Iran, and in the years 2021 to 2023, he successfully received four titles from the membership schemes of the National Elite Foundation in Iran. He is currently an Assistant Professor at the Electrical Engineering Department of Arak University, Arak, Iran. His specialized interests are fault protection, detection, classification, and location in HVAC and HVDC transmission lines, control of reactive power and FACTS devices, evaluation and improvement of power quality, and power system studies.

Journal of Green Energy Research and Innovation

Optimal Placement of Distributed Energy Resources to Reduce Losses, Improve Voltage Profile, and Convert it into a Self-healing Smart Grid

Ali Kazemi, Ali Morsagh Dezfuli

Highlight

- Achieving a self-healing network with high reliability and minimal losses
- Optimal placement of DGs in the network using the particle swarm algorithm
- Enhancing the voltage profile and system reliability
- Detecting and rectifying disruptions with minimal human intervention

Graphical Abstract

Use your device to scan and read the article online

Citation

A. Kazemi, and A. Morsagh Dezfuli, " Optimal Placement of Distributed Energy Resources to Reduce Losses, Improve Voltage Profile, and Convert it into a Self-healing Smart Grid," *Journal of Green Energy Research and Innovation*, vol. 1, no. 1, pp. 16-33, 2024.

https://doi.org/10.61186/jgeri.1.1.16

JGERI Journal of Green Energy Research and Innovation

Online ISSN: 3041-9018

Journal of Green Energy Research and Innovation

Journal Homepage: www.jgeri.araku.ac.ir

Optimal Placement of Distributed Energy Resources to Reduce Losses, Improve Voltage Profile, and Convert it into a Self-healing Smart Grid

Ali Kazemi [1]*, Ali Morsagh Dezfuli [2]

[1] *Department of Electrical and Computer Engineering, Technical and Vocational University (TVU), Mazandaran, Iran.*
[2] *Department of Electrical Engineering, Faculty of Engineering, Shahid Chamran University of Ahvaz, Ahvaz 61357-85311, Iran.*

* ***Corresponding Author:*** *Ali.kazemi2004@gmail.com*

ARTICLE INFO

Keywords:
Smart grid,
Self-healing,
Optimal location,
Distributed energy resources.

Article history:
Received: 04 December 2023;
Revised: 11 January 2024;
Accepted: 23 January 2024;

Article type:
Research Article

ABSTRACT

This study focuses on achieving a self-healing network with high reliability and minimal losses by discussing the optimal placement of distributed generation (DG) sources in the network using the particle swarm algorithm (PSO). Optimal placement not only reduces losses but also enhances the voltage profile and enhances system reliability. Consequently, the paper explores the concept of a self-healing smart grid. Smart grids possess a crucial attribute known as self-healing, designed to enhance the system's dependability. The self-healing power grid can detect and rectify disruptions within its infrastructure with minimal or even absent human intervention. This study examines a standard IEEE 69-bus network and presents results demonstrating the network's safety, the prevention of blackouts, the reduction of losses, and the substantial enhancement of the voltage profile.

1. Introduction

The growing demand for clean and affordable energy, along with advancements in renewable resources technology, has led to a rising trend in distributed generation. Conversely, the utilization of distributed generation (DGs) units in energy distribution networks can yield several outcomes, including loss reduction, enhanced dependability, improved voltage profile, and enhanced power quality in electrical distribution networks. The strategic placement of DGs inside a distribution network is crucial for attaining these objectives. Within distribution networks, the voltage profile is inadequate in terms of voltage magnitude, and power loss is unavoidable. Therefore, the investigation of the impact of DGs is necessary to enhance the voltage profile magnitude, minimize losses, and improve reliability. Additionally, determining the optimal location of these sources is crucial in achieving these objectives. Parametric relations and cost functions are utilized in [1] to determine the optimal placement of DGs in a network with unbalanced loads. Additionally, the group search optimizer (GSO) is employed as a novel method for resolving unbalanced power flow. This is one of the recently developed algorithms in the field of neural networks. The paper [2] presents a method for determining the best location for DGs by minimizing the overall energy loss. This method uses nonlinear programming and optimal power flow (OPF) techniques, taking into account operational

constraints and uncertainties in load and power generation resources in the IEEE 33-bus test system. The unit commitment (UC) problem is addressed in [3] using a novel evolutionary approach. The conventional objective function of the UC problem involves taking into account the pertinent parameters of the wind farm and aiming to enhance the quality of life by incorporating wind units. This can be achieved by minimizing the annual economic losses, which encompass the expenses associated with installation, operation, and maintenance, in addition to fluctuations in voltage and losses of power in the buses. The paper [4] discusses a novel multi-objective whale optimization algorithm (MOWOA) designed specifically for solving multi-objective problems. The study [5] focuses on enhancing the cost function or cost-effectiveness of electricity generation by strategically allocating wind, solar, and hydroelectric systems. The system assesses the degree of penetration (ranging from 0 to 100%) of various systems and develops generators that effectively transition to renewable resources.

The advanced search group algorithm (ESGA) [6] has been used for the purpose of optimizing the placement of DGs in distribution networks. The system utilizes radial networks (RDNs) to minimize power losses, enhance voltage stability, and improve voltage profiles. It effectively enhances network performance by employing appropriate power. Reference [7] presents a method that utilizes non-linear programming and the crow search algorithm to optimize the placement and sizing of hybrid SFCLs in distribution systems with synchronous DG. The objective is to minimize the size of the SFCLs and the operating time of the OCR, while also enhancing protection coordination with minimizing installation expenses. The paper [8] presents an optimal approach for positioning and assessing type IV induction generators in extensive wind farms. The objective is to effectively incorporate type IV induction generators and wind farms into unbalanced three-phase distribution networks. This study focuses on minimizing losses by utilizing Unified Power Quality Conditioner (UPQC) as a means of reactive power support, in conjunction with the Particle Swarm Optimization (PSO) algorithm. The outcomes of a two-step economic plan in [9] for incorporating synchronous DGs into conventional distribution networks validate the enhancement of protection coordination and economic metrics in comparison to power flow studies. Ref. [10] presents a method based on evolutionary optimization for determining the optimal location and reconfiguration of DGs in the standard IEEE 33-bus system. This method leads to considerable enhancements in voltage characteristics, reduction in power loss, and improved system reliability.

According to [11], an optimal approach is suggested for determining the quantity and placement of DGs in distribution networks, using nodal pricing as the basis. This study employs an enhanced artificial bee colony algorithm on a practical 38-bus system with voltage- and frequency-sensitive loads, with the objective of maximizing the profit of the distribution company. The researchers in [12] propose a highly effective approach to optimize the placement and capacity of DGs and transformers tap in distribution networks by analyzing and considering uncertainties. This is realized by minimizing the loss and improving the voltage stability using probabilistic nonlinear optimization. The study [13] employs three multi-objective algorithms to determine the optimal placement and quantity of DGs in power systems. The effectiveness of this approach is evaluated

using the standard IEEE 33-bus distribution network, and the results demonstrate a notable decrease in active power losses by strategically placing DGs, thereby enhancing system performance. In [14], a proposed approach suggests integrating electric vehicles (EVs) into unbalanced distribution systems using an optimal coordinated strategy. By employing Vehicle-to-Grid (V2G) technology and demand-side management for EVs, this method effectively finds resources that result in decreased power losses, enhanced voltage parameters, and lowered operating expenses. In their study, researchers in [15] suggest an optimal method for determining the location, generation level, and scheduling of energy storage sources with DGs in distribution networks. This methodology utilizes loss sensitivity factors and addresses uncertainties to prevent voltage deviation and minimize the voltage deviations and active power losses.

The objective of [16] is to reduce active and reactive power losses in power networks by implementing a genetic algorithm (GA) to maximize the capacity of DGs. Through simulation on standard IEEE 30- and 118-bus systems, this technique proves to be a promising strategy for sustainable energy systems. In [17], a novel approach is suggested to enhance voltage stability and reduce power losses in radial distribution networks. This approach involves the optimal positioning of DGs, network reconfiguration, and voltage control at buses using a gray wolf optimization algorithm for a multi-objective function. It enhances the voltage stability of the tested system to a notable extent. The researchers in [18] examine how the rated power and overall capacity of solar modules impact energy loss in radial distribution networks. They find that their multi-objective control strategy is more effective than alternative approaches in attaining reduced energy loss. The recommended power rating for each individual unit and the overall capacity for all units are provided to ensure the installation of an efficient solar system.

The strategy proposed in [19] aims to enhance voltage regulation in order to optimize distributed energy storage in imbalanced distribution networks. The researchers in this study utilize thorough voltage analysis to ascertain the most advantageous placement and dimensions of Distributed Energy Storage Systems (DESS) while simultaneously reducing costs with an enhanced gray wolf minimization technique. This approach effectively enhances voltage projects in unbalanced distribution networks, while also ensuring economic efficiency.

Based on the analysis of various articles and references, it has been observed that the strategic placement of generation sources in order to minimize losses, enhance voltage stability, and reduce network expenses has been achieved through methods such as optimization algorithms, solving non-linear equations, energy storage, and adjusting transformers tap. However, none of these approaches have addressed the issue of network self-healing, which will be the focus of this article.

This paper presents the architecture of a self-healing network that exhibits great dependability and minimal losses. To achieve this objective, the PSO algorithm will be employed to locate DG units throughout the network. Among the existing algorithms, this algorithm provides the most optimal solution, and the main reason for selecting this specific algorithm is its convergence speed, which presents the desired results in the least possible time. Identifying the most suitable locations for these sources will not only lead to a substantial reduction in losses but also enhance the voltage profile and the system's

reliability. Subsequently, the discussion will focus on the enhancement of network intelligence and self-healing capabilities. In this study, we examined the conventional 69-bus network and analyzed the simulation outcomes. Next, the second section will discuss the allocation of DGs to minimize losses, while the third section will outline the suggested self-repairing algorithm. This article is structured into five sections, with Section 1 serving as an introductory overview of the topic. Section 2 provides an explanation of the relationships associated with the placement of DGs to minimize losses, utilizing the PSO algorithm. Section 3 provides a comprehensive explanation of the theoretical framework behind the proposed self-healing algorithm. Section 4 outlines the outcomes of the software simulation test, while Section 5 provides the final conclusion.

2. Allocation of DGs to reduce losses

The PSO has been adopted here to find the proper size and location of DGs in a distribution system. The optimization problem is formulated as follows:

$$Min\ f\ (x)s.t.\ x_i \in X_i,\ i = 1,2,...,N \tag{1}$$

where $f(x)$ is the objective function, and x is the sum of each of the selected x_i variables. The value of X_i is the sum of the possible amplitude of each variable, and N is the number of variables.

2.1. Objective function

The optimization problem aims to determine the optimal size and precise placement of DGs to maximize the ratio of the benefits derived from employing these resources to their associated costs. Augmenting the quantity of DGs amplifies the advantages of this scheme, although it concurrently escalates the capital cost and substantially raises the overall cost. Consequently, as the number of DGs rises, so does the magnitude of their expenses. The objective function is defined by Equation (2):

$$\max f = \frac{Benefit}{Cost} \tag{2}$$

2.2. Advantages

- **Reduced power purchase**

The first advantage of using DGs is that with the generation of power by DG, the purchase of power from the main grid is reduced. Therefore, this reduction can be considered as an advantage in DGs in the form of Equation (3):

$$PS\ (\$/KWh) = \sum_{i=1}^{N_{DG}} P_{DG}^{i} \times \rho \tag{3}$$

Here, PS is the profit from the sale of power. N_{DG} is the number of installed DGs, P_{DG}^{i} is the amount of power produced by the ith DG, and ρ is the price of electricity. Considering the 5-year study period, inflation and interest rates should be considered in electricity cost calculations. The price of electricity per year can be calculated by Equation (4):

$$\rho^{i}\ (\$/KWh) = \rho^{0} \times \left(\frac{1+\ln fR}{1+\ln tR}\right)^{i-1} \tag{4}$$

Here ρ^0 is the cost of electricity in the first year, ρ^i is the cost of electricity in the ith year, and InfR and IntR denote the inflation and interest rates, respectively.

- **Loss reduction**

Another advantage of using DG is the reduction of losses due to energy generation in local loads and the elimination of transmission lines [20, 21]. Losses in the distribution system depend on the current and resistance of the transmission lines. Losses are a function of system topology and the size and location of DGs in the system. The loss reduction equation can be shown as Equation (5):

$$B_{Loss} = \left(Loss_{NDG} - Loss_{DG}\right) \times \rho \tag{5}$$

Here, $Loss_{NDG}$ and $Loss_{DG}$ show the losses without and with the use of DGs.

- **Reduced energy not-supplied (ENS)**

Reliability is another benefit that can be achieved using DGs and the ENS model. Fault location and fault clearance along the fault branch are used to calculate ENS [22, 23]. Sectionalizers and reclosers can reduce the range of fault impact and reduce the number of users experiencing long-term outages [23, 24]. The repair duration includes the time required to isolate the faulty branch, connect an emergency node, and repair the fault location. DGs that direct the power to the split branch can play a major role in improving reliability.

ENS costs can be calculated as in [25] according to Equation (6):

$$C_{ENS} = \sum_{i=1}^{N_{branch}} \sum_{j=1}^{N_t} \lambda_i L_i \rho_{\text{int}} t_i D_j \tag{6}$$

Here, C_{ENS} is equal to the cost of ENS per year, N_{branch} is the number of branches in the system, N_t is the number of loads interrupted due to fault in the ith branch, λ_i is the fault rate for each branch per kilometer per year, L_i is the length of the branch, t_i is the length of the repair period, ρ_{int} is the consumer price, and D_j denotes the load rate due to the fault in the ith branch.

The benefit of using DGs in reliability is as Equation (7):

$$\Delta C_{ENS} = C_{NDG}^{ENS} - C_{DG}^{ENS} \tag{7}$$

where C_{NDG}^{ENS} and C_{DG}^{ENS} are the ENS cost without DG and with DG. Also, the price of ENS should be calculated every year on the basis of bank interest and inflation and in the form of Equation (8):

$$\rho_i^{\text{int}} = \rho_0^{\text{int}} \times \left(\frac{1+\ln fR}{1+\ln tR}\right)^{i-1} \tag{8}$$

2.3. Costs

In this section, three types of costs are considered for DGs: initial, maintenance and performance, and investment costs [26].

- **Initial cost**

Initial costs include the costs related to the purchase, installation, and connection of DG units. The initial cost of DG is given in Equation (9) [26]:

$$IC_{DG}\left(\$/KWh\right)=\sum_{i=1}^{N_{DG}} C_i^{investment} \tag{9}$$

Here $C_i^{investment}$ is the cost necessary for purchasing and connecting the *i*th DG, and IC_{DG} is the total capital cost of all DGs.

- **Investment cost**

The investment cost includes the annual cost of fuel, taking into account the interest rate. In this case, the investment cost will be calculated in the form of Equation (10) [26]:

$$OC_{DG}\left(\$/KWh-year\right)=\sum_{i=1}^{N_{DG}} C_i^{operation} \tag{10}$$

The amount $C_i^{operation}$ is the investment cost of the *i*th DG and OC_{DG} is the investment cost for all DGs. This is an annual cost, and interest rates and inflation should be considered in them [26].

$$C_i^{operation}=C_0^{operation}\times\left(\frac{1+\ln fR}{1+\ln tR}\right)^{i-1} \tag{11}$$

- **Maintenance and operation cost**

The cost of maintenance and operation, which includes the costs related to the maintenance of DG units, is defined as Equation (12):

$$MC_{DG}\left(\$/KWh-year\right)=\sum_{i=1}^{N_{DG}} C_i^{maintenance} \tag{12}$$

where $C_i^{maintenance}$ is the maintenance and operation cost of the *i*th DG and MC_{DG} is the total cost for maintenance and operation of all DGs. This is an annual cost, and the amounts of interest and inflation should be considered in it. According to Equation (13), we have:

$$C_i^{maintenance}=C_0^{maintenance}\times\left(\frac{1+\ln fR}{1+\ln tR}\right)^{i-1} \tag{13}$$

2.4. Constraints

The constraints of the objective function include the following:

- **System voltage level**

$$V_{\min}\le V_i^{n}\le V_{\max}\quad n=1,2,\ldots,N \tag{14}$$

where V_i is the node voltage in year *i*, and *N* is the number of nodes of the system.

- **Short-circuit limits**

$$S_{\min}^{b}\le S_i^{b}\le S_{\max}^{b}\quad b=1,2,\ldots,B \tag{15}$$

where S_i^{b} is the apparent power at branch *b* in year *i*, and *B* represents the number of branches (transformers and lines).

- **Active and reactive power of the DG**

$$P_{DG\min}^{k} \le P_{DGi}^{k} \le P_{DG\max}^{k} \quad k = 1,2,\ldots,K \tag{16}$$

$$Q_{DG\min}^{k} \le Q_{DGi}^{k} \le Q_{DG\max}^{k} \quad k = 1,2,\ldots,K \tag{17}$$

where P_{DGi}^{k} and Q_{DGi}^{k} are the active and reactive power output of generator k in year i, and K is the number of DGs.

3. The proposed self-healing algorithm

This section provides a comprehensive description of the proposed self-healing algorithm for the network. The self-healing reconfiguration process is described here. When a fault occurs, the power recovery system detects the fault based on the data related to the distribution network in real time. Subsequently, it proposes an accurate and efficient reconfiguration technique to precisely identify the location of the fault, separate the faulty region, and promptly restore the unaffected regions. The challenge of self-healing reconfiguration in distribution networks can be characterized as a multi-objective, multi-period hybrid, multi-boundary nonlinear optimization problem, taking into account factors such as the number of switching operations, feeder load margin, load improvement amount, network restrictions, and user priority. Prior to elucidating the executed method, we provide an explanation of the objective functions, constraints, and the algorithm employed in the simulation [27].

3.1. Objective function

Different objective functions for the reconfiguration algorithm of self-healing distribution networks are presented according to different reconfiguration target conditions. The following two objectives are considered in this paper [27].

1) Objective functions with the least number of switching operations and minimum power loss

$$\min F(I,Y,Z) = \min\left\{ b_1 \left[\sum_{i=1}^{m} a_i (1 - y_i) + \sum_{j=1}^{n} a_{m+j} z_j \right] + b_2 \sum_{i=1}^{l} |I_i|^2 R_i \right\} \tag{18}$$

y_i and z_i show the status of disconnection and loop switches, m and n are the number of disconnection and loop switches, a_i is the weight coefficient, i denotes the number of branches, I_i represents the present amplitude of branch i, R_i is the resistance of branch i, b_1 is the cost coefficient of switch operations, and b_2 is the weight coefficient of active power loss.

2) To avoid overload and ensure the security and quality of the power supply, the objective function with uniform load becomes:

$$LB_i = \frac{S_i}{S_i^{\max}} \tag{19}$$

$$LB_{sys} = \frac{1}{n}\sum_{i=1}^{Nb}\frac{S_i}{S_i^{\max}} \quad (20)$$

where LB_i and LB_{sys} are the indices of load balance of branches and the system, S_i denotes the current flow on branch i, $S_i^{\max}$ is the capacity of the unit, and N_b represents the number of branches of the system. Due to the rapid increase in load and slow energy production, the load distribution of distribution networks is very uneven and has many disadvantages for the system, including increased energy consumption, reduced power quality, and overload risk. There are two main means of achieving load balancing. The first tool is to transfer the load between different feeders in the system and the other is to transfer the load between different phases in the feeder.

3.2. Constraints

The constraints of the self-healing reconfiguration algorithm of distribution networks include a set of equality constraints, including power flow constraints, and inequality constraints, including limits on feeder capacity, line current, bus voltage, and transformer overload [28].

a. Capacity limit of the feeder

$$S_j \le S_{j\max} \quad (21)$$

where S_j is the current power on route φ, and $S_{j\max}$ is the maximum power on that route.

b. Line current limit

$$I_{ij} \le I_{ij\max} \quad (22)$$

here, I_{ij} is the current flow on the route ij, and $I_{ij\,max}$ is the maximum current on that route.

c. Bus voltage limit

$$V_{j\min} \le V_j \le V_{j\max} \quad (23)$$

where $V_{j\max}$ and $V_{j\min}$ are the upper and lower limits of the node j voltage.

d. Transformer overload limit

$$S_t \le S_{t\max} \quad (24)$$

S_t is the transformer power, and $S_{t\,max}$ is the maximum power of the transformer.
In the self-healing reconfiguration process, inequality constraints are guaranteed by adding a penalty function to the objective functions.

3.3. Metaheuristic reconfiguration self-healing Algorithm

This part of the paper discusses the metaheuristic reconfiguration self-healing algorithm based on the tree structure.

- Metaheuristic rules

We divide the switches into the following three sets:
Set A: Switches that cannot be closed.
Set B: Switches that cannot be opened.

Set C: Switches that cannot be freely activated.
The following rules of thumb are provided with respect to the characteristics of distribution networks and self-healing reconfiguration requirements:
• Prioritizing operations to the switches connected to the transformer.
• Prioritizing the use of closed-loop switches to the power supply terminal. The situations where the load is connected to the distribution network affects the system loss, and the shorter the distance between the load and the power supply terminal, the less network loss.
• Prioritizing the operation of the lines with the maximum current margin.

3.4. Algorithm procedure

Step 1: First, search and find all the out-of-service areas, calculate the amount of load loss, and mark all the switches in this area.
Step 2: Count the number (defined as n) of loop switches that can be operational and do not belong to set A between the charging region and the out-of-service region. If $n = 0$, this means that there is no way to restore power and terminate the process.
Step 3: If $n \neq 0$ ‘, select a loop switch as the root node according to subjective rules; other nodes in the out-of-service area are formed into a tree according to the connection relationship. Then, according to the distance from the root node, put the numbers in the route of the buses and lines saved by the layer.
Step 4: Close the loop switch and return to Step 1 if the constraints are met.
Step 5: If the constraint is not satisfied, search the tree from the bottom up and open the switches of this layer until the constraint is satisfied, then return to Step 1. If the switches in this layer belong to sets B and C, open only the switches for set C. If the switches in this layer belong to set B, open all. Constraints are removed until the root node's loop switch is turned on, which means the loop switch cannot be closed, so mark it as set A. This algorithm process is also shown in Figure 1.

3.4.1. Self-healing reconfiguration of the distribution network with DGs

DGs generally adopt an active power or voltage control strategy when connected to the grid. When the agent is disconnected from the grid, the voltage/frequency control system is selected. According to different control strategies, DGs can be divided as follows: DGs that can run independently and DGs that cannot. Under the assumption of ensuring the safety of the power system, according to the different types of DGs, when a fault occurs in the distribution networks, the DGs that can operate independently form a controllable island, while the DGs that cannot operate independently are disconnected; the rest of the network is rebuilt using a self-healing reconfiguration method. Figure 2 shows this process.

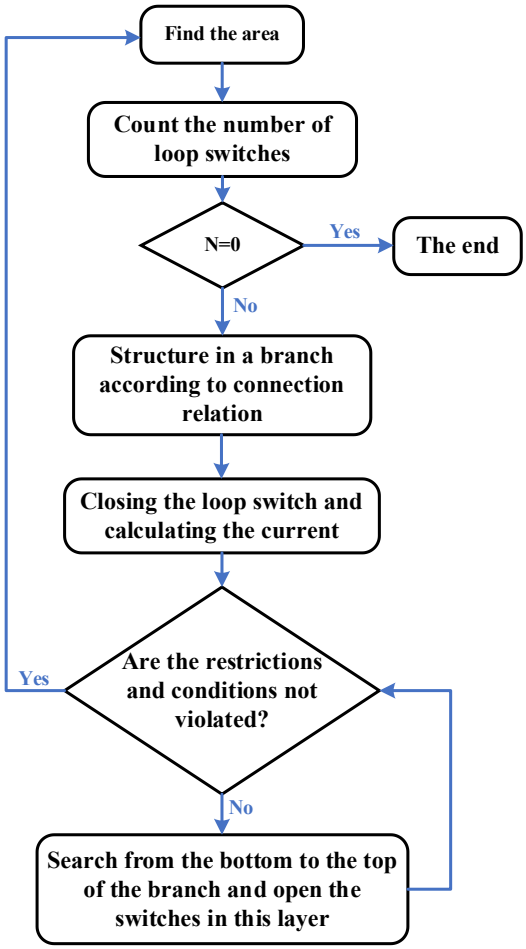

Figure 1. The flowchart of the metaheuristic reconfiguration self-healing algorithm.

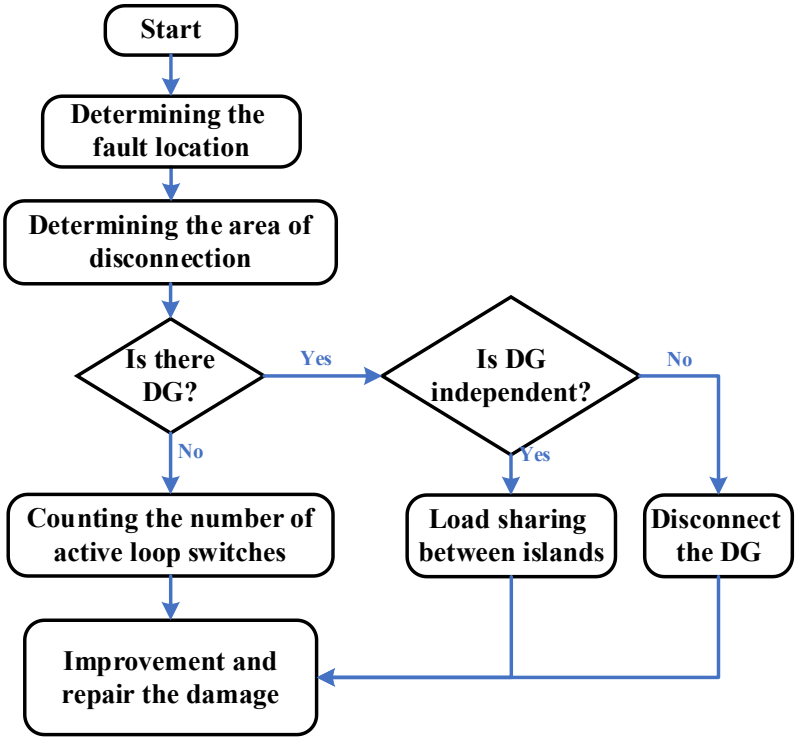

Figure 2. Self-healing reconfiguration of the distribution network with DGs.

An additional limitation of distribution networks with DGs is island power limitation, i.e., the load on an island must be less than the total supply from DG for this island.

$$P_{DG} + \sum_{\phi} P_i \geq 0 \tag{25}$$

where P_{DG} is the output power of the DG in the island, ϕ is the set of islands, and P_i is the loads within the island.

4. Simulation results

4.1. Allocation of DGs to reduce losses

The system under study is the standard IEEE 69-bus system, depicted in Figure 3. The power consumption of buses is 3.8 MW and 2.7 MVar in total, which are fed at a nominal voltage of 12.66 kV, in which case the network loss is equal to 224.98 kW.

Table 1 shows the location and size of energy sources and network losses after optimization. At the end of the optimization process, the global search reaches convergence around the optimal point during the 16th iteration. The utilization of DGs results in a consistent oscillation of the voltage profile around 1 per-unit (p.u.), as depicted in Figure 4. This phenomenon demonstrates a significant enhancement in voltage. Before the installation of DGs, the voltage profile in p.u. shows a significant reduction of 91% at the end of the lines.

To enhance the comparison in Figure 4, the voltage profile is juxtaposed prior to and subsequent to the implementation of energy sources. The addition of a 1.57 MW energy source at the end of the network resulted in a 10% improvement in the voltage profile at that location. Additionally, it should be noted that the storage devices are situated in the same location as the energy sources.

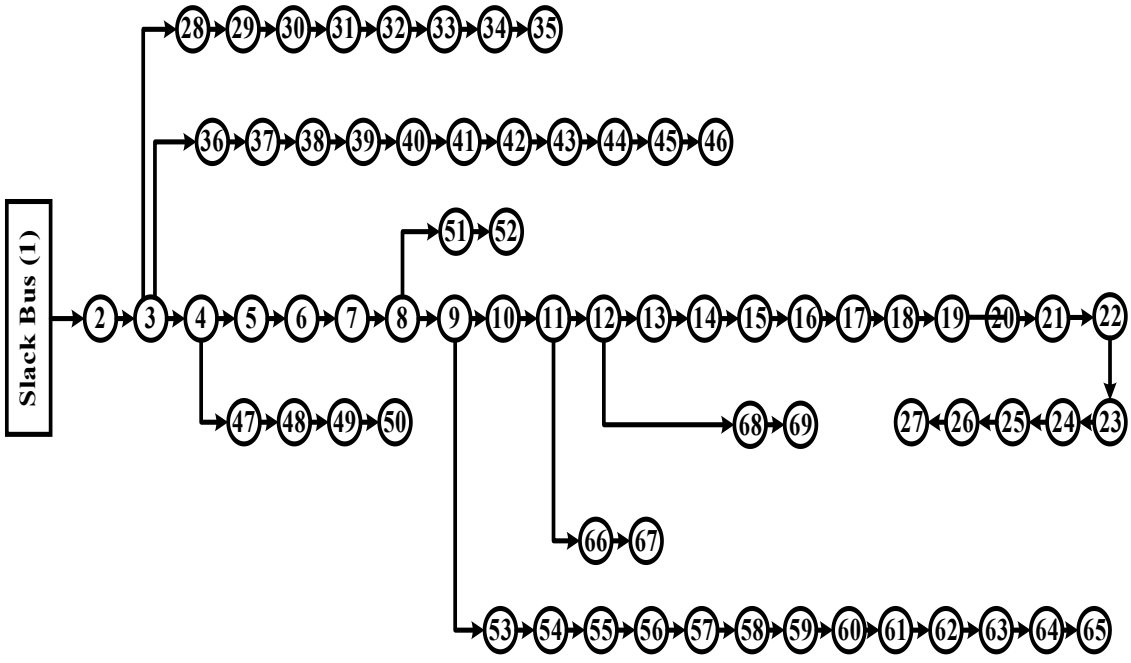

Figure 3. The standard IEEE 69-bus system under study [25].

Table 1. Location and optimal size of energy sources by the PSO method.

No.	Capacity	Location	No. of birds	Iteration s	Loss before installation of sources	Loss after installation of sources
DER 1	1.5766 MW	61	100	20	224.94kW	97.2kW
DER 2	0.46196 MW	17				

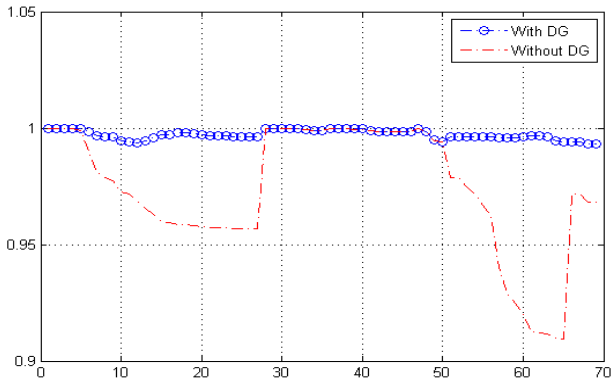

Figure 4. A comparison of voltage profiles before and after installation of DGS in the network.

4.2. Self-healing of the 69-bus distribution network

As previously mentioned, there are several DG protections switches in the vicinity. These switches are designed to open in the event of a fault during islanding. Additionally, there are a set of open switches that can be connected to create secondary and healing routes. In the event of a fault and disconnection of the faulty point, these switches help address any issues that may arise. Power quality, dependability, and stability in the network should not be compromised. While it is possible to define several intricate and diverse structures, the notable benefits of this technology include its rapid self-healing, reduced expenses, and overall simplicity.

Initially, the network is partitioned into 8 sections. Bus 1 to 3 comprise the primary route and do not have any associated load, so they are excluded from this segmentation. Partitioned areas are:

$$Area: [4-27; 28-35; 36-46; 47-50; 51-52; 53-65; 66-67; 68-69]$$

In this scenario, it is feasible to exclude less significant feeders with a low load in order to minimize the costs associated with switching and establishing an alternative route. Here, all feeders are provided with zoning to ensure that they can supply all network loads in case of fault occurrence. This zoning is also depicted in Figure 5. Then all areas are connected to each other through an open switch that can be connected at different points, which are alternative routes for the power of different feeders in case of fault. These switches are defined for different feeders as follows:

$$Disc\ Switches: [27-35; 35-46; 46-52; 27-50; 50-65; 65-68; 67-69]$$

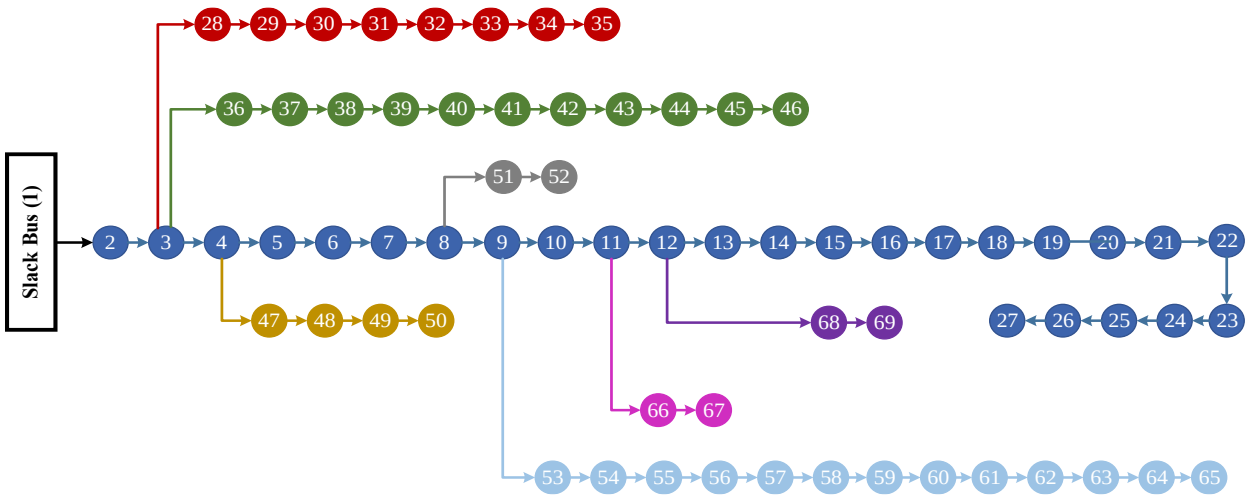

Figure 5. Network zoning.

These routes with connectable switches are also shown in Figure 6. The algorithm outlined below describes a method for finding self-healing. The first step involves identifying the specific area where the fault occurred and the affected consumer. Next, the algorithm checks the number of loop switches in the network. Starting from the fault location, it forms a loop by connecting the switch above the fault and establishes an alternative route. By opening the isolated switch, the data's status is altered, thereby isolating the DG source. This isolation allows for the delivery of load power by disconnecting the DG and connecting the upstream loop switches, enabling power flow. Self-healing is only possible if the voltage and power limits are upheld. In such cases, the self-healing is carried out using the same switch position. However, if the conditions are not met, the upstream switches are altered until the desired conditions are achieved. In order to evaluate the simulation's performance, we introduce a hypothetical fault in bus 28 and then in bus 26. We then calculate the switching cost and maintenance cost using Equation (18) and taking into account the self-healing characteristics of the network.

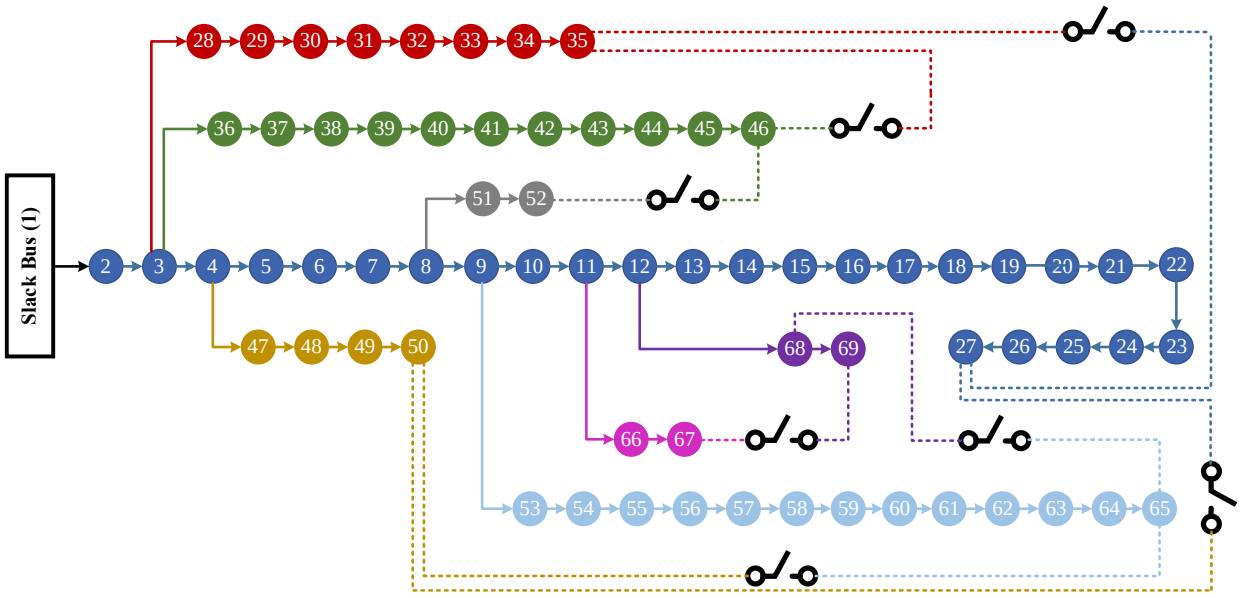

Figure 6. Secondary routes considered for the 69-bus network.

- A fault at bus 28

Given that bus 61 has a substantial load capacity of 1.3 MW, with 0.8 MW accounting for one-third of the overall network load, and the approximate capacity of bus 61 is 1.6 MW, the cost calculation formulation has concluded that in the event of islanding, DG should solely be accountable for supplying power to its own bus load, taking into consideration voltage constraints and the expenses associated with switching. Upon detecting a fault through the sensors and measurement devices, the self-healing network initiates the process of self-healing the network based on the prevailing conditions and the switching cost function. According to the information presented in Table 2, when a fault occurs at bus 28, the bus with DG becomes islanded and the route 65-68 as the first priority with the least total cost and the route 27-35 as the second priority with higher cost are established. The self-healing function is depicted in Figure 7.

- A fault at bus 26

The consideration of bus 26 was only due to the distance of the bus from the slack bus and it was random. An attempt was made to select one of the farthest buses from the slack bus. Considering that the desired method has been validated, the possibility of considering other points for fault is unimpeded. In this case, the self-healing approach is demonstrated in Table 3 and Figure 8, illustrating the performance of this function. When simulating self-healing, it is observed that the self-healing algorithm selects the route with the lowest cost after each fault. This is because, in other tested faults, routes 35-46 or 27-50 were found to have high costs and are not chosen unless low-cost routes are excluded or not taken into account.

Table 2. Self-healing strategy for a fault at bus 28.

Fault	No.	Switch status	Case	Cost
Bus 28	1	61-62 open 60-61 open	Islanded DG	65.7056
	2	65-68 closed 27-35 closed	Power source restoration	

Table 3. Self-healing strategy for a fault at bus 26.

Fault	No.	Switch status	Case	Cost
Bus 26	1	61-62 open 60-61 open	Islanded DG	103.2107
	2	46-52 closed 50-65 closed	Power source restoration	

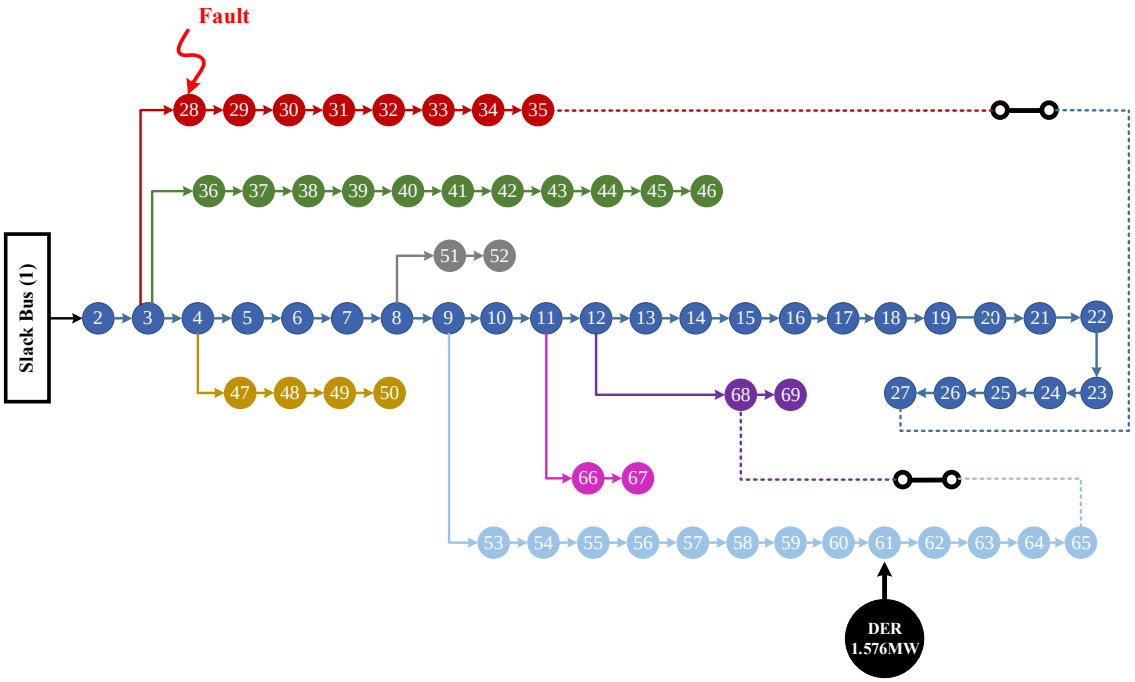

Figure 7. Self-healing performance in the case of a fault at bus 28.

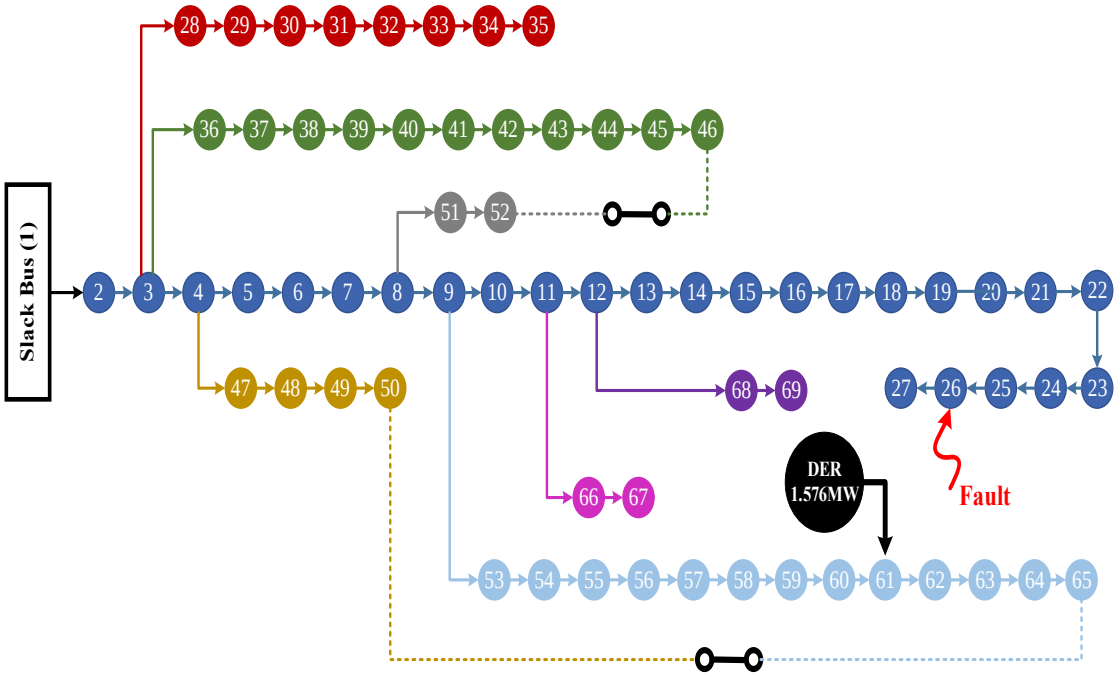

Figure 8. Self-healing performance in the case of a fault at bus 26.

5. Conclusions

This paper presents the design of a self-healing network with high reliability, minimal losses, and an improved voltage profile. The objective is to determine the best placement and capacity for DG units. In order to evaluate the effectiveness of the suggested approach, the algorithm was implemented on the standard IEEE 69-bus network. The simulation results of the self-healing process validated that, apart from selecting the route with the least cost, the algorithm substantially decreased the overall power loss and enhanced the

voltage profile. Moreover, through the implementation of intelligent devices, the network has been optimized, resulting in a highly efficient infrastructure. Additionally, the self-healing capabilities of this smart network have further enhanced its efficiency, minimizing human errors to an almost negligible extent. Consequently, the network's reliability has significantly improved, leaving a remarkable impression. In the end, it should be said that in future studies, the costs related to switches, including purchase, maintenance, and costs related to switching, can be considered in locating distributed generation resources. Also, the hidden costs of distributed generation resources, including the efficiency and switching of power electronic circuits and life span, are items that can be effective in locating the distributed generation resources. As a verification, the location of the fault, the type of fault, and the number of distributed generation sources added to the network can be considered as variables for the next location studies.

References

[1] M. Falah Nezhadnaeini, M. Hajivand, M. Abasi, and S. Mohajerami, "Optimal Allocation of Distributed Generation Units Based on Different Objectives by a Novel Version Group Search Optimizer Algorithm in Unbalance Load System," *Rev Roumaine des Sciences Techniques-Series Electrotechnique et Energetique*, vol. 61, no. 4, pp. 338–342, 2016.

[2] S. M. R. H. Shawon, X. Liang, and M. Janbakhsh, "Optimal Placement of Distributed Generation Units for Microgrid Planning in Distribution Networks," *IEEE Transactions on Industry Applications*, vol. 59, no. 3, pp. 2785-2795, 2023.

[3] M. Abasi, M. Falah Nezhadnaeini, M. Karimi, and N. Yousefi, "A Novel Metaheuristic Approach to Solve Unit Commitment Problem in the Presence of Wind Farms," *Rev Roumaine des Sciences Techniques-Series Electrotechnique et Energetique*, vol. 60, no. 3, pp. 253–262, 2015.

[4] K. Subbaramaiah and P. Sujatha, "Optimal DG Unit Placement in Distribution Networks by Multi-Objective Whale Optimization Algorithm & Its Techno-Economic Analysis," *Electric Power Systems Research*, vol. 214, 108869, 2023.

[5] I. P. Idoko, T. R. Ayodele, et al., "Maximizing the Cost Effectiveness of Electric Power Generation Through the Integration of Distributed Generators: Wind, Hydro and Solar Power," *Bulletin of the National Research Centre*, vol. 47, 166, 2023.

[6] T. H. B. Huy, D. N. Vo, K. H. Truong, and T. Van Tran, "Optimal Distributed Generation Placement in Radial Distribution Networks Using Enhanced Search Group Algorithm," *IEEE Access*, vol. 11, pp. 103288-103305, 2023,

[7] M. Sadeghi, and M. Abasi, "Optimal Placement and Sizing of Hybrid Superconducting Fault Current Limiter to Protection Coordination Restoration of the Distribution Networks in the Presence of Simultaneous Distributed Generation," *Electric Power Systems Research*, vol. 201, 107541, 2021.

[8] M. Pushkarna, H. Ashfaq, et al., "An Optimal Placement and Sizing of Type-IV DG With Reactive Power Support Using UPQC in an Unbalanced Distribution System Using Particle Swarm Optimization," *Energy System,* vol. 15, pp.353-370, 2022.

[9] S.M. Sadeghi, M. Daryalal, and M. Abasi, "Two-stage Planning of Synchronous Distributed Generations in Distribution Network Considering Protection Coordination Index and Optimal Operation Situation," *IET Renewable Power Generation*, vol. 16, no. 11, pp. 2338-2356, 2022.

[10] M. A. Shaik, P. L. Mareddy, and N. Visali, "Enhancement of Voltage Profile in the Distribution system by Reconfiguring with DG placement using Equilibrium Optimizer," *Alexandria Engineering Journal*, vol. 61, no. 5, pp. 4081-4093, 2022.

[11] M. Dashtdar, M. Najafi, et al., "Placement and Optimal Size of DG in the Distribution Network Based on Nodal Pricing Reduction with Nonlinear Load Model Using the IABC Algorithm," *Sadhana*, vol. 47, 73, 2022.

[12] S. Das, O. B. Fosso, and G. Marafioti, "Probabilistic Planning of Distribution Networks with Optimal DG Placement Under Uncertainties," *IEEE Transactions on Industry Applications*, vol. 59, no. 3, pp. 2731-2741, 2023.

[13] B. N. Alajmi, M. F. AlHajri, et al., "Multi-objective Optimization of Optimal Placement and Sizing of Distributed Generators in Distribution Networks," *IEEJ Transactions on Electrical and Electronic Engineering*, vol. 18, no. 6, pp. 817-833, 2023.

[14] S. Mondal, and M. De, "Optimal Allocation and Smart Scheduling of Distributed Energy Resources and Electrical Vehicles to Enhance Economical Operation of Unbalanced Distribution System," *Electrical Engineering*, vol. 105, pp. 3493–3510, 2023.

[15] A. Ahlawat, and D. Das, "Optimal Sizing and Scheduling of Battery Energy Storage System with Solar and Wind DG Under Seasonal Load Variations Considering Uncertainties," *Journal of Energy Storage*, vol. 74, 109377, 2023.

[16] S. Mirsaeidi, S. Li, et al., "A Power Loss Minimization Strategy Based on Optimal Placement and Sizing of Distributed Energy Resources," *International Journal of Numerical Modelling: Electronic Networks, Devices and Fields*, vol. 35, no. 4, 2022.

[17] A. K. Barnwal, L. K. Yadav, and M. K. Verma, "A Multi-Objective Approach for Voltage Stability Enhancement and Loss Reduction Under PQV and P Buses Through Reconfiguration and Distributed Generation Allocation," *IEEE Access*, vol. 10, pp. 16609-16623, 2022.

[18] L. C. Kien, T. T. Nguyen, et al., "A Study on the Placement of Photovoltaic Units in the North and South of Vietnam for Energy Loss Reduction by Using a Proposed Slime Mould Algorithm," *Neural Computing and Applications*, vol. 35, pp. 23225–23247, 2023.

[19] Y. Li, and H. Cai, "Improving Voltage Profile of Unbalanced Low-Voltage Distribution Networks via Optimal Placement of Single-Phase Distributed Generation and Shunt Capacitors," *International Journal of Electrical Power & Energy Systems*, vol. 137, 107799, 2022.

[20] M. Abasi, M. Joorabian, A. Saffarian, and S. G. Seifossadat, "A Comprehensive Review of Various Fault Location Methods for Transmission Lines Compensated by FACTS Devices and Series Capacitors," *Journal of Operation and Automation in Power Engineering*, vol. 9, no. 3, pp. 213-225, 2021.

[21] M. Abasi, A. Saffarian, M. Joorabian, and S. G. Seifossadat, "Location of Double-Circuit Grounded Cross-Country Faults in GUPFC-Compensated Transmission Lines Based on Current and Voltage Phasors Analysis," *Electric Power Systems Research*, vol. 195, 107124, 2021.

[22] M. Abasi, A. Torabi Farsani, A. Rohani, and M. Aghazadeh Shiran, "Improving Differential Relay Performance During Cross-Country Fault Using a Fuzzy Logic-based Control Algorithm," *5th Conference. on Knowledge-Based Engineering and Innovation (KBEI)*, Iran, 2019.

[23] M. Abasi, A. Torabi Farsani, A. Rohani, and A. Beigzadeh, "A Novel Fuzzy Theory-Based Differential Protection Scheme for Transmission Lines," *International Journal of Integrated Engineering*, vol. 12, no. 8, pp. 149-160, 2020.

[24] M. Abasi, N. Heydarzadeh, and A. Rohani, "Broken Conductor Fault Location in Power Transmission Lines Using GMDH Function and Single-Terminal Data Independent of Line Parameters," *Journal of Applied Research in Electrical Engineering*, vol. 1, no. 1, pp. 22-32, 2021.

[25] B. Liu, Z. Yuan, and H. Bao, "Intelligent Optimization Algorithm for the Locating and Sizing of Distributed Generation Planning," *China International Conference on Electricity Distribution (CICED)*, pp.1-6, 2010.

[26] M. H. Moradi and M. Abedini, "A Combination of Genetic Algorithm and Particle Swarm Optimization for Optimal DG Location and Sizing in Distribution Systems," *International Journal of Electrical Power & Energy Systems*, vol. 34, no. 1, pp. 66-74, 2012.

[27] D. Li, S. Wang, J. Zhan, and Y. Zhao, "A Self-Healing Reconfiguration Technique for Smart Distribution Networks with DGs," *International Conference on Electrical and Control Engineering (ICECE)*, pp. 4318-4321, 2011.

[28] J. Moshtagh, and S. Ghasemi, "Optimal Distribution System Reconfiguration Using Nondominated Sorting Genetic Algorithm (NSGA-II)," *Journal of Operation and Automation in Power Engineering*, vol. 1, no. 1, pp. 12-21, 2013.

Declaration of Competing Interest

The authors declare that they have no known competing financial interests or personal relationships that could have appeared to influence the work reported in this paper. The ethical issues, including plagiarism, informed consent, misconduct, data fabrication and/or falsification, double publication and/or submission, redundancy, have been completely observed by the authors.

Credit Authorship Contribution Statement

Ali Kazemi: Conceptualization, Formal analysis, Investigation, Methodology, Roles/Writing - original draft, Writing - review & editing. **Ali Morsagh Dezfuli:** Conceptualization, Resources, Methodology, Roles/Writing - original draft, Writing - review & editing.

Bibliography

Ali Kazemi received his B.Sc. and M.Sc. degrees in Electrical Engineering (Power Systems) from Islamic Azad University, Sari branch, Sari, Iran, in 2009 and 2015, respectively. His fields of interest include smart grids, distribution networks, renewable energies, and system operation. Currently he is working as an adjunct professor at Department of Electrical and Computer Engineering, Technical and Vocational University (TVU), Mazandaran, Iran.

Ali Morsagh Dezfuli was born in Dezful, Iran in 1992. He received the B.Sc. degree from the Jundi-Shapur University of Technology of Dezful, Dezful, Iran in 2015, the M.Sc. degree from the Shahid Rajaee Teacher Training University of Tehran, Tehran, Iran in 2017 and he is a PhD candidate at Shahid Chamran University of Ahvaz, Ahvaz, Iran all in Power Electrical Engineering. His research interests are: Voltage and Frequency Control of Microgrid, Power Electronics, FACTs Devices and Power System Protection.

Journal of Green Energy Research and Innovation

The Impact of Wind Direction on Wind Farms' Output Power and Income

AliAsghar Karimi Taleb, Hojatollah Makvandi, Ashknaz Oraee

Highlights

- Modifying The quadratic power curve equation
- The derivation of new parameters for predicting the output power of a WT
- Wind direction and its variation for predicting power and income of a WT
- Proposing a new approach to study the wind power potential of a region

Graphical Abstract

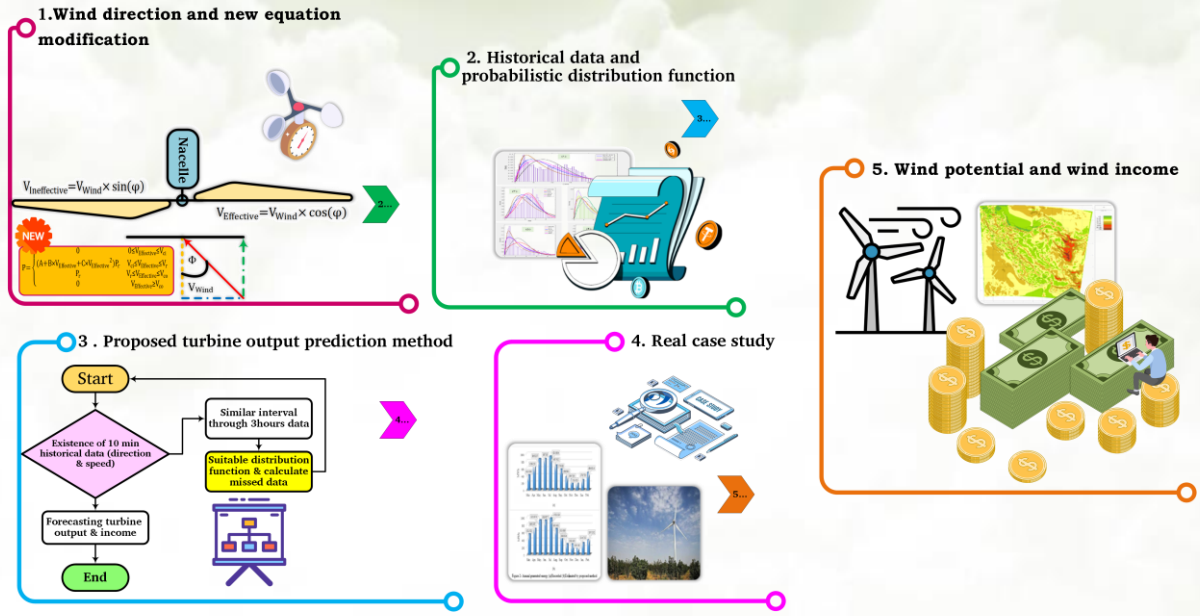

Use your device to scan and read the article online

Citation

A. A. Karimi Taleb, H. Makvandi, and A. Oraee " The Impact of Wind Direction on Wind Farms' Output Power and Income," *Journal of Green Energy Research and Innovation*, vol. 1, no. 1, pp. 34-47, 2024.

https://doi.org/10.61186/jgeri.1.1.34

JGERI Journal of Green Energy Research and Innovation

Online ISSN: 3041-9018

Journal of Green Energy Research and Innovation

Journal Homepage: www.jgeri.araku.ac.ir

The Impact of Wind Direction on Wind Farms' Output Power and Income

Ali Asghar Karimi Taleb [1]*, Hojatollah Makvandi [2], Ashknaz Oraee[3]

[1] *Khuzestan Water and Power Authority, Ahvaz, 613481395, Iran.*
[2] *Abadan Oil Refining Company, Abadan, Iran.*
[3] *Faculty of Electrical and Medical Engineering, Sadjad University of Technology, Mashhad, Iran.*

* ***Corresponding Author:*** *a.karimii.t@gmail.com*

ARTICLE INFO

Keywords:
Wind energy,
Wind speed prediction,
Wind turbine,
Wind farm income.

Article history:
Received: 26 November 2023;
Revised: 10 January 2024;
Accepted: 21 January 2024;

Article type:
Research Article

ABSTRACT

The main methodology in every wind power prediction model involves converting wind speed into power using the power output curve of the wind turbine. However, preceding studies that have introduced models for such curves have not considered the impact of wind direction and its recurring fluctuations over time on predicting wind turbine power output. The main focus of these studies has just been on the magnitude of wind speed and the relationship between wind speed and turbine power. The present study models the effect of wind direction on wind turbine power output and uses it to modify the quadratic power curve equations. Using these modified equations and considering the turbine mechanism to follow the wind direction, a method is presented for predicting wind turbine power output under frequent changes in wind direction over time. To deal with the lack of access to long-term and high-resolution wind data, registered historical data and probabilistic distribution functions are used to produce lost data with software. To demonstrate the efficacy of the suggested approach, the real data recorded for a 1.5 MW turbine installed in Khaf in Razavi Khorasan, Iran, are used as a case study. Finally, the potential wind power and potential income of the four windy regions in Iran were assessed based on the payment mechanism of the Organization of Renewable Energy and Electricity Efficiency of Iran, assuming the same installed capacity. The effect of wind direction and its variations over time, which can affect power output of wind turbine and income, is the main focus of this section of paper.

1. Introduction

With the increase in the effect of wind power in power systems, new challenges have emerged due to wind energy variability and uncertainty [1, 2]. A precise prediction of the power generation of a wind farm (WF) is a great help in dealing with these challenges [3]. Transforming wind speed to wind power using a wind turbine power curve (WTPC) is the main approach of wind power prediction models. In the past decades, there has been increasing interest in the WTPC as a part of wind energy research [4, 5]. The power generation of a wind turbine (WT) is influenced by various factors, including wind speed, wind direction, air density (determined by temperature, pressure, and humidity), and

turbine settings [6]. Properly assessing the effects of all the influencing parameters involves significant intricacy. The WTPC, which represents the turbine's power output at a given wind speed, offers a practical method for modeling the performance of WTs [7]. The approaches for modeling power curves can be categorized as discrete, deterministic/probabilistic, parametric/nonparametric, and stochastic methods. Alternatively, they can be classified based on the data utilized for modeling [8]. Generally, it is preferred to use the general equation in WTPC modeling in wind energy potential studies. The parametric methods rely on solving mathematical model equations, and nonparametric methods have been adopted to discover how input data of wind and turbine power output are interrelated [6]. Authors in [9] introduced parametric modeling's of the WTPC constructed using four and five-parameter logistic equations. The parameters of these expressions were determined by sophisticated methods such as genetic algorithm (GA), evolutionary programming (EP), particle swarm optimization (PSO), and differential evolution (DE). A comparative analysis was conducted to examine several approaches for mathematically modeling WTs, specifically focusing on three WTs that are currently available in the market. The analysis utilized an algorithm developed and described in reference [10]. In their study, authors in [11] suggested incorporating operational data from WTs to generate bivariate probability distribution functions that may accurately describe the power curve of existing turbines. This approach enables the detection of any deviations from the expected behavior. The utilization of empirical copulas is suggested. The statistical concept of copulas enables the individual distribution shape of wind speed and power to be described independently from the information regarding their interdependence. The study conducted by [12] involved the utilization and comparison of three distinct machine learning models: a self-supervised neural network known as Generalized Mapping Regressor (GMR), a feed-forward Multi-layer Perceptron (MLP), and a General Regression Neural Network (GRNN). The objective was to estimate the correlation between wind speed and power generation in a WF. Precise representations of power curves are crucial for predicting power output and conducting real-time monitoring of turbines.

Several methodologies have been suggested in different studies to simulate WTPCs. Many academics have employed these methods, which involve adopting data from manufacturers' specifications and actual data from WFs in a range of wind power applications [13]. Choosing the proper power curve models can enhance the efficiency of wind energy systems [14]. The most recent approach employed in papers involves the use of Sigmoid models, which are characterized using a comprehensive expression comprising several parameters. Currently, two types of models are being utilized, namely exponential models (EM) and algebraic models (AM) [15, 16]. WTPCs clearly illustrate the correlation between wind speed and the amount of electrical power generated by a WT. The manufacturers offer them as the primary choice, and they can also be presented in a tabular style using pairs of values [17]. Researchers commonly believe that in a horizontal axis WT (HAWT), the turbine will generate a specific amount of power when the wind speed is recorded directly in front of its hub [18, 19]. Alternatively, the

manufacturers can provide a graph that allows the derivation of such value pairs by observation. Stakeholders and promoters can utilize these values to determine both the anticipated power output and the energy value that a specific WT can harness from the wind. The only additional information required is the probability distribution of wind speeds at the location in question. The International Electrotechnical Commission (IEC) has provided a defined technique for establishing curves in its paper IEC-61400-12-1 [20]. In this fashion, the measured WTPC is commonly obtained by applying the so-called method of bins for the normalized data sets. In practical applications, WTs and, consequently, WFs encounter operating conditions that deviate from the ideal conditions observed in controlled environments such as manufacturer laboratories and wind tunnels where WTPCs are assessed. Within a WF, WTs are typically exposed to various conditions, influenced by factors such as air temperature, moisture, turbulence caused by phenomena like the wake effect and shear effect, the presence of ice, reduced performance due to aging, and other potential factors [21]. The modeling of WTPC is crucial in various analysis applications, research endeavors, and software tools due to the need to handle such curves. The WTPC models have diverse and extensive uses. They can also be used to determine a WF's suitable position and arrangement [22] and examine the impact of external influences [23, 24].

Previous studies have just used the magnitude of the wind velocity vector and the relationship between velocity and power to estimate turbine power output. None of these studies have considered the effect of wind direction and its repeated variations over time in calculating the turbine power output. This paper models the wind direction and uses it to modify the quadratic power curve equations, which is the most widely used method for estimating WT power output. The contributions of the article are as follows:

- Modifying the quadratic power curve equation
- Deriving new parameters for predicting a WT output power
- Considering wind direction and its variations in predicting the power output of a WT and farm income
- Proposing a novel method to study the wind power capacity of a region

This part describes the organization of the paper. Section 2 describes the model. Next, Section 3 tests the proposed methodology on the WT of Khaf, Iran, to show its effectiveness and discusses the results thoroughly. Finally, the conclusions and perspectives for future work are provided in Section 4.

2. Model Analysis

2.1. Modified quadratic power curve

As already stated, the quadratic power curve (QPC) is the method most commonly used to estimate the power output of a WT [25, 26] based on the wind velocity's magnitude. Wind direction and its variations are not considered in the quadratic power curve.

Variability is inherent to wind, which strongly affects the power output of a WT. Wind direction changes even within seconds. Therefore, regardless of the wind direction, its variations cause a great deal of error in estimating WT power output, so it needs to be included in these calculations. The perpendicular component of wind velocity to the plate of the turbine blades is the factor that rotates the turbine blades. As shown in Figure 1, if the wind angle with the line perpendicular to the plate of the turbine blades is φ, then Vwind × cosφ and Vwind × sinφ are two components of Vwind. Vwind cosφ is the vertical component that rotates turbine blades and is called VEffective, which should be modified based on QPC equations. The modified form (MQPC) is shown in Equation (1).

In these equations, V_{ci}, V_{co}, V_r, P_r, and P are the cut-in speed, cut-out speed, rated speed, rated power, and estimated turbine power, respectively. In Equation (1), $V_{Effective}$ is not the size of the wind speed. This variable is the perpendicular component of the wind velocity to the plate of turbine blades, named effective wind speed ($V_{Effective}$). $V_{Effective}$ rotates the turbine's blades. Another important point to mention in Equation (1) is that when the wind direction is taken into account, $V_{Effective}$ changes in the intervals of Equation (1). For example, regardless of the direction of the wind, at a given time, if the wind speed was within the range between the nominal speed and the cut-in speed, the turbine power output could be calculated by using the polynomials in Equation (1), which is greater than zero.

On the other hand, by considering the wind direction, given that $cos\varphi$ is smaller than 1, $V_{Effective}$ will be lower than the wind speed ($|V_{wind}|$), and it may also be lower than the cut-in speed. So, the power output will be zero. Another instance is when the wind speed is higher than the cut-out speed. If the wind direction was not considered, the power output would be equal to zero. However, if the wind direction is taken into account, the effective wind speed ($V_{Effective}$) may be lower than the cut-out speed, so the turbine power output will be equal to the rated power. The parameters *A, B*, and *C* are the same in both QPC and MQPC because they depend on the turbine's construction and are independent of the regional wind's characteristics.

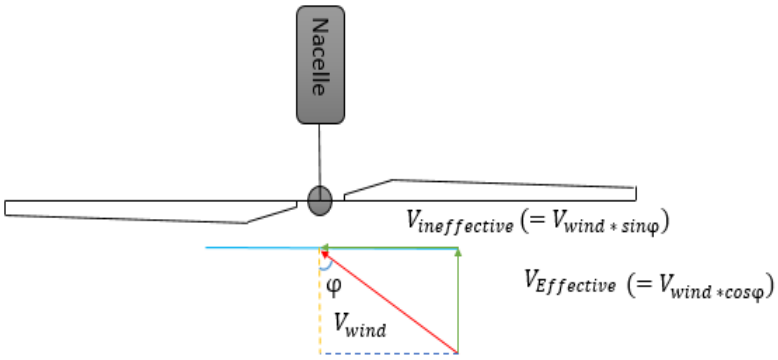

Figure 1. Wind speed components.

$$P = \begin{cases} 0 & 0 \le V_{Effective} \le V_{ci} \\ (A + B \times V_{Effective} + C \times V_{Effective}{}^2)\, P_r & V_{ci} \le V_{Effective} \le V_r \\ P_r & V_r \le V_{Effective} \le V_{co} \\ 0 & V_{Effective} \ge V_{co} \end{cases} \quad (1)$$

$$A = \frac{1}{(V_{ci} - V_r)^2}[V_{ci}(V_{ci} + V_r) - 4V_{ci}V_r(\frac{V_{ci} + V}{2V_r})^3]$$

$$B = \frac{1}{(V_{ci} - V_r)^2}[4(V_{ci} + V_r)(\frac{V_{ci} + V}{2V_r})^3 - (3V_{ci} + V_r)]$$

$$C = \frac{1}{(V_{ci} - V_r)^2}[2 - 4(\frac{V_{ci} + V}{2V_r})^3]$$

2.2. The proposed method for predicting WT power output

This paper proposes a method for predicting turbine output, focusing on the effect of wind direction and its variations on WT output power. In the proposed method, the turbine mechanism in tracking the wind direction is the most important factor, a factor not considered in previous studies. Furthermore, the proposed method includes the turbine's monthly stop period for turbine services, grid errors, turbine start-up, etc., in power calculations.

The turbine mechanism in following the wind direction depends on turbine technology and operator setting, which varies for each turbine and site. The wind tracking mechanism of WT aims to set the blades' plate in a direction perpendicular to the wind, thereby increasing the effective wind speed. This will highly increase the power output of the turbine. The settings considered in how to follow the wind direction and turbine yawing in the present work are as follows:

Yaw velocity: yaw velocity is one of the most important characteristics of a turbine. The faster the yaw speed is, the faster the turbine will follow the wind's direction. So, the turbine will have a shorter time deviation angle with the wind direction, which increases the power output.

Maximum yaw error: Due to mechanical considerations and to avoid the reduction in the useful life of the turbine, turbines should not yaw in small changes of yaw angle. The maximum angle between wind velocity and the line perpendicular to the blades' plate that the turbine does not yaw is called maximum yaw error.

Yaw lag: Due to variations in wind direction at certain times, the yawing system waits a while until the wind stabilizes. This delay is yaw lag.

Maximum angle: In some sudden and momentary changes in wind direction that are very large, it is technically and economically better that the turbine does not yaw. The

maximum yaw angle that the yaw system works is called the maximum angle. If the angle between the wind direction and the line perpendicular to the blades' plate (yaw angle) gets larger than the maximum angle, the turbine will turn off, and it should be driven under favorable conditions.

Launch time: For various reasons, such as annual maintenance and $V_{Effective}$ higher than the cut-out speed, the WT will be switched off. When launching, the power output becomes zero, which is considered in the proposed method.

Simulation steps of the proposed method: To estimate turbine power output, wind speed and wind direction data are first predicted for a desired time period (e.g., 1 year) at appropriate time intervals (e.g., 10 minutes). Then, in order to obtain the power output in each interval, the wind speed and the direction variations of the wind to the previous interval are used. At last, $V_{Effective}$ is obtained, and the power output is calculated using Equation (1) and according to the turbine yawing setting. In the yaw lag period, the wind direction variations are considered for some next intervals, and if the wind direction variations are unstable, the turbine does not yaw. If the wind direction change is greater than the maximum angle, in addition to turning off the turbine, a launch time is also considered. Another important point in simulating is when the yaw angle exceeds the maximum yaw error. In this situation, the turbine yaw system should follow the wind direction to increase power output. In this case, by considering yaw velocity (φ rad/s), $V_{Effective}$ is calculated, and by using MQPC equations, the power output of WT is calculated. Finally, by adding the power output in each second, the average power output in each interval is calculated. Disconnected periods due to turbine maintenance and grid errors are also considered.

2.3. Wind speed and wind direction data

A challenge in WT power output studies is the lack of access to long-term and high-resolution wind data (e.g., 10 minutes). Therefore, for an acceptable result, the wind data must be completed or produced for an appropriate time period. In the Organization of Renewable Energy and Electricity Efficiency of Iran's (SATBA) website [27], incomplete wind speed and direction data are available at 10-minute intervals for different regions. Therefore, wind data should be completed over a proper interval for more accurate analysis and proper study.

For this purpose, the 3-hour resolution wind speed data and wind direction in a longer interval (e.g., 15 years) provided by Iran's Meteorological Organization, the MATLAB software, and wind speed and wind direction characteristics (such as the relationship between speed variations and wind direction with height) were used. So, 3-hour synoptic data of wind speed and direction were first analyzed, and the trend of wind speed and wind direction variations was studied. The time periods with the same trends in a year were identified. To complete wind data for intervals without any information, the time period of the intervals was first identified. Secondly, similar time intervals with registered data were detected. Now, to produce wind data for intervals with no recorded data, the most suitable distribution function was chosen among the most widely used probabilistic

distribution functions, including Rayleigh, Normal, Logarithmic Normal, and Gamma, by using MATLAB software and its most suitable fitted parameters were calculated. Using the probability distribution obtained, wind speed and wind direction data were produced for intervals without recorded data. In addition to finding similar intervals, wind directional features were adopted to complete wind data.

At varying heights, the direction of the wind does not change, and these changes can be ignored. Furthermore, according to the study area, the direction of the wind had similar orientations during certain periods of the year. By considering these wind characteristics, one-year wind data were completed in different areas.

2.4. Cost calculation for generated wind power in Iran

In Iran, the government guarantees the purchase of the generated renewable energy. A 20-year warranty contract is made between SATBA and wind energy producers for wind energy. SATBA monthly pays for wind energy produced. According to the government's decree on February 10, 2016, the purchasing base rate of guaranteed wind power for WFs with a capacity of more than 50 megawatts and equal to or less than 50 megawatts is set at 3400 and 4200 Rials per kilowatt-hour, respectively.

SATBA's method for calculating the price of produced energy per hour is as follows:

- Equivalent production = Pure hourly production * CPF (Cost of Preparation Factor)
- New purchasing rate = Contract purchasing rate * Adjustment factor
- Price of energy produced per hour = New purchasing rate * Equivalent production

In these equations, CPF is a coefficient given by Iran's Grid Management Co. (IGMC) every hour of the day. This coefficient varies for different hours of the day and for days, weeks, and months of the year. In fact, this coefficient is used to pay the cost of being ready to produce wind power to the producer. Pure hourly production refers to the wind energy generated per hour in kilowatt-hours. The contract purchasing rate is equal to the rate quoted in the contract between SATBA and the wind energy producer, and the adjustment factor is used to compensate for the effects of currency depreciation and inflation.

In this study, the adjustment coefficient is ignored since the aim is to compare the wind energy produced in one year. For this study, CPF from June 21, 2016 to June 21, 2017, which are available on IGMC's website, was used [28].

3. Case Study and Results

This study used the real data of a 1.5 MW WT installed by the Behin Ertebat Mehr Co. in Khaf as a case study. The installed turbine is a WD77-1.5MW model of WINDEY Company, with a cut-out speed, cut-in speed, and nominal speed of 25, 3, and 11 m/s, respectively, and a tower height of 80 meters. The simulation used the recorded data in 10-minute intervals of the average wind speed and direction at an 80-meter height at Khaf farm. Also, the settings for tracking the turbine based on information from the Khaf turbine are as follows:

Yaw velocity: 0.47 degrees per second

Maximum yaw error: 5 degrees

Yaw lag: 4 minutes

Maximum angle: 80 degrees

Launch time: 2 minutes

3.1. Forecasting output power for a 1.5 MW WT

Figure 2a displays the recorded monthly data of generated energy. According to this data, the total annually generated energy is 6653.031 MWh. Without considering wind direction and its variation and using QPC equations, the common method of previous studies, the estimated generated energy would be 7568.794 MWh. Figure 2b shows the monthly estimated generated energy using Equation (1) and the proposed method. According to this estimated data, the total annually generated energy is 6833.365 MWh. The results for annually generated energy in various modes are presented in Table 1. Accordingly, without wind direction calculations, the estimated power output will highly deviate from the actual generated power (about 14%). In fact, the energy generation estimated by this method (without considering wind direction and generation interruption) is the maximum energy that the turbine can generate, in which the wind is assumed to be perpendicular to the turbine plate at all moments, and there are no failures or interruptions for the turbine. The results on the proposed approach are very close to the real power output of the WT so that the difference is only about 2.5%, which is a relatively small error. This low error indicates the efficacy of this approach. Moreover, the energy generated by the proposed method, regardless of the interruption effect, is also calculated, representing the impact of the wind direction on the turbine power output calculations.

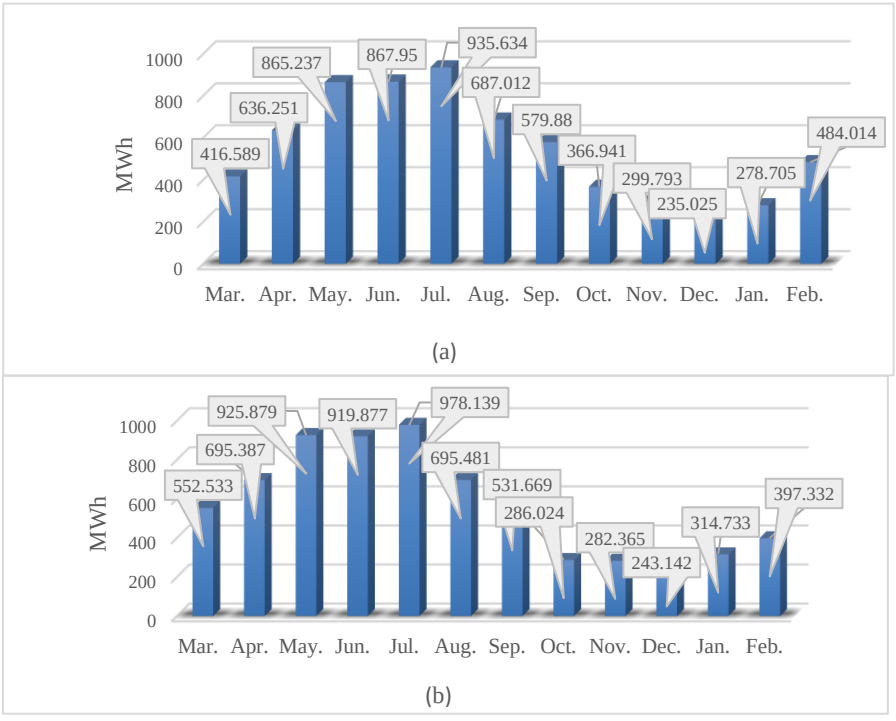

Figure 2. Annually generated energy: (a) recorded and (b) estimated by the proposed method.

Table 1. Annual energy generation and estimated error in each scenario.

Estimated data			Recorded data	
Without turbine direction	Including wind direction and turbine interruption	Including wind direction without turbine interruption		
5768.794	6822.561	7105.094	6653.031	**Annual generated energy (MWh)**
13.76	2.55	6.79	-	**Error (%)**

3.2. Interactive effect of wind direction and speed on wind power production

The difference between the two conventional methods and the proposed method, without considering the variations in wind direction in the calculation of produced energy of the Khaf turbine, indicates the effect of wind direction variations. Table 2 presents this difference (as a percentage of the real energy produced in each month) and the average wind speed. Wind power generation is highly sensitive to wind speed. Hence, it is expected that the higher the wind speed, the higher the generated power. However, the evaluation of Figure 2 and Table 2 indicates interesting results. The output power is low in October and November despite high average wind speed. The reasons for the low power generation in these two months can be found in Table 2, which shows that wind direction variations are very high in these two months. The high wind direction variations reduce wind power production despite the high wind speed in these months. These calculations show the significant role of wind direction and variations in WT power output. The important conclusion is that to potentiate the wind power of an area, one should not only evaluate wind average speed but also consider wind direction and its changes over time. This factor is not only effective but also decisive.

Table 2. The difference in the estimated energy between the proposed method and the conventional method in Khaf.

Month	Ave. wind speed (m/s)	Diff. in estimated energy (%)
Mar.	6.2	9.82
Apr.	7.5	4.46
May.	8.5	1.96
Jun.	11.2	0.77
Jul.	13.5	0.89
Aug.	15.2	5.75
Sep.	15.0	11.57
Oct.	14.7	26.28
Nov.	10.2	12.87
Dec.	9.6	16.52
Jan.	6.4	14.58
Feb.	6.2	8.55

3.3. Estimating energy generation and WF income in Iran

This section analyzes the energy production and income of an identical WF (identical in installed capacity and turbines) in four regions of Iran, including Manjil, Kahak, Binalood, and Khaf. These WFs are located in Gilan, Qazvin, Khorasan Razavi, and Khorasan Razavi provinces, respectively. These zones are the only areas in Iran where WFs have been built. Among these areas, Khaf in Khorasan Razavi is an exceptional zone in terms of potential wind energy. These zones are analyzed using the previous method (without considering wind direction) and the method proposed in this paper (without considering interruption in energy production).

For this purpose, data on wind speed and direction at a height of 40 meters and in 10-minute intervals are used. Moreover, the identical WF consists of 66 × 1.5 MW turbines (turbines with the same characteristics as the Khaf turbine). So, the total capacity of WF is 99 MW. In this calculation, the effect of turbines on each other is ignored, and the wind speed and direction of the whole site are assumed to be identical for all turbines. Table 3 summarizes the results.

Table 3. Annually generated energy and income of a 99MW WF.

		Khaf	Manjil	Binalood	Kahak
Previous Method	Net Production (GWh)	459.186	361.918	370.396	306.424
	Equivalent Production (GWh)	499.723	357.641	412.362	359.761
	Income (Billion Toman)	169.906	121.598	140.203	122.319
Proposed Method	Net Production (GWh)	407.290	319.092	339.355	254.167
	Equivalent Production (GWh)	449.063	313.537	381.085	299.544
	Income (Billion Toman)	152.682	106.602	129.569	101.845
Diff. (Billion Toman)		17.224	14.996	10.634	20.474

According to Table 3, the difference in energy production and revenue calculated for the two methods are the highest in Kahak and the lowest in Binalood due to wind direction variations in these areas.

Most of the Kahak WF production is during peak demand hours. So, CPF is often higher than 1, so its equivalent production is significantly higher than its net production. Therefore, although Kahak WF's net production is much lower than that of the other areas, its income is appropriate. Unlike Kahak WF, just a fraction of Manjil wind production is during grid peak hours.

Therefore, CPF is often lower than 1, and its equivalent production is significantly lower than its net production. So, although Manjil WF's net production is appropriate, its income is not that good. Khaf and Binalood WF's equivalent production is 10.26% and 13.20%, respectively, which is higher than net production due to the predominance of CPFs greater than one.

4. Conclusions

A precise prediction of the power output of a WF is a great help in facing the variability and uncertainty of wind energy. The present work modified the quadratic power curve equation according to wind direction and its variation. Using the modified quadratic power curve equation and yawing system of WT, a method was developed for predicting the power output of a WT. To solve the problem of the lack of access to data on long-term and high-resolution wind speed and wind direction, historical data and probabilistic distribution functions were used to produce wind data for intervals with no recorded data.

In this method, wind direction and its variation were considered. The suggested method was applied to the actual recorded values, and the results supported the efficiency of the proposed method. Also, they showed a significant impact of the wind direction and its variations on the turbine power output. Another important result of this study is that to study the potential wind power of an area, besides wind speed, the wind direction and its variations over time should be taken into account.

The potential wind power of the four regions of Manjil, Khaf, Binalood, and Kahak was estimated based on the proposed methodology and considering the common effect of wind speed and direction. It was determined that the Khaf zone had a great potential wind power. On the other hand, despite the high average wind speed in the Kahak zone, the potential wind power was lower than that of the other regions due to high wind direction variations.

The correlation between wind power production and grid peak hours was another main result of this study, which highly influences WF income. So, WFs that are more productive at the grid peak hours can earn more because of applying CPF greater than one. In this regard, among the studied regions, Kahak is the best. But, Manjil has the worst situation among the four studied areas.

Future researchers are recommended to consider the effect of wind direction on reliability indices. It is also suggested to model wind direction and its variations in various methods for predicting wind power, both parametric and nonparametric. Furthermore, it is advised to employ the proposed methodology to investigate the potential of wind power in a particular region.

References

[1] F. Bilendo, H. Badihi, N. Lu, P. Cambron, and B. Jiang, "An Intelligent Data-Driven Machine Learning Approach for Fault Detection of Wind Turbines," *in 2021 6th International Conference on Power and Renewable Energy (ICPRE)*, pp. 444-449, 2021.

[2] M. F. Nezhadnaeini, M. Hajivand, M. Abasi, and S. Mohajeryami, "Optimal Allocation of Distributed Generation Units Based on Two Different Objectives by A Novel Version Group Search Optimizer Algorithm in Unbalanced Loads System," *Rev Roumaine des Sciences Techniques-Series Electrotechnique et Energetique,* vol. 61, no. 4, pp. 338–342, 2016.

[3] M. Abasi, M. Joorabian, A. Saffarian, and S. G. Seifossadat, "A Comprehensive Review of Various Fault Location Methods for Transmission Lines Compensated by FACTS Devices and Series Capacitors," *Journal of Operation and Automation in Power Engineering*, vol. 9, no. 3, pp. 213-225, 2021.

[4] X. Jin, Z. Xu, and W. Qiao, "Condition Monitoring of Wind Turbine Generators Using Scada Data Analysis," *IEEE Transactions on Sustainable Energy*, vol. 12, no. 1, pp. 202-210, 2020.

[5] M. Sadeghi, and M. Abasi, "Optimal Placement and Sizing of Hybrid Superconducting Fault Current Limiter for Protection Coordination Restoration of The Distribution Networks in The Presence of Simultaneous Distributed Generation," *Electric Power Systems Research*, vol. 201, 107541, 2021.

[6] C. Carrillo, A. F. Obando Montano, J. Cidras, and E. Diaz-Dorado, "Review of Power Curve Modelling for Wind Turbines," *Renewable and Sustainable Energy Reviews*, vol. 21, pp. 572-581, 2013.

[7] M. Abasi, A. T. Farsani, A. Rohani, and M. A. Shiran, "Improving Differential Relay Performance During Cross-Country Fault Using a Fuzzy Logic-Based Control Algorithm," *in 2019 5th Conference on Knowledge Based Engineering and Innovation (KBEI)*, pp. 193-199, 2019.

[8] M. Abasi, M. Falah Nezhadnaeini, M. Karimi, and N. Yousefi, "A Novel Metaheuristic Approach to Solve Unit Commitment Problem in the Presence of Wind Farms," *Rev Roumaine des Sciences Techniques-Series Electrotechnique et Energetique*, vol. 60, no. 3, pp. 253–262, 2015.

[9] M. Lydia, A. I. Selvakumar, S. S. Kumar, and G. E. P. Kumar, "Advanced Algorithms for Wind Turbine Power Curve Modeling," *IEEE Transactions on Sustainable Energy*, vol. 4, no. 3, pp. 827-835, 2013.

[10] V. Thapar, G. Agnihotri, and V. K. Sethi, "Critical Analysis of Methods for Mathematical Modelling of Wind Turbines," *Renewable Energy*, vol. 36, no. 11, pp. 3166-3177, 2011.

[11] S. Gill, B. Stephen, and S. Galloway, "Wind Turbine Condition Assessment Through Power Curve Copula Modeling," *IEEE Transactions on Sustainable Energy*, vol. 3, no. 1, pp. 94-101, 2011.

[12] A. Marvuglia, and A. Messineo, "Monitoring of Wind Farms Power Curves Using Machine Learning Techniques," *Applied Energy*, vol. 98, pp. 574-583, 2012.

[13] J. Yan, H. Zhang, Y. Liu, S. Han, and L. Li, "Uncertainty Estimation for Wind Energy Conversion by Probabilistic Wind Turbine Power Curve Modelling," *Applied Energy*, vol. 239, pp. 1356-1370, 2019.

[14] D. Villanueva, and A. Feijoo, "A Review on Wind Turbine Deterministic Power Curve Models," *Applied Sciences*, vol. 10, no. 12, 4186, 2020.

[15] S. Seo, S. D. Oh, and H. Y. Kwak, "Wind Turbine Power Curve Modeling Using Maximum Likelihood Estimation Method," *Renewable Energy*, vol. 136, pp. 1164-1169, 2019.

[16] D. Villanueva, A. Sixto, A. Feijoo, A. Fernandez, and E. Miguez, "Methods to Apply A 3-Parameter Logistic Model to Wind Turbine Data," *Applied Sciences*, vol. 10, no. 9, 3317, 2020.
[17] S. M. Sadeghi, M. Daryalal, and M. Abasi, "Two-Stage Planning of Synchronous Distributed Generations in Distribution Network Considering Protection Coordination Index and Optimal Operation Situation," *IET Renewable Power Generation*, vol. 16, no. 11, pp. 2338-2356, 2022.
[18] M. Abasi, A. Saffarian, M. Joorabian, and S. G. Seifossadat, "Location of Double-Circuit Grounded Cross-Country Faults in GUPFC-Compensated Transmission Lines Based on Current and Voltage Phasors Analysis," *Electric Power Systems Research*, vol. 195, 107124, 2021.
[19] S. Han, Y. Qiao, et al., "Wind Turbine Power Curve Modeling Based on Interval Extreme Probability Density for the Integration of Renewable Energies and Electric Vehicles," *Renewable Energy*, vol. 157, pp. 190-203, 2020.
[20] G. Demurtas "Power Curve Measurement with Spinner Anemometer According to IEC 61400-12-2.", DTU Wind Energy. DTU Wind Energy I No. 0440, 2015.
[21] M. Abasi, A. T. Farsani, A. Rohani, and A. Beigzadeh, "A Novel Fuzzy Theory-Based Differential Protection Scheme for Transmission Lines," *International Journal of Integrated Engineering*, vol. 12, no. 8, pp. 149-160, 2020.
[22] S. Markarian, F. Fazelpour, and E. Markarian, "Optimization of Wind Farm Layout Considering Wake Effect and Multiple Parameters," *Environmental Progress & Sustainable Energy*, vol. 38, no. 5, 13193, 2019.
[23] R. K. Pandit, D. Infield, and J. Carroll, "Incorporating Air Density into A Gaussian Process Wind Turbine Power Curve Model for Improving Fitting Accuracy," *Wind Energy*, vol. 22, no. 12, pp. 1675-1687, 2019.
[24] S. Diaz, J. A. Carta, and J. M. Matias, "Performance Assessment of Five MCP Models Proposed for the Estimation of Long-Term Wind Turbine Power Outputs at a Target Site Using Three Machine Learning Techniques," *Applied Energy*, vol. 209, pp. 455-477, 2018.
[25] P. Giorsetto, and K. F. Utsurogi, "Development of a New Procedure for Reliability Modeling of Wind Turbine Generators," *IEEE Transactions on Power Apparatus and Systems*, vol. 102, no. 1, pp. 134-143, 1983.
[26] M. Abasi, N. Heydarzadeh, and A. Rohani, "Broken Conductor Fault Location in Power Transmission Lines Using GMDH Function and Single-Terminal Data Independent of Line Parameters," *Journal of Applied Research in Electrical Engineering*, vol. 1, no. 1, pp. 22-32, 2021.
[27] Ministry of Energy, Renewable Energy and Energy Efficiency Organization (SATBA).
[28] Iran Grid Management Company.

Declaration of Competing Interest

The authors declare that they have no known competing financial interests or personal relationships that could have appeared to influence the work reported in this paper. The ethical issues, including plagiarism, informed consent, misconduct, data fabrication and/or falsification, double publication and/or submission, redundancy, have been completely observed by the authors.

Credit Authorship Contribution Statement

AliAsghar Karimi Taleb: Conceptualization, Formal analysis, Project administration, Supervision, Validation, Roles/Writing - original draft. **Hojatollah Makvandi:** Conceptualization, Investigation, Methodology, Resources, Visualization, Writing - review & editing. **Ashknaz Oraee:** Formal analysis, Investigation, Software, Roles/Writing - original draft.

Bibliography

AliAsghar Karimi Taleb received the B.Eng. degree in Electronic Engineering from Razi University Kermanshah, Kermanshah, Iran., in 2014, and the MSc. degree in Power System Engineering from Sharif University of Technology, Tehran, Iran, in 2017. He is a PhD candidate in Electrical Power Engineering in Shahid Chamran University of Ahvaz, Ahvaz, Iran. He works as a design and supervision expert for the installation of electrical facilities and structures, Khuzestan Water and Power Authority (KWPA), Ministry of Energy of Iran, Ahvaz, Iran. His current research interests include smart grid and microgrid and influence of renewable energy on power systems.

Hojatollah Makvandi was born in 1975 in Iran. He received the Ph.D. degree in Electrical Power Engineering in 2020 from the Dezful Branch, Islamic Azad University, Dezful, Iran. He is a utility and power plant manager in the Abadan Oil Refining Company. His research interests include gas and steam turbine, micro-grid and islanding, and FACTS devices.

Ashknaz Oraee (Member, IEEE) received the B.Eng. degree in Electrical Engineering from Kings College London, London, U.K., in 2011, and the Ph.D. degree in Electrical Engineering from Cambridge University, Cambridge, U.K., in 2015, focusing on electrical machine design and optimization. She is a member of faculty in Sadjad University, Mashhad, Iran. Her current research interests include electrical machines and drives for renewable power generation.

Journal of Green Energy Research and Innovation

Optimization of CIGS/CIGS Tandem Solar Cells by Adjusting Layer Thickness Using Silvaco-TCADe

Bahareh Boroomandnasab, Mohammad Hossein Zolfaghari

Highlights

- **Design and simulation of CIGS/CIGS back-to-back solar cells using Silvaco-Atlas software**
- **Optimizing the performance of the CIGS/CIGS tandem solar cell**
- **Studying the effect of electrode metal and comparison of different materials**

Graphical Abstract

Use your device to scan and read the article online

Citation

B. Boroomandnasab, and M.H. Zolfaghari, "Optimization of CIGS/CIGS Tandem Solar Cells by Adjusting Layer Thickness Using Silvaco-TCAD," *Journal of Green Energy Research and Innovation*, vol. 1, no. 1, pp. 48-54, 2024.

https://doi.org/10.61186/jgeri.1.1.48

JGERI Journal of Green Energy Research and Innovation

Online ISSN: 3041-9018

Journal of Green Energy Research and Innovation

Journal Homepage: www.jgeri.araku.ac.ir

Optimization of CIGS/CIGS Tandem Solar Cells by Adjusting Layer Thickness Using Silvaco-TCAD

Bahareh Boroomandnasab [1]*, Mohammad Hossein Zolfaghari [2]

[1] *Department of Electrical and ICT, Faculty of Technical Engineering, Institute for Higher Education, ACECR, Khouzestan, IRAN.*
[2] *Instrument and Control Engineer at Well Services of Iran (WSI).*

* ***Corresponding Author:*** *boroomand@acecr.ac.ir*

ARTICLE INFO

Keywords:
CIGS/CIGS tandem solar cell,
Absorbing layer,
Electrode,
Cds.

Article history:
Received: 18 December 2023;
Revised: 23 January 2024;
Accepted: 03 February 2024;

Article type:
Research Article

ABSTRACT

This research designed and simulated CIGS/CIGS back-to-back solar cells using Silvaco-Atlas software. We considered CIGS absorbing layer thickness and sub-cells as critical parameters to optimize the performance of the CIGS/CIGS tandem solar cell. The research comparatively examined the effect of different electrode metals, such as molybdenum, aluminum, titanium, and silver, on the efficiency. The electrical parameters of the best CIGS/CIGS tandem solar cell configuration were a short-circuit current density (Jsc) of 15.65 mA/cm^2, an open-circuit voltage (Voc) of 1.86 V, a fill factor (FF) of 86.04%, and a conversion efficiency (η) of 27.12%. The optimal CIGS absorbing layer thickness of the top and bottom cells corresponding to the maximum conversion efficiency obtained were 0.17 and 6.3 µm, respectively. In contrast, the optimal thickness of the Cds layer was 0.04 µm. Silver had the best performance in connecting layers between several metals. The results can be used to develop low-cost and high-efficiency solar cells.

1. Introduction

Solar energy is a renewable energy that has the potential to produce energy for future generations. Every hour, Earth receives about four times as much solar energy as humans consume in a year. Therefore, if it can be converted into usable energy, such as electrical energy, we will no longer need to worry about the lack of energy in the world. In this regard, efforts in investigating and manufacturing solar cell devices have been growing in recent years [1]. Despite all the merits of thin-film cells compared to silicon cells, they suffer from the drawback of the amount of crystal defects, which increases electron-hole recombination in these cells. In thin-film solar cells, by calculating the appropriate thickness for the active layer versus the absorption coefficient, a process can be created to absorb all the wavelengths of light that shine on the cell. In the same vein, the propagation length of the electron-hole production created in the absorbent layer must be greater than the thickness of the absorbent layer in order to obtain a sufficient amount of electron-holes. Accordingly, choosing the suitable material with the proper thickness for thin-layer cells is very important. Amorphous silicon (a-Si), CIGS, and CdTe perform

best among various materials investigated in this field. These materials are used as absorbent layers in all thin-film cells due to their direct energy gap, high absorption coefficient, and compatibility of electrons with layers with higher energy gaps, such as CdS [2]. CIGS is one of the best candidates for making solar cells due to its unique properties, such as direct and controllable band gap energy, high radiation endurance, and the ability to deposit on flexible surfaces, such as metal foils [3]. The CIGS compound material has exceptional advantages, such as a high optical absorption coefficient (105 cm^{-1}) [4], a modifiable band gap from 1.02 eV for $CuInSe_2$ (CIS) up to 1.68 eV for $CuGaSe_2$ (CGS) [5], long-term stability, and high theoretical efficiency. High-efficiency CIGS-based devices can be made using many different manufacturing techniques [4]. The highest absorption coefficient in the CIGS layer is obtained when there is no gallium in the structure; that is, the layer acts as a CIS. Due to the high absorption coefficient of this layer, which is around 99%, the incoming photons are absorbed into this layer, and this absorption process occurs up to a depth of about one micron. This is why a thickness of one to two microns suffices when making a solar cell from this layer [6]. This becomes important if we need about three hundred microns of silicon to make a solar cell with silicon. The important thing is that although $CuInSe_2$ has a high absorption power, it has a small band gap energy. This problem can be solved by adding gallium. Some gallium atoms will replace indium, and the composition will be CuInxGa1-xSe2, which will achieve the highest efficiency by optimizing the amount of gallium to indium in this structure [7]. In today's world, the importance of solar cells has increased, so the goal is to make solar cells with higher efficiency and lower cost. Thin-film solar cells have a lower manufacturing cost than silicon solar cells, but their efficiency is lower. Therefore, this work aimed to optimize the performance of the double junction tandem solar cells based on CIGS/CIGS and extract the optimal electrical parameters of the structure studied. In this context, a numerical simulation of CIGS/CIGS tandem solar cell as a function of the CIGS absorbing layer thickness and its band gap of the sub-cells was performed using a two-dimensional device simulator Silvaco-Atlas in order to get the best structure simulated configuration, which corresponds the higher values of Voc for top and bottom cells and the good current matching between them.

2. Structure and simulation method

The CIGS/CIGS tandem solar cell structure considered in this study, which is schematically presented in Figure 1, consists of a double junction solar cell based on a CIGS connected optically and electrically with a ZnO layer as a transparent conducting oxide layer. The doping concentrations and thicknesses for different layers composing the structure simulated here are displayed in Figure 1. The detailed design of the CIGS top cell consists of a n-type ZnO transparent contact layer, a n-type CdS buffer layer, and a p-type CIGS absorbing layer. On the other hand, the bottom cell structure consists of a layer set composed of an n-ZnO window layer to ensure the electrical and optical connection between the two sub-cells, an n-CdS buffer layer, a p-CIGS absorbing layer, and finally, a

silver layer on a glass substrate usually used as the back contact. We used the TCAD Atlas simulator in Silvaco to simulate the solar cell. Atlas is a physically based two- and three-dimensional device simulator, which allows for solving Poisson's equation numerically coupled with the continuity equations for both electrons and holes under steady-state conditions. Physical models, such as Shockley-Reid-Hall (SRH) mechanisms, Auger and Langevin mechanisms of recombination, have been applied. In order to obtain the photon production rates along with the continuity equations, the solar spectra (AM1.5G) were imported into Atlas using the BEAM statement [8]. The change of current density versus voltage (J-V) under light was obtained, from which the main PV parameters were extracted, and Jsc, Voc, fill factor (FF), and PCE were calculated. Then, the effect of the electrode metal and the thickness of the CIGS layers in the upper and lower cells were investigated and the most optimal state of the structure was obtained.

3. Simulation Results and Discussion

The CIGS/CIGS tandem solar cell structure obtained by Silvaco-Atlas is shown in Figure 2. The current density-voltage characteristics (J-V) of the CIGS/CIGS tandem cell are plotted in Figure 3 for the input base parameters given in Table 1.

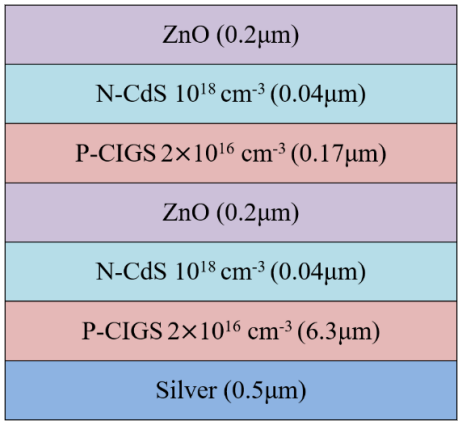

Figure1. The schematic structure of the CIGS/CIGS tandem solar cell.

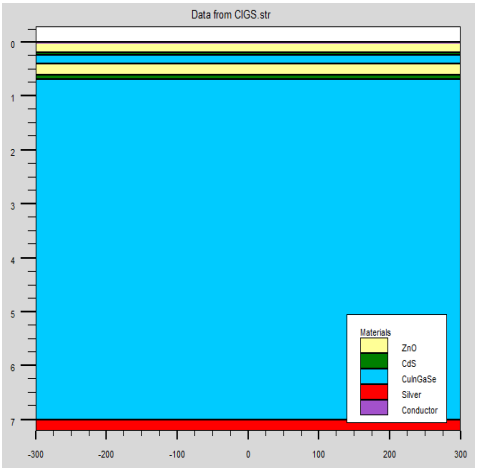

Figure 2. The Silvaco-Atlas structures file of the CIGS/CIGS tandem solar cell.

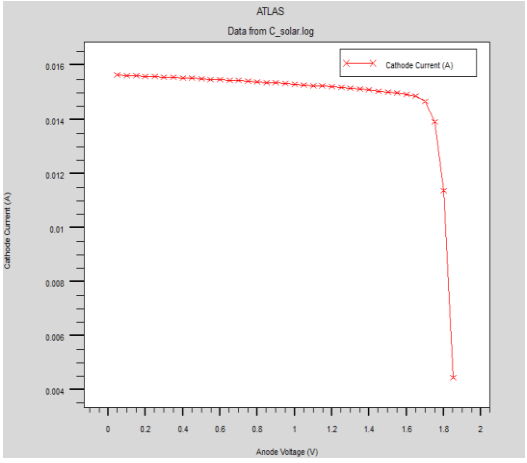

Figure3. The J-V characteristics of the CIGS/CIGS tandem cell before optimization.

Table 1. Material parameters used in the simulation.

Layer properties	ZnO	Cds	CIGS
$Eg\ (eV)$	3.3	2.4	1.13
εr	9	10	13.9
$\chi e\ (eV)$	4.1	4.5	4.8
$\mu n(cm^2/Vs)$	100	100	100
$\mu p(cm^2/Vs)$	25	25	25
$Nc\ (cm^{-3})$	2.2×10^{18}	2.2×10^{18}	2.2×10^{18}
$Nv\ (cm^{-3})$	1.8×10^{19}	1.8×10^{19}	1.8×10^{19}
Gaussian Defect States			
$NDG, NVG(cm^{-3})$	D: 10^{17}	A: 10^{18}	D: 10^{14}
$EA\ , ED\ (eV)$	Mid gap	Mid gap	Mid gap
$WG\ (eV)$	0.1	0.1	0.1
σe (cm^2)	10^{-12}	10^{-17}	5×10^{-13}
σh (cm^2)	10^{-15}	10^{-12}	10^{-15}
Surface recombination velocity for electrons (holes) (cm.s^{-1})			
At CdS/CIGS interface	10^5	10^5	10^5
At CdS/CIGS interface	10^5	10^5	10^5
at front contact	10^5	10^5	10^5
at back contact	10^5	10^5	10^5

By matching the values of the short-circuit current density of the CIGS top cell and those of the bottom cell, we can determine the optimal CIGS absorbing layer thickness for the CIGS top cell, which corresponds to the good current matching between the sub-cells and leads to the maximum efficiency of the CIGS tandem cell. We varied the CIGS absorbing layer thickness of the CIGS top from 0.17 µm to 0.26 µm, and the thickness of the CIGS bottom cell from 5 µm to 6.3 µm. When the CIGS top cell is thicker, it absorbs more light, leaving less light to the CIGS bottom cell. Therefore, the CIGS bottom cell exhibits poor performance. For CIGS, the bottom cell's thicker layer means more light absorbance. Figure 4 indicates that Jsc increases by decreasing top CIGS and increasing bottom CIGS layer thickness. Figure 4(c) also illustrates that a thicker CdS buffer layer will allow more current to pass between the two cells. Using Silvaco software, we investigated the effect of the electrode and compared different materials, such as molybdenum, aluminum, titanium, and silver, on solar cell efficiency. As shown in Figure 5, silver metal performs best among the metals used in the solar cell structure under discussion. After that, aluminum, molybdenum, and finally, titanium are more suitable. According to the investigations in the previous sections, the optimal thickness for different layers was calculated, and the suitable metal for the electrodes was considered. Finally, electrical parameters Jsc, Voc, FF, and η were calculated and compared with previous research. According to Table 2, we improved the structure.

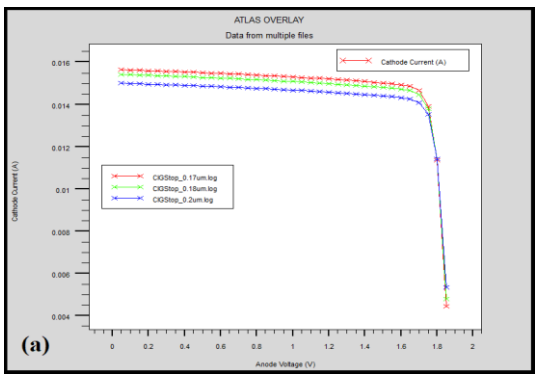

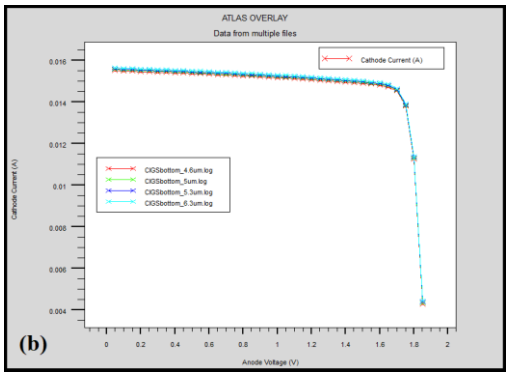

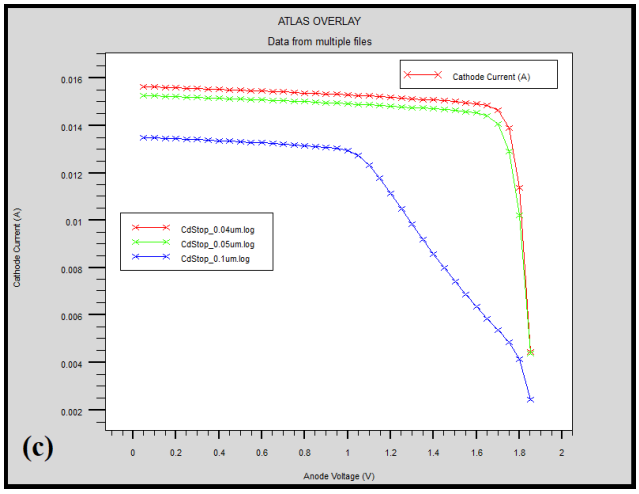

Figure 4. J-V characteristics of CIGS (a) top CIGS layer thickness, (b) bottom CIGS layer thickness, and (c) buffer layer thickness.

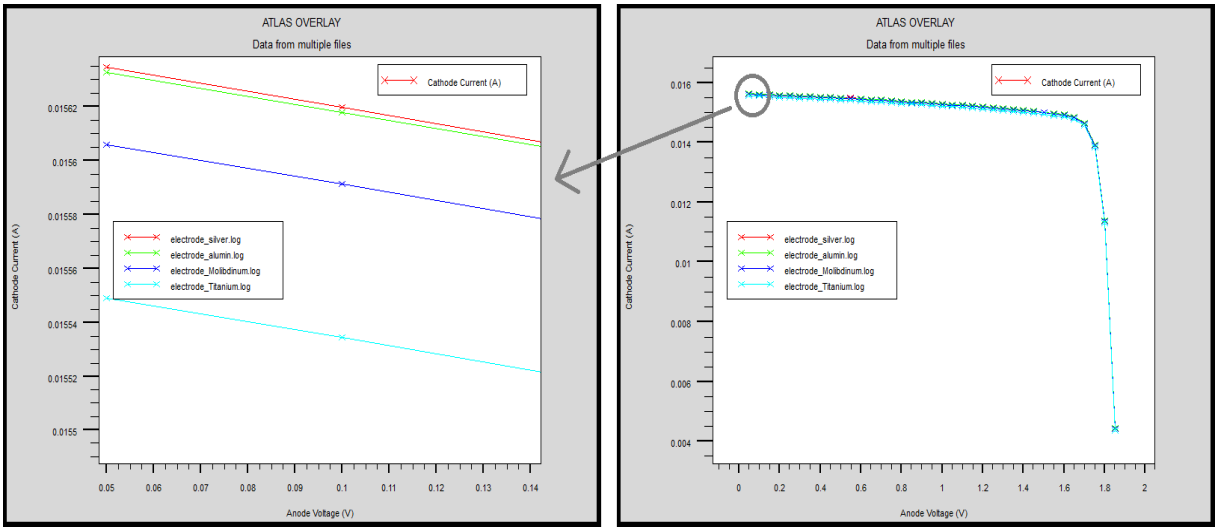

Figure 5. The J-V characteristics for different electrode metals**.**

Table 2. Electrical parameters of CIGS/CIGS tandem cell.

	J_{sc}	V_{OC}	FF%	η%
Simulation [9]	16.35	1.80	85.09	25.11
Simulation [10]	16.89	1.77	82.54	27.03
Manufacture [11]	8.24	1.13	65.6	6.11
Our Simulation	15.65	1.86	86.04	27.12

4. Conclusions

CIGS/CIGS tandem cells with different thicknesses of CIGS absorber layers and different CdS for top and bottom cells were numerically simulated using Silvaco-Atlas to find the best CIGS/CIGS tandem solar cell configuration and select the optimal CIGS device parameters. After optimization, the conversion efficiency improved from 27.03% to 27.12% for a CIGS/CIGS tandem cell. The Voc value was equal to 1.86 V. It is equal to the sum of the separate voltages of the upper and lower cells. By matching the short-circuit current density values between the sub-cells (Jsc=Jsct=Jscb), we determined an excellent current match of 15.65 mA/cm^2 provided by the CIGS/CIGS tandem cell, increasing the performance of the simulated structure.

We considered the thickness of the CIGS absorber layer and Cds layer to improve the performance of the CGIS/CIGS tandem cell. It was found that the thickness of the optimal CIGS absorbing layer was 0.17 µm for the upper cell and 6.3 µm for the lower cell, and the thickness of the Cds layer was 0.04 µm. The most suitable metal for connecting was the silver electrode.

References

[1] A. W. Ho-Baillie, J. Zheng, et al., "Recent Progress and Future Prospects of Perovskite Tandem Solar Cells," *Applied Physics Reviews*, vol. 8, no. 4, 041307, 2021.

[2] N. Mufti, T. Amrillah, et al., "Review of CIGS-Based Solar Cells Manufacturing by Structural Engineering," *Solar Energy*, vol. 207, pp. 1146-1157, 2020.

[3] J. Ramanujam, D. M. Bishop, et al., "Flexible CIGS, CdTe and a-Si: H Based Thin Film Solar Cells: A Review," *Progress in Materials Science*, vol. 110, 100619, 2020.

[4] A. Romeo, M. Terheggen, et al., "Development of Thin Film Cu (In, Ga) Se2 and CdTe Solar Cells," *Progress in Photovoltaics: Research and Applications*, vol. 12, pp. 93–111, 2004.

[5] T. Dullweber, G. Hanna, et al., "Study of the Effect of Gallium Grading in Cu (In, Ga) Se2," *Thin Solid Films*, vol. 361, pp. 478-481, 2000.

[6] B. Barman, and P. K. Kalita, "Influence of Back Surface Field Layer on Enhancing the Efficiency of CIGS Solar Cell," *Solar Energy*, vol. 216, pp. 329-337, 2021.

[7] Y. Zhao, S. Yuan, et al., "High Efficiency CIGS Solar Cells by Bulk Defect Passivation Through Ag Substituting Strategy," *ACS Applied Materials & Interfaces*, vol. 12, no. 11, pp. 12717-12726, 2020.

[8] A. Sarkar "Device Simulation Using Silvaco ATLAS Tool." Technology Computer Aided Design. *CRC Press*, pp. 203-252, 2013.

[9] M. Elbar, S. Tobbeche, and A. Merazga, "Effect of Top-Cell CGS Thickness on the Performance of CGS/CIGS Tandem Solar Cell," *Solar Energy*, vol. 122, pp. 104–112, 2015.

[10] B. Bouanani, A. Joti, F. S.B. Bouiadjra, and A. Kadid, "Band Gap and Thickness Optimization for Improvement of CIGS/CIGS Tandem Solar Cells Using Silvaco Software," *Optik*, vol. 204, 164217, 2020.

[11] S. Y. Chae, S. J. Park, et al., "Highly Stable Tandem Solar Cell Monolithically Integrating Dye-Sensitized and CIGS Solar Cells," *Scientific Reports*, vol. 6, no. 1, p. 30868, 2016.

Declaration of Competing Interest

The authors declare that they have no known competing financial interests or personal relationships that could have appeared to influence the work reported in this paper. The ethical issues, including plagiarism, informed consent, misconduct, data fabrication and/or falsification, double publication and/or submission, redundancy, have been completely observed by the authors.

Credit Authorship Contribution Statement

Bahareh Boroomandnasab: Conceptualization, Formal analysis, Project administration, Supervision, Validation, Roles/Writing - original draft. **Mohammad Hossein Zolfaghari:** Conceptualization, Investigation, Methodology, Resources, Visualization, Writing - review & editing.

Bibliography

Bahareh Boroomandnasab was born in 1988, in Dezful, Iran. She received her Bachelor's, Master's, and Ph.D. degrees in Electronics Systems Engineering from Shahid Chamran University of Ahvaz, Ahvaz, Iran in 2011, 2013, and 2019, respectively. She is currently an Assistant Professor in Institute for Higher Education, ACECR, Khouzestan, IRAN. Her research interests include semiconductor device design, simulation and fabrication.

Mohammad Hossein Zolfaghari He is currently an Instrument and Control Engineer at Well Services of Iran (WSI) company. He has four years of experience in the maintenance, troubleshooting, and repairing of electronic devices, with a proven ability to work efficiently both as a team player and independently due to working as a team member and individually. Furthermore, his interpersonal skills have been developed during his work as a lecturer of robotics and embedded programming; he has one article at prestigious conferences in the field of simulation of semiconductor devices.

Journal of Green Energy Research and Innovation

Power Equations for Non-Detection Zone of Islanding Detection in Renewable-Energy-based Microgrids with Multiple Connection Points to Microgrids

Saman Darvish Kermani, Vahid Davatgaran, Arsalan Beigzadeh, Mahmood Joorabian

Highlights

- Presenting the power equations for active and reactive power in renewable-energy-based multi-microgrids
- Presenting procedures for over/under voltage protection, over/under frequency protection
- The proposed approach is very broad across different types of microgrids
- The proposed local islanding identification methods often have a significant NDZ

Graphical Abstract

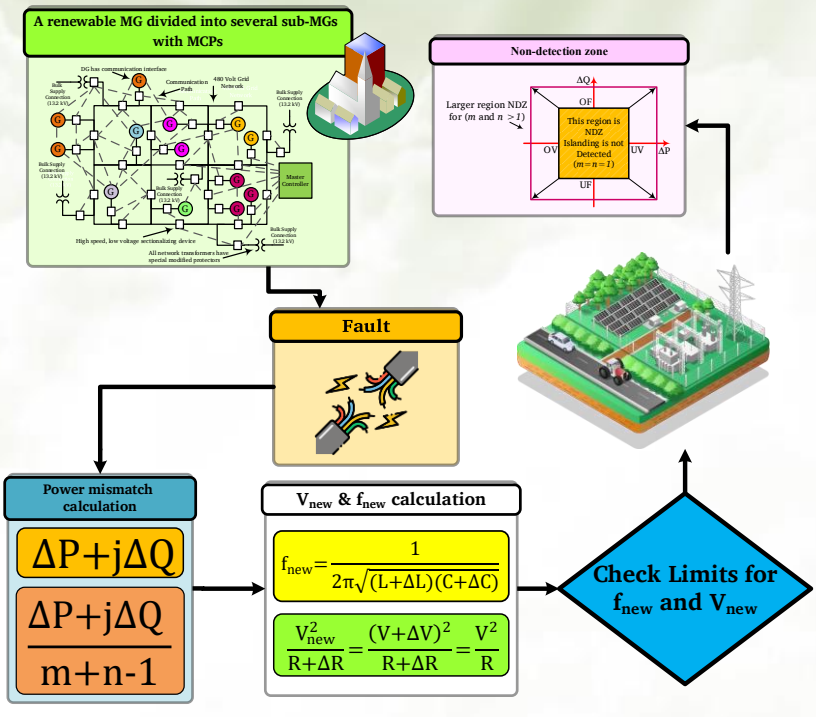

Islanding detection and protection of microgrid

Use your device to scan and read the article online

Citation

S. Darvish Kermani, V. Davatgaran, A. Beigzadeh, and M. Joorabian, "Power Equations for Non-Detection Zone of Islanding Detection in Renewable-Energy-based Microgrids with Multiple Connection Points to Micro-Grids," *Journal of Green Energy Research and Innovation*, vol. 1, no. 1, pp. 55-65, 2024.

https://doi.org/10.61186/jgeri.1.1.55

JGERI Journal of Green Energy Research and Innovation

Online ISSN: 3041-9018

Journal of Green Energy Research and Innovation

Journal Homepage: www.jgeri.araku.ac.ir

Power Equations for Non-Detection Zone of Islanding Detection in Renewable-Energy-based Microgrids with Multiple Connection Points to Micro-Grids

Saman Darvish Kermani [1], Vahid Davatgaran [2], Arsalan Beigzadeh[3], Mahmood Joorabian [4]*

[1] *GHD Advisory Melbourne VIC 3000 Australia.*
[2] *Department of Electrical Engineering, Technical and Vocational University (TVU), Tehran, Iran.*
[3] *Department of Maintenance, Iran Khodro Co, Tehran, Iran.*
[4] *Department of Electrical Engineering, Faculty of Engineering, Shahid Chamran University of Ahvaz, Ahvaz, Iran.*

* *Corresponding Author: mjoorabian@scu.ac.ir*

ARTICLE INFO

Keywords:
Microgrid,
Power equation,
Passive and Active,
Islanding detection.

Article history:
Received: 19 December 2023;
Revised: 10 January 2024;
Accepted: 21 January 2024;

Article type:
Research Article

ABSTRACT

Microgrids (MGs), which can incorporate renewable energies such as wind and solar, can be divided into several sub-MGs with multiple connection points (MCPs) to the grids. However, this configuration is not ideal for MG operation due to the lack of adequate protection and operation mechanisms that ensure the safe and reliable functioning of distributed generation. A key issue with these MGs is the identification of islanding, which is challenging due to the presence of a broad non-detection zone (NDZ). Passive islanding identification approaches primarily depend on over/under voltage protection (OVP/UVP), over/under frequency protection (OFP/UFP), and monitoring metrics, such as phase jump at the point of common coupling (PCC). This study examines the power equations for real and reactive power in renewable-energy-based MGs (referred to as renewable MGs) with multiple connections to different grids and MGs, which are of significant size. The analysis focuses on the NDZ of OVP/UVP and OFP/UFP approaches. Passive approaches observe the changing system parameters that occur when the MG is isolated, while active methods depend on the system's reaction to a minor disturbance introduced to identify the isolation situation. Traditional passive islanding detection approaches exhibit a significant NDZ that may compromise the accuracy of islanding detection in these types of MGs. Even if one grid is disconnected, the MG remains connected to other grids, preventing islanding. Consequently, typical active islanding detection methods are unable to identify the off-grid status.

1. Introduction

Islanding identification is crucial in the process of connecting microgrids (MGs) to electrical grids. The detection approaches are primarily categorized into remote and local methods, which depend on electrical signal measurements taken at the grid and MG sides, respectively. MGs are capable of harnessing renewable energies for power generation.

They can be divided into smaller sub-MGs with MCPs to the rest of the grids. However, the current network protection systems and operations do not support the immune and dependable operation of distributed generation, making them unsuitable for MG operation [1-3]. The majority of remote techniques used for islanding identification depend on the connectivity between the power grid and the MG. Remote methods lack a non-detection zone (NDZ) and are, hence, significantly reliable techniques for detecting islanding. Although the implementation of remote methods can be costly for small MGs, they offer significant advantages for large MG practices [4-6]. Local islanding identification is conducted by passive, active, and hybrid techniques by finding grid parameters at the MG side, including voltage, frequency, current, and harmonic distortion. Passive approaches observe the changing system characteristics when the microgrid is isolated. On the other hand, active methods depend on the grid's reaction to a minor injected disturbance to detect the islanding condition. The hybrid strategy is a fusion of the active and passive techniques used to overcome NDZ [7-19]. Islanding in a power network can only occur when there is an equilibrium between the active and reactive powers. The equations for P and Q, as well as the NDZ of the MG for grid connection, are developed and investigated in the references [20, 21]. The utilization of power equations for NDZ in islanding detection of MG with several connection points to grids and/or other MGs is thoroughly studied in reference [22]. This study investigates the power equations for real and reactive power in the presence of NDZ using OVP/UVP (overvoltage/undervoltage protection) and OFP/UFP (over-frequency/under-frequency protection) approaches. The analysis focuses on significant-size renewable MGs that are connected to several grids and other MGs. Traditional passive islanding identification approaches have a significant non-detection zone (NDZ), potentially compromising the accuracy of islanding identification in these specific kinds of MGs. Even if one grid is disconnected, the MG remains connected to other grids, preventing islanding. Consequently, typical active islanding identification methods are unable to identify the off-grid status. The paper presents active, reactive power equations and procedures for OVP/UVP and OFP/UFP and analyzes the NDZ area for MGs. The results show the broad NDZ area for OUP and OVP methods in different types of MGs.

The rest of the paper is organized as follows: Section 2 explains the MGs, MCPs, and islanding techniques. Section 3 describes and analyzes passive method equations of islanding. Then, the paper is focused on relation criteria and thresholds of frequency, active power, and reactive power. Concluding remarks are finally presented in Section 4.

2. Microgrids with MCPs to Grids and/or Microgrids

Nowadays, renewable MGs are developed and use different kinds of energy, such as solar energy, to produce power. Some power consumers, such as hospitals and airports, are some examples of MGs with MCPs to grids constituting several large and important sub-MGs that should always be in service. Therefore, the stability of such unified MGs is so important while all low-voltage cells are connected and synchronized. One example of large MGs with two connection points to other grids is illustrated in Figure 1, but islanding identification in this kind of MGs is more complicated compared to other MGs, as

mentioned in [1-3]. The primary limitation of passive and active techniques lies in their reliance on the fluctuations of measured quantities, which may not be substantial, especially in scenarios such as i) microgrids with NCPs to the grid, ii) microgrids connected to multiple grids, and iii) microgrids with numerous smaller sub-microgrids. Figure 2 depicts a highly sophisticated low-voltage grid network capable of functioning as a unified MG, where all low-voltage cells are interconnected and synchronized. Alternatively, the network is divided into separate autonomous cells. Using local passive and active islanding identifications is not recommended here since these kinds of MGs have a large NDZ.

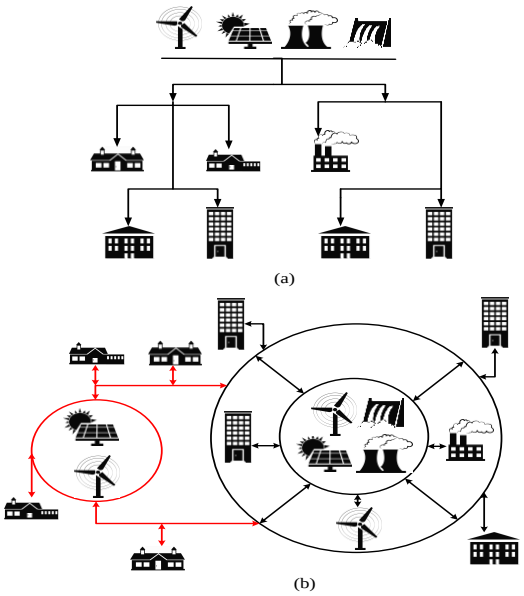

Figure 1. Topologies for grids; (a) Traditional grid, (b) large renewable MG with two connection points to grids.

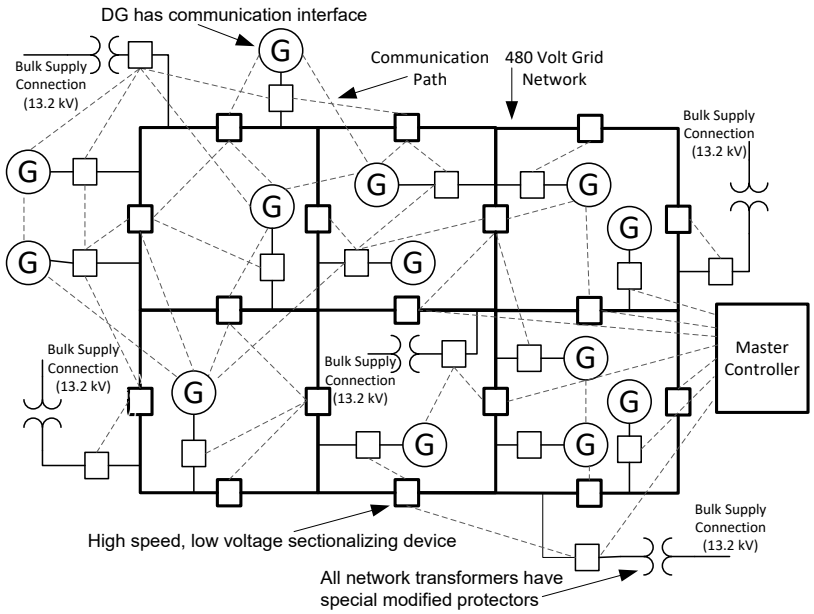

Figure 2. A renewable MG divided into several sub-MGs with MCPs to the rest of the grids; similar to figures 2-11 given in [1].

3. Power Equations for Non-Detection Zone in Renewable Microgrids with MCPs to Grids and/or Microgrids

Figure 3 illustrates a universal method for examining islanding in a renewable MG with MCPs connected to distinct grids and other MGs. A regional RLC load is placed at the point of common coupling (PCC). The resonant frequency f and power quality Qf is defined as follows [20, 21]:

$$f = \frac{1}{2\pi\sqrt{LC}} \tag{1}$$

$$Q_f = R\sqrt{\frac{C}{L}} \tag{2}$$

$$Q_L = \frac{V^2}{2\pi f L} \tag{3}$$

$$Q_C = 2\pi f C V^2 \tag{4}$$

where f(Hz), L(H), C(F), R(Ω), V(v), Q_L(kVAR) and Q_C(kVAR) are frequency, reactance, capacitance, resistance, voltage, reactive power of reactance, and reactive power of capacitance, respectively. In Figure 3, the power mismatch $\Delta P + j\Delta Q$ is observed between MG generation and RLC load. Prior to removing Grid 1, the power is supported by grids and the rest of the MGs. For simplicity, suppose every MGs and grids equally supply this power mismatch. So, every MG and grid supply power mismatch is $\frac{\Delta P + j\Delta Q}{m+n-1}$, where m *and* n denote the number of MGs and grids, respectively. In Figure 4, Grid 1 is disconnected from the network, and the power mismatch $\frac{\Delta P + j\Delta Q}{m+n-1}$ can be represented as mismatch loads $\Delta R. \Delta L. \Delta C$. The frequency and voltage values are modified to V_{new} and f_{new}, correspondingly. Nevertheless, the limited magnitude of these changes can be attributed to the interconnection between MG and the other power systems.

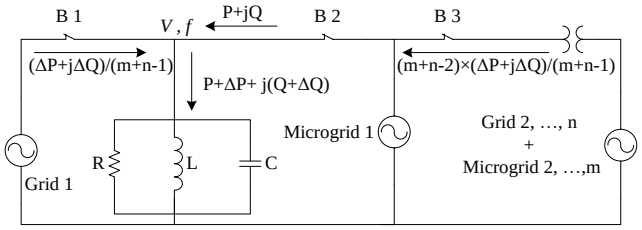

Figure 3. A renewable MG with MCPs to grids for islanding study.

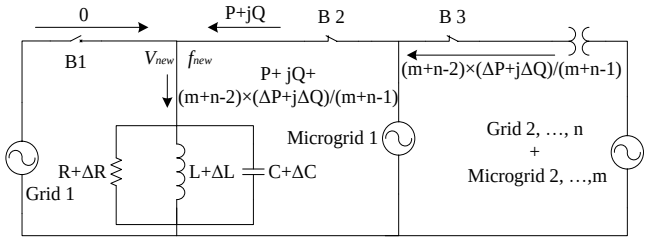

Figure 4. Circuit breaker 1 (B1) opens and mismatch power $\frac{\Delta P + j\Delta Q}{m+n-1}$ represented by $\Delta R. \Delta L. \Delta C$.

$$f_{new} = \frac{1}{2\pi\sqrt{(L+\Delta L)(C+\Delta C)}} \tag{5}$$

$$\frac{f_{new}-f}{f} = \frac{\frac{1}{2\pi\sqrt{(L+\Delta L)(C+\Delta C)}} - \frac{1}{2\pi\sqrt{LC}}}{\frac{1}{2\pi\sqrt{LC}}}$$

$$= \frac{\frac{1}{2\pi\sqrt{(L+\Delta L)(C+\Delta C)}}}{\frac{1}{2\pi\sqrt{LC}}} - \frac{\frac{1}{2\pi\sqrt{LC}}}{\frac{1}{2\pi\sqrt{LC}}}$$

$$= \frac{\sqrt{LC}}{\sqrt{(L+\Delta L)(C+\Delta C)}} - 1 \tag{6}$$

In order to use f_{max} and f_{min} as thresholds for under/over frequency (UF/OF), the following criteria need to be satisfied:

$$\frac{f_{min}-f}{f} \le \frac{\sqrt{LC}}{\sqrt{(L+\Delta L)(C+\Delta C)}} - 1 \le \frac{f_{max}-f}{f}$$

$$\frac{f_{min}}{f} - 1 \le \frac{\sqrt{LC}}{\sqrt{(L+\Delta L)(C+\Delta C)}} - 1 \le \frac{f_{max}}{f} - 1$$

$$\frac{f_{min}}{f} \le \frac{\sqrt{LC}}{\sqrt{(L+\Delta L)(C+\Delta C)}} \le \frac{f_{max}}{f}$$

$$\left(\frac{f_{min}}{f}\right)^2 \le \frac{LC}{(L+\Delta L)(C+\Delta C)} \le \left(\frac{f_{max}}{f}\right)^2$$

$$\left(\frac{f_{min}}{f}\right)^2 \le \frac{LC}{LC + L\Delta C + C\Delta L + \Delta L\Delta C} \le \left(\frac{f_{max}}{f}\right)^2 \tag{7}$$

where f_{max} and f_{min} are maximum and minimum frequency, respectively. Simplifying with the approximation of $\Delta L\Delta C \approx 0$:

$$\left(\frac{f_{min}}{f}\right)^2 \le \frac{LC}{LC + L\Delta C + C\Delta L} \le \left(\frac{f_{max}}{f}\right)^2$$

$$\left(\frac{f}{f_{max}}\right)^2 \le \frac{LC + L\Delta C + C\Delta L}{LC} \le \left(\frac{f}{f_{min}}\right)^2$$

$$\left(\frac{f}{f_{max}}\right)^2 \le 1 + \frac{\Delta C}{C} + \frac{\Delta L}{L} \le \left(\frac{f}{f_{min}}\right)^2$$

$$\left(\frac{f}{f_{max}}\right)^2 - 1 \le \frac{\Delta C}{C} + \frac{\Delta L}{L} \le \left(\frac{f}{f_{min}}\right)^2 - 1 \tag{8}$$

$\frac{\Delta Q}{m+n-1}$ mismatch can be shown as:

$$\frac{\Delta Q}{m+n-1} = V^2\left(\frac{1}{2\pi f(L+\Delta L)} - 2\pi f(C+\Delta C)\right)$$
$$= V^2\left[\frac{1}{2\pi fL\left(1+\frac{\Delta L}{L}\right)} - 2\pi fC\left(1+\frac{\Delta C}{C}\right)\right]$$
$$= \left[\left(\frac{V^2}{2\pi fL}\right)\frac{1}{\left(1+\frac{\Delta L}{L}\right)} - (2\pi fCV^2)\left(1+\frac{\Delta C}{C}\right)\right]$$
$$= \frac{Q_L}{\left(1+\frac{\Delta L}{L}\right)} - Q_C\left(1+\frac{\Delta C}{C}\right) \quad (9)$$

Based on Q_f definition:

$$Q_f \times P = Q_L = Q_C \quad (10)$$

Normalize $\frac{\Delta Q}{m+n-1}$ in Equation (9) based on P:

$$\frac{\Delta Q}{(m+n-1)P} = \frac{\left(\frac{Q_L}{P}\right)}{\left(1+\frac{\Delta L}{L}\right)} - \left(\frac{Q_C}{P}\right)\left(1+\frac{\Delta C}{C}\right)$$
$$= \frac{Q_f}{\left(1+\frac{\Delta L}{L}\right)} - Q_f\left(1+\frac{\Delta C}{C}\right)$$
$$= Q_f\left[\frac{1}{\left(1+\frac{\Delta L}{L}\right)} - \left(1+\frac{\Delta C}{C}\right)\right]$$
$$= Q_f\frac{1-\left(1+\frac{\Delta L}{L}\right)\left(1+\frac{\Delta C}{C}\right)}{1+\frac{\Delta L}{L}}$$
$$= Q_f\frac{1-\left(1+\frac{\Delta C}{C}+\frac{\Delta L}{L}+\frac{\Delta L}{L}\times\frac{\Delta C}{C}\right)}{1+\frac{\Delta L}{L}}$$
$$= Q_f\frac{-\left(\frac{\Delta C}{C}+\frac{\Delta L}{L}+\frac{\Delta L}{L}\times\frac{\Delta C}{C}\right)}{1+\frac{\Delta L}{L}} \quad (11)$$

Simplified with approximation of $\Delta L\Delta C \approx 0$ and $1+\frac{\Delta L}{L} \approx 1$:

$$\frac{\Delta Q}{(m+n-1)P} \approx -Q_f\left(\frac{\Delta C}{C}+\frac{\Delta L}{L}\right) \quad (12)$$

From Equation (8) and Equation (12), NDZ of reactive power is:

$$\left(\frac{f}{f_{max}}\right)^2 - 1 \le \frac{\Delta Q}{-Q_f(m+n-1)P} \le \left(\frac{f}{f_{min}}\right)^2 - 1$$
$$Q_f\left(\left(\frac{f}{f_{max}}\right)^2 - 1\right) \le \frac{-\Delta Q}{(m+n-1)P} \le Q_f\left(\left(\frac{f}{f_{min}}\right)^2 - 1\right) \quad (13)$$

Finally,

$$Q_f\left(1-\left(\frac{f}{f_{min}}\right)^2\right) \leq \frac{\Delta Q}{(m+n-1)P} \leq Q_f\left(1-\left(\frac{f}{f_{max}}\right)^2\right) \tag{14}$$

By the same token, the correlation between the voltage and active power is deduced. Prior to the disconnection of Grid 1, the MG active power is V^2/R. After disconnecting Grid 1, the load active power is $V^2/(R+\Delta R)$. If it is assumed that the system is under constant power regulation, then the equilibrium of active power may be expressed as:

$$\frac{V_{new}^2}{R+\Delta R} = \frac{(V+\Delta V)^2}{R+\Delta R} = \frac{V^2}{R} \tag{15}$$

Equation (15) can be simplified as:

$$\begin{aligned}
&\frac{(V+\Delta V)^2}{V^2} = \frac{R+\Delta R}{R} \\
&\frac{V^2+2V\Delta V+\Delta V^2}{V^2} = 1+\frac{\Delta R}{R} \\
&1+\frac{2\Delta V}{V}+\frac{\Delta V^2}{V^2} = 1+\frac{\Delta R}{R} \\
&2\frac{\Delta V}{V}+\left(\frac{\Delta V}{V}\right)^2 = \frac{\Delta R}{R}
\end{aligned} \tag{16}$$

Before disconnecting Grid 1 from the system, Grid 1 supplies $\frac{\Delta P}{m+n-1}$ to the RLC load:

$$\frac{\Delta P}{m+n-1} = \frac{V^2}{R+\Delta R} - \frac{V^2}{R} \tag{17}$$

Normalize $\frac{\Delta P}{m+n-1}$ with $P = \frac{V^2}{R}$:

$$\begin{aligned}
\frac{\Delta P}{(m+n-1)P} &= \frac{\frac{V^2}{R+\Delta R} - \frac{V^2}{R}}{\frac{V^2}{R}} = \frac{\frac{RV^2-(R+\Delta R)V^2}{(R+\Delta R)R}}{\frac{V^2}{R}} \\
&= \frac{R-(R+\Delta R)}{R+\Delta R} = -\frac{\Delta R}{R+\Delta R} = -\frac{\frac{\Delta R}{R}}{\frac{R+\Delta R}{R}} = -\frac{\frac{\Delta R}{R}}{1+\frac{\Delta R}{R}}
\end{aligned} \tag{18}$$

Substituting Equation (16) into Equation (18) and simplifying the equation with $V_{new} = \Delta V + V$, it is obtained:

$$\frac{\Delta P}{(m+n-1)P} = -\frac{\frac{\Delta R}{R}}{1+\frac{\Delta R}{R}} = -\frac{2\frac{\Delta V}{V}+\left(\frac{\Delta V}{V}\right)^2}{1+2\frac{\Delta V}{V}+\left(\frac{\Delta V}{V}\right)^2}$$
$$= -\frac{1+2\frac{\Delta V}{V}+\left(\frac{\Delta V}{V}\right)^2-1}{1+2\frac{\Delta V}{V}+\left(\frac{\Delta V}{V}\right)^2} = -\frac{\left(\frac{\Delta V}{V}+1\right)^2-1}{\left(\frac{\Delta V}{V}+1\right)^2}$$
$$= \frac{1-\left(\frac{\Delta V}{V}+1\right)^2}{\left(\frac{\Delta V}{V}+1\right)^2} = \frac{1}{\left(\frac{\Delta V+V}{V}\right)^2}-1$$
$$= \frac{V^2}{(\Delta V+V)^2}-1 = \frac{V^2}{V_{new}^2}-1 = \left(\frac{V}{V_{new}}\right)^2-1 \quad (19)$$

To ensure that V_{new} falls between the voltage thresholds, V_{min} and V_{max}, the following condition must be satisfied, resulting in the non-disruptive zone (NDZ) of active power:

$$\left(\frac{V}{V_{max}}\right)^2-1 \le \frac{\Delta P}{(m+n-1)P} \le \left(\frac{V}{V_{min}}\right)^2-1 \quad (20)$$

where V_{min}, V_{max} are minimum and maximum voltage, respectively. Therefore, the NDZ for UV/OV and UF/OF approaches to one MG and one grid $m=1$ and $n=1$ can be observed in Figure 5. Mathematically approach, in Equations (14) and (20), power mismatch $\frac{\Delta P}{m+n-1}$ and $\frac{\Delta Q}{m+n-1}$ are smaller than ΔP *and* ΔQ when m *and* n are larger than 1, and the power mismatch of the MG is lesser. Therefore, the region of the NDZ increases. For example, based on standard IEEE 1547 [15] in Equations (14) and (20) for $Q_f = 1$. $f_{min} = 0.99f$. $f_{max} = 1.01f$. $V_{min} = 0.9V$. $V_{max} = 1.1V$:

$$(-2.03\%) \times (m+n-1) \le \frac{\Delta Q}{P} \le (1.97\%) \times (m+n-1) \quad (21)$$

$$(-17.36\%) \times (m+n-1) \le \frac{\Delta P}{P} \le (23.46\%) \times (m+n-1) \quad (22)$$

Considering Equations (21) and (22), The region of NDZ in passive islanding identification approaches, as shown in Figure 5, expands due to the compensation of ΔP and ΔQ by other grids and MGs. Consequently, no discrepancies appear in the frequency and voltage. As a result, the passive islanding identification approaches will exhibit significant NDZs for these particular kinds of MGs. Furthermore, the connection of many grids to the MG ensures that even if one grid is disconnected, islanding can be prevented. Consequently, typical active islanding identification approaches will be unable to identify the off-grid status.

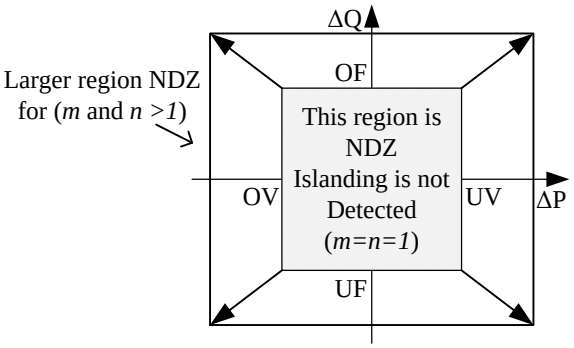

Figure 5. The NDZ of OV/UV and OF/UF for MG in Figure 3. $m = n = 1$, m and $n > 1$.

4. Conclusions

MGs that are presented constitute some sub-MGs with MCPs to different grids. As a consequence of a large NDZ area in these kinds of MGs, traditional methods cannot always detect islanding. OVP/UVP and OFP/UFP are primarily employed as passive islanding detection techniques, monitoring parameters such as voltage amplitude and frequency at the PCC. This study presents a derivation and analysis of the equations for real and reactive power, as well as the procedures for OVP/UVP and OFP/UFP. The presented equations can be applied to any type of multi-terminal microgrid. The findings indicate that the NDZ of the OVP and UVP methods is very broad across different types of MGs. Identifying islanding in renewable microgrids can be complex due to their ability to remain stable by connecting to many grids. Additionally, local islanding identification methods often have a significant NDZ. Even if one grid is disconnected, the renewable microgrid remains connected to other grids, preventing islanding. Consequently, conventional active islanding identification methods are unable to detect the off-grid condition.

References

[1] S. M. Hossain, S. Koley, A. Winter, and J. H. Enslin, "A Technical and Economic Feasibility Study of Campus Microgrid Implementation," *IEEE 13th International Symposium on Power Electronics for Distributed Generation Systems (PEDG)*, pp. 1-6, 2022.

[2] R. Bakhshi-Jafarabadi, J. Sadeh, J. D. J. Chavez, and M. Popov, "Two-Level Islanding Detection Method for Grid-Connected Photovoltaic System-Based Microgrid with Small Non-Detection Zone," *IEEE Transactions on Smart Grid*, vol. 12, no. 2, pp. 1063-1072, 2021.

[3] M. Falah Nezhadnaeini, M. Hajivand, M. Abasi, and S. Mohajerami, "Optimal Allocation of Distributed Generation Units Based on Different Objectives by a Novel Version Group Search Optimizer Algorithm in Unbalance Load System," *Revue Roumaine Des Sciences Techniques Serie Electrotechnique et Energetique*, vol. 61, no. 4, pp. 338-342, 2016.

[4] J. Yin, L. Chang, and C. Diduch, "Recent Developments in Islanding Detection for Distributed Power Generation," *IEEE Power Engineering, Large Engineering Systems Conference on Power Systems*, vol. 28, pp. 124-128, 2004.

[5] R. Bakhshi-Jafarabadi, and J. Sadeh, "New Voltage Feedback-Based Islanding Detection Method for Grid-Connected Photovoltaic Systems of Microgrid with Zero Non-Detection Zone," *IET Renewable Power Generation*, vol. 14, no. 10, pp. 1710-1719, 2020.

[6] S. Sanati, and Y. Alinejad-Beromi, "Fast and Complete Mitigation of Residual Flux in Current Transformers Suitable for Auto-Reclosing Schemes Using Jiles-Atherton Modeling," *IEEE Transactions on Power Delivery*, vol. 37, no. 2, pp. 765-774, 2022.
[7] M. Ezzt, M. I. Marei, M. Abdel-Rahman, and M. M. Mansour, "A Hybrid Strategy for Distributed Generators Islanding Detection," *IEEE Power Engineering Society Conference and Exposition in Africa*, pp. 1-7, 2007.
[8] A. Mohanty, B. Rout, and R. Pradhan, "A Comparative Studies on Different Islanding Detection Methods for Distributed Generation Systems," *Energy Sources, Part A: Recovery, Utilization, and Environmental Effects*, vol. 45, no. 1, pp. 2284-2316, 2023.
[9] M. Sadeghi, and M. Abasi, "Optimal Placement and Sizing of Hybrid Superconducting Fault Current Limiter to Protection Coordination Restoration of the Distribution Networks in the Presence of Simultaneous Distributed Generation," *Electric Power Systems Research*, vol. 201, 107541, 2021.
[10] M. Khodaparastan, H. Vahedi, F. Khazaeli, and H. Oraee, "A Novel Hybrid Islanding Detection Method for Inverter-Based DGs Using SFS and ROCOF," *IEEE Transactions on Power Delivery*, vol. 32, no. 5, pp. 2162-2170, 2017.
[11] S. Sanati, and Y. Alinejad-Beromi, "Avoid Current Transformer Saturation Using Adjustable Switched Resistor Demagnetization Method," *IEEE Transactions on Power Delivery*, vol. 36, no. 1, pp. 92-101, 2021.
[12] S. M. Sadeghi, M. Daryalal, and M. Abasi, "Two-Stage Planning of Synchronous Distributed Generations in Distribution Network Considering Protection Coordination Index and Optimal Operation Situation," *IET Renewable Power Generation*, vol. 16, no. 11, pp. 2338-2356, 2022.
[13] S. Akhlaghi, A. A. Ghadimi, and A. Akhlaghi, "A Novel Hybrid Islanding Detection Method Combination of SMS and Q-f for Islanding Detection of Inverter-Based DG," *2014 Power and Energy Conference at Illinois (PECI), Champaign*, IL, USA, pp. 1-8, 2014.
[14] M. Abasi, M. Falah Nezhadnaeini, M. Karimi, and N. Yousefi, "A Novel Meta Heuristic Approach to Solve Unit Commitment Problem in the Presence of Wind Farms," *Revue Roumaine Des Sciences Techniques Serie Electrotechnique et Energetique*, vol. 60, no. 3, pp. 253-262, 2015.
[15] C. C. Hou, and Y. C. Chen, "A Hybrid Islanding Detection for Distributed Generation Systems Using Pulse Current Injection," *2012 IEEE International Symposium on Industrial Electronics*, 2012.
[16] M. Abasi, A. Torabi Farsani, A. Rohani, and A. Beigzadeh, "A Novel Fuzzy Theory-Based Differential Protection Scheme for Transmission Lines," *International Journal of Integrated Engineering*, vol. 12, no. 8, pp. 149-160, 2020.
[17] N. Kothari, and B.G. Fernandes, "A Hybrid Active Islanding Detection Technique for Single-Phase Inverter-Based Distributed Generation System," *2015 IEEE International Conference on Industrial Technology (ICIT)*, , 2015.
[18] S. Sanati, and Y. Alinejad-Beromi, "Prevention of the Current Transformer Saturation by Using Negative Resistance," *IET Generation, Transmission & Distribution*, vol. 15, no. 3, pp. 1751-8687, 2021.
[19] S. D. Kermany, M. Joorabian, S. Deilami, and M. A. S. Masoum, "Hybrid Islanding Detection in Microgrid with Multiple Connection Points to Smart Grids Using Fuzzy-Neural Network," *IEEE Transactions on Power Systems*, vol. 32, no. 4, pp. 2640-2651, 2017.
[20] Z. Ye, A. Kolwalkar, Y. Zhang, P. Du, and R. Walling, "Evaluation of Anti-Islanding Schemes Based on Nondetection Zone Concept," *IEEE Transactions on Power Electronics*, vol. 19, no. 5, pp. 1171-1176, 2004.
[21] Z. Mi, and F. Wang, "Power Equations and Non-Detection Zone of Passive Islanding Detection and Protection Method for Grid Connected Photovoltaic Generation System," *Pacific-Asia Conference on Circuits, Communications and Systems, Chengdu*, pp. 360-363, 2009.
[22] P. Kumar, V. Kumar, and B. Tyagi, "Sequence-Based Hybrid Technique for Islanding Detection for Microgrid With RES," *IEEE Transactions on Industry Applications*, vol. 58, no. 1, pp. 185-200, 2022.

Declaration of Competing Interest

The authors declare that they have no known competing financial interests or personal relationships that could have appeared to influence the work reported in this paper. The ethical issues, including plagiarism, informed consent, misconduct, data fabrication and/or falsification, double publication and/or submission, redundancy, have been completely observed by the authors.

Credit Authorship Contribution Statement

Saman Darvish Kermani: Conceptualization, Formal analysis, Investigation, Methodology, Resources, Roles/Writing- original draft. **Vahid Davatgaran:** Methodology, Resources, Roles/Writing - original draft, Writing - review & editing. **Arsalan Beigzadeh**: Conceptualization, Supervision, Methodology, Roles/Writing- original draft. **Mahmood Joorabian:** Conceptualization, Project administration, Validation, Visualization, Roles/Writing - original draft.

Bibliography

Saman Darvish Kermani received his PhD degree in 2016 from Shahid Chamran University of Ahvaz, Ahvaz, Iran in the field of electrical engineering. He is currently working at GHD Advisory Melbourne VIC 3000 Australia in the field of renewable energy. His main research interests include optimization, nature-inspired metaheuristic algorithms, islanding, microgrid, smart grid, power quality, modeling of electrical networks, and distributed renewable resources.

Vahid Davatgaran was born in 1987 in Iran. He received his B.Sc., M.Sc., and Ph.D. degrees in Electrical Engineering (Power Systems) from Shahid Chamran University of Ahvaz, Iran, in 2010, 2013, and 2019, respectively. He is currently an assistant professor at Department of Electrical Engineering, Technical and Vocational University (TVU), Tehran, Iran. His fields of interest include operation and planning of power systems, microgrids and renewable energies, smart grids, and reactive power control in power systems.

Arsalan Beigzadeh was born in Ahvaz, Iran, in 1992. He received his B.Sc. degree in Electrical Engineering from Jundi Shapour University of Technology, Dezful, in 2015 and his M.Sc. degree in Electrical Power systems from Shahid Chamran University of Ahvaz, Ahvaz in 2018. He is currently working on a variety of research projects in association with Iran Power Ministry. His fields of interest include distribution systems, distribution system protection, power quality, and microgrids.

Mahmood Joorabian was born in Iran, in 1961. He received his B.E.E degree from University of New Haven, CT, USA, M.Sc. degree in Electrical Power Engineering from Rensselaer Polytechnic Institute, NY, USA and Ph.D. degree in Electrical Engineering from University of Bath, Bath, UK in 1983, 1985 and 1996, respectively. He has been with the Department of Electrical Engineering at Shahid Chamran University of Ahvaz, Ahvaz, Iran as Senior Lecturer (1985), Assistant Professor (1996), Associate Professor (2004) and Professor (2009). His main research interests are fault location, FACTS devices, power system protection, power quality, and applications of intelligence technique in power systems.

Journal of Green Energy Research and Innovation

Utilizing Hybrid Sine Cosine Shuffled Frog Leaping Algorithm for Optimal Energy Management in the Residential building with Renewable Energy Resources and Corresponding Uncertainties

Behdad Arandian

Highlight

- Integration of WT and PV systems in residential building is modeled
- Different loading models are incorporated as load control program
- Both connected and island operation of residential building are considered
- Daily energy cost is minimized by using HSFL algorithm.
- Load control handles generation uncertainty of renewable energy resources

Graphical Abstract

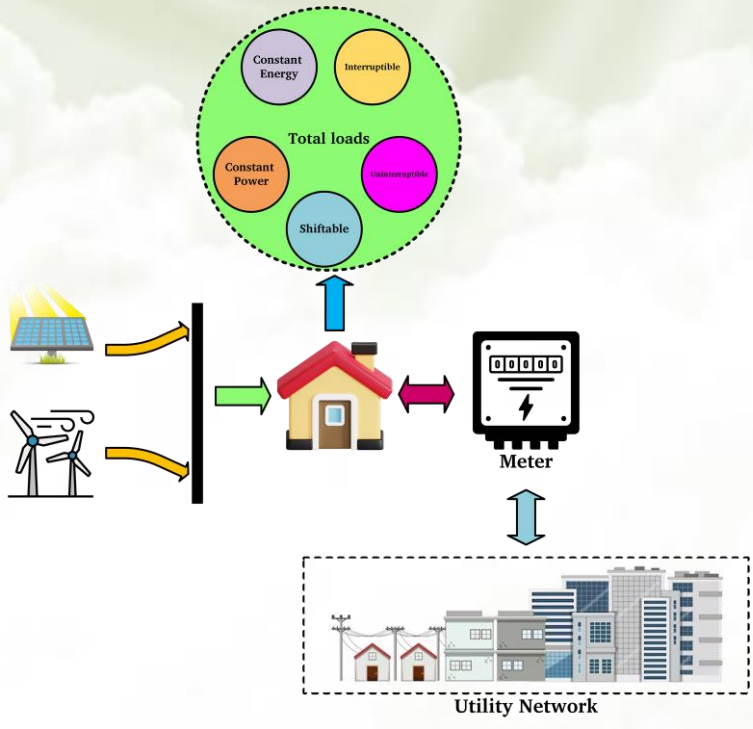

Use your device to scan and read the article online

Citation

B. Arandian, "Utilizing Hybrid Sine Cosine Shuffled Frog Leaping Algorithm for Optimal Energy Management in the Residential building with Renewable Energy Resources and Corresponding Uncertainties," *Journal of Green Energy Research and Innovation*, vol. 1, no. 1, pp. 66-79, 2024.

https://doi.org/10.61186/jgeri.1.1.65

JGERI Journal of Green Energy Research and Innovation

Online ISSN: 3041-9018

Journal of Green Energy Research and Innovation

Journal Homepage: www.jgeri.araku.ac.ir

Utilizing Hybrid Sine Cosine Shuffled Frog Leaping Algorithm for Optimal Energy Management in the Residential building with Renewable Energy Resources and Corresponding Uncertainties

Behdad Arandian *

Department of Electrical Engineering, Dolatabad Branch, Islamic Azad University, Isfahan, Iran.

* ***Corresponding Author:*** *b.arandian@iauda.ac.ir*

ARTICLE INFO

Keywords:
Sine cosine algorithm,
Shuffled frog leaping algorithm,
Renewable energy,
Residential building,
Energy management.

Article history:
Received: 23 December 2023;
Revised: 06 February 2024;
Accepted: 17 February 2024;

Article type:
Research Article

ABSTRACT

In this study, optimal energy management is addressed in the residential building. The residential building is equipped with renewable energies including wind turbines (WT) and photovoltaic (PV) systems. Stochastic programming is used to model the uncertainty of renewable energy resources. To manage these uncertainties and reduce the total daily cost of energy, the load control program is adopted. In this respect, five different types of loads are modeled in the building, including interruptible, uninterruptible, constant-energy, constant-power and movable loads. The above charges are properly adjusted and shipped to minimize energy costs and address the uncertainties of renewable energy by hybrid sine cosine shuffled frog leaping algorithm. The residential building is considered as later active in the network, which transfers energy from network to the building and vice versa. The simulation results show that the proposed model can efficiently harness all the energy possible from WT-PV systems, manage uncertainties, minimize total daily costs and operate as an island. All of these objectives are achieved by optimal load distribution and control within the proposed load control program.

1. Introduction

The integration of energy resources is one of the interesting problems of electrical engineering and several types of energy resources have been modeled and studied for good integration [1]. In real networks, the grid is often equipped with different types of renewable and non-renewable energy, such as wind turbines, photovoltaic systems and hydropower systems as renewable energy sources, as well as micro-turbines, internal combustion engines (ICE), and the fuel cell (FC) as non-renewable energy resources. It is therefore useful to study the correlation and the cogeneration of these resources. This problem has been approached in different ways, for example by combining hydro, WT and PV [2, 3], WT and PV [4], WT and PV-thermal [5], MT, FC and ICE [6], PV-FC [7], and PV-thermal [8]. Studies show that such a correlation exerts a significant influence on the network and that it is necessary to take this element into account in the problem.

The correlation of renewable energy sources can also be studied in the problem of household energy management. This problem manages energy consumption in homes

and the building. Domestic energy management has been well taken into account, including various renewable and non-renewable energy resources such as WT [9], PV [10, 11], geothermal biomass [12]. In addition, the management of domestic energy has been approached from different angles, such as reduction of emissions to the environment [6], operation and management of wireless networks [13], control analysis the load [14], the comfortable lifestyle [15] and electrical systems loading [8] and increasing of energy performance [16]. Energy storage systems are also useful technologies that can be used properly in energy management [6, 8].

Load control (demand response) is one of the preferred methods for managing energy exchange in buildings. Load control is a broad term that offers a variety of methods to improve the operation of the system by managing demand rather than generation [17, 18]. Loads and their models are one of the main components of load control. There are different types of loads, such as interruptible loads [19], constant power or power loads [20], and switchable loads [21]. Thus, the load control program, as a demand management method (DSM), optimally adjusts and modifies loads to meet loads, while minimizing total daily energy costs.

This study presents an optimization strategy aimed at minimizing the total daily energy cost in the residential building. Despite the fact that this building is equipped with WT and PV systems as an internal renewable energy source, it is connected to the distribution network. This means that the building can receive its energy from the internal generation system or the distribution network (network) and also sends its surplus energy to the grid. Such an operation can help the building to reduce energy costs because it can sell energy to the upstream network at high-cost periods. It is assumed that the building comprises five types of loads, namely interruptible load, constant power load, constant energy load, uninterrupted load, and load that can be moved. Optimization programming manages energy in the building subject to the correlation of WT and PV energy resources as well as the load control program such as the DSM. The uncertainty of the WT and PV generation systems is managed by proper charge control and the total daily cost of the energy is minimized. So, the contribution of this paper is complete model of various parts in the system with consideration of renewable energy uncertainties. Also new optimization algorithms are improved and applied on the system.

The rest of this study is organized as follows. Section 2 describes the proposed model. Section 3 discusses the mathematical modeling used in this study. Section 4 provides the data required for simulation studies. In Section 5, numerical results are given. Finally, Section 6 presents conclusions and recommendations for future work.

2. The Proposed Method

The schematic structure of the proposed model is shown in Figure 1. In spite of considering WT and PV systems as internal production units, the building is also connected to the distribution network (network).

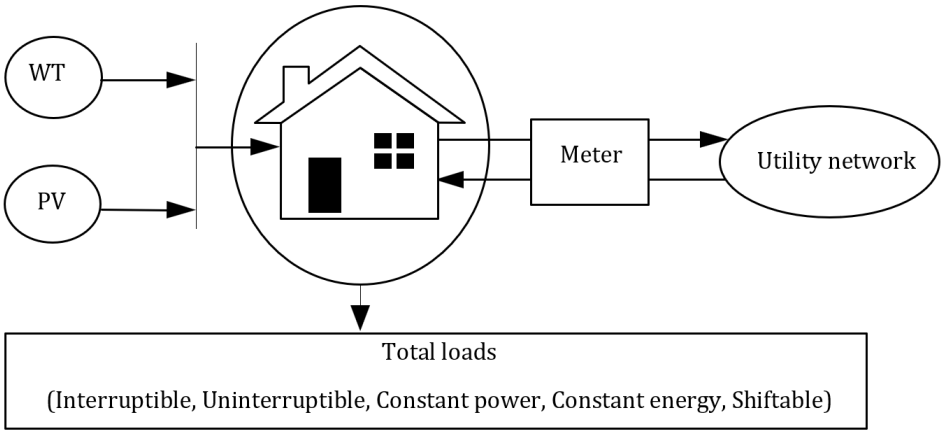

Figure 1. Schematic structure of the proposed model for energy management in building.

There is a counter between the building and the network to record the reception and sending energies. Energy management in the building is carried out by controlling loads and surplus produced energy can be send to the grid and make profits at the right time of the operation horizon. There are five different types of loads in the building and the plan can properly adjust the loads to manage energy and minimize the total daily energy cost in the building.

3. Mathematical Modeling

3.1. Optimization Programming

The energy management tool given in the residential building minimizes the total daily cost of energy in the building, as defined by Equation (1) as an objective function. It calculates the expected value of the cost in all the performance scenarios related to the uncertainty of the WT and PV generation systems. It should be noted that the probability of each scenario is less than one and the sum of all probabilities is equal to one, as indicated by the Equations (2) and (3).

$$TC = \sum_{s=1}^{N} \sum_{t=1}^{24} (P_{UN.st} \times \rho_s \times \alpha_t) \quad (1)$$

$$0 \leq \rho_s \leq 1 \quad (2)$$

$$\sum_{s=1}^{N} \rho_s = 1 \quad (3)$$

The energy exchange between the building and the distribution network is calculated by the Equation (4). The load is a positive variable Equation (5) and is modeled by five different load types, including loads 1 to 5 Equation (6), which are modeled and described in subsections 3.2 to 3.6 The building can send power to the grid or receive power from the grid. If this calculated power is negative, the building sends electrical energy to the grid, otherwise the network sends electrical energy to the building.

As a result, the exchange power between the building and the grid can be positive or negative, as shown in Equation (7). However, the line capacity between the building and the network limits this exchange power, as indicated by the Equation (8).

$$P_{UN.st} = P_{load,t} - P_{PV,st} - P_{WT,st} \quad (4)$$

$$P_{load,t} \geq 0 \quad (5)$$

$$P_{load,t} = P_{load1,t} + P_{load2,t} + P_{load3,t} + P_{load4,t} + P_{load5,t} \quad (6)$$

$$-\infty \leq P_{UN.st} \leq +\infty \quad (7)$$

$$|P_{UN.st}| \leq P_{line.max} \quad (8)$$

3.2. Interruptible Load

One of the load types in this study is interruptible loads. The energy consumed by interruptible loads is not required to be continued. This type of loads can consume energy at different times with several start and stop commands. Such operation can be defined for certain devices such as electric motors. Load 1 is an interruptible load and it is a positive variable, as the Equation (9) shows. A binary variable is defined as Equation (10) and it is fixed as Equation (11). Then, the load profile of the interruptible load is modeled by Equation (12).

$$P_{load1,t} \geq 0 \quad (9)$$

$$B_{load1,t} \in \{0,1\} \quad (10)$$

$$\sum_{t=1}^{24} B_{load1,t} = NL1 \quad (11)$$

$$P_{load1,t} = B_{load1,t} \times P_{load1,rated} \quad (12)$$

3.3. Constant Energy Load

Another load types considered in this study is constant energy loads. This load type uses fixed energy level during the day, regardless of the operating time. Such a procedure can be considered as operation of billable devices. They can be loaded at intermittent intervals with different powers. Charge 2 is a constant energy charge and it is a positive variable, as the Equation (13) shows. The energy of the load is defined in Equation (14) and its power is limited by Equation (15).

$$P_{load2,t} \geq 0 \quad (13)$$

$$\sum_{t=1}^{24} P_{load2,t} \times t = EL2 \quad (14)$$

$$P_{load2,t} \leq P_{load2,rated} \quad (15)$$

3.4. Constant Power Load

Constant power loads follow a constant profile during the hours of the day, such as lighting demand. Load 3 is a constant power load and it is a positive variable, as the Equation (16) shows. The constant charge is defined by Equation (17).

$$P_{load3,t} \geq 0 \tag{16}$$

$$\sum_{t=1}^{24} P_{load3,t} = P_{load3,rated} \tag{17}$$

3.5. Uninterrupted Load

Some loads must have consecutive and uninterrupted operation such as the washing machine. This means that the operation of these devices cannot be interrupted before the end of their work. Load 4 is modeled as a load with a consecutive operation. It is a positive variable like Equation (18). A binary variable is defined as Equation (19) and the uninterrupted operation is modeled by Equation (20). The loading profile for this load is modeled by Equation (21).

$$P_{load4,t} \geq 0 \tag{18}$$

$$B_{load4,t} \in \{0,1\} \tag{19}$$

$$\sum_{t=i}^{i+NL4} B_{load4,t} = NL4 \tag{20}$$

$$P_{load4,t} = B_{load4,t} \times P_{load4,rated} \tag{21}$$

3.6. Shiftable Load

The usage time of certain charges can be changed during the day. This means that the operation of these devices is not limited to specific hours. Load 5 is modeled as a load with varying duty cycle as movable loads. It is a positive variable like Equation (22). A binary variable with a maximum limitation is defined as Equation (23) and the load profile for this load is modeled by Equation (24).

$$P_{load5,t} \geq 0 \tag{22}$$

$$B_{load5,t} \in \{0,1\} \tag{23}$$

$$P_{load4,t} = B_{load5,t} \times P_{load5,rated} \tag{24}$$

4. Data and Setting of Problem

Figure 1 shows the schematic structure of the residential building. A photovoltaic system of 20 kW WT and one of 20 kW are installed for this building [2]. The electric powers produced by the WT and PV systems are illustrated in Figures 2 and 3, respectively [2]. The nominal power of the load 1 since the interrupted load is 20 kW, it must work 8 hours a day. The nominal energy of the load 2 being constant, it is 50 kWh and its nominal power of 5 kW [4]. The nominal power of the load 3 with a constant load

power is 25 kW and its load profile is given in Figure 4 [4]. Since the nominal power of the load 4 is a continuous load of 15 kW, it must operate for 6 consecutive hours per day [4]. It is assumed that 90% of the total load is considered a load that can be moved (load 5). The line capacity between the network and the building is 42 kW. The price of electric energy is changed throughout the day and three levels are taken into account, as shown in Figure 5 [20].

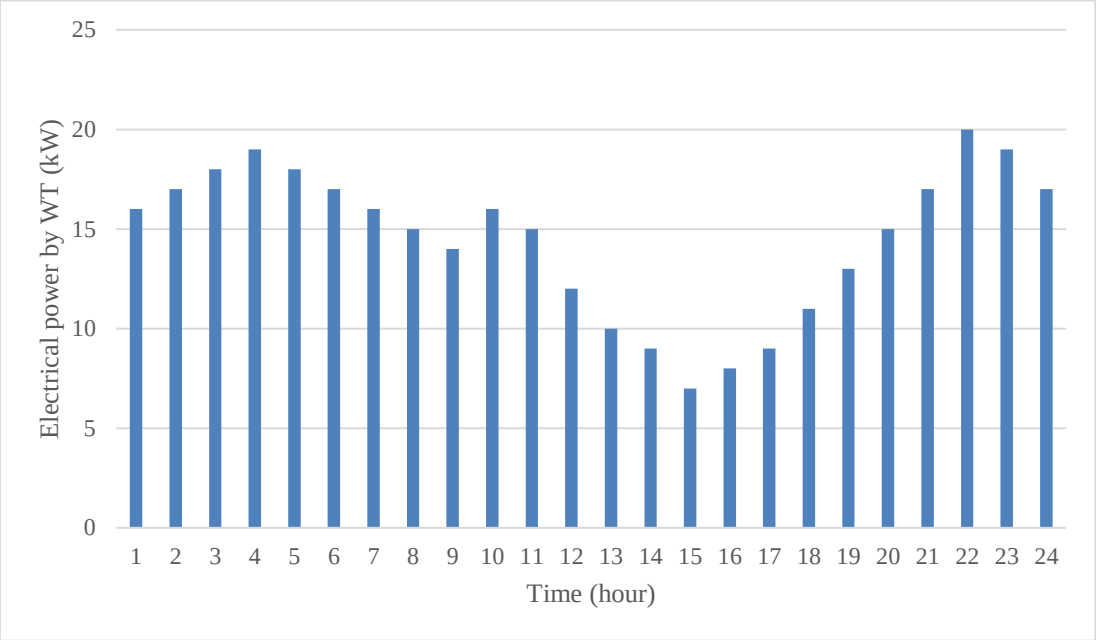

Figure 2. Electrical power by WT [2].

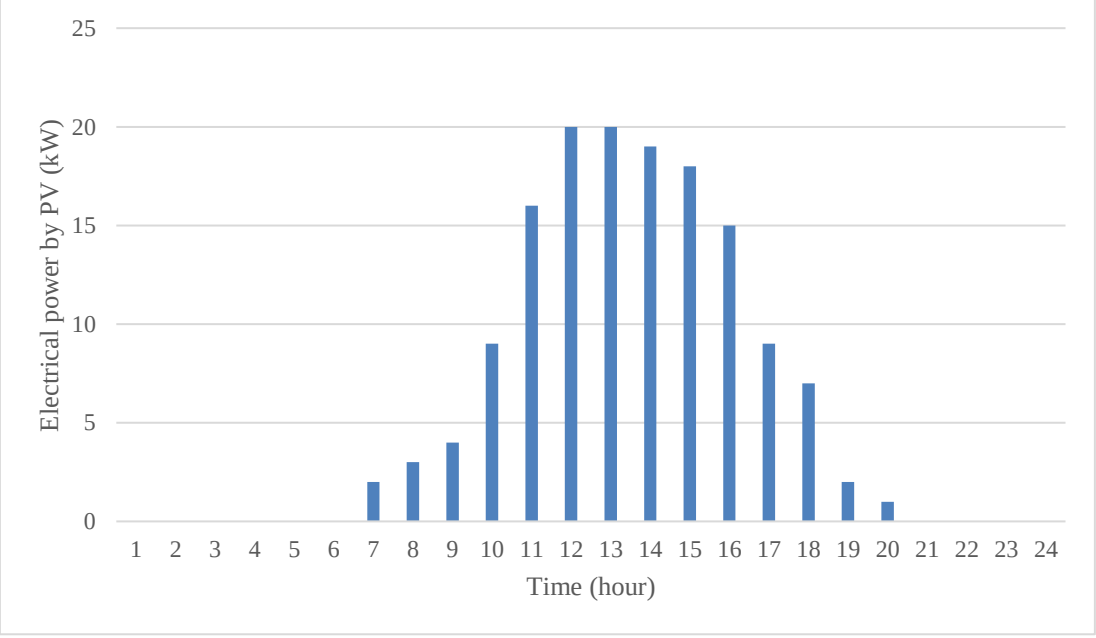

Figure 3. Electrical power by PV [2].

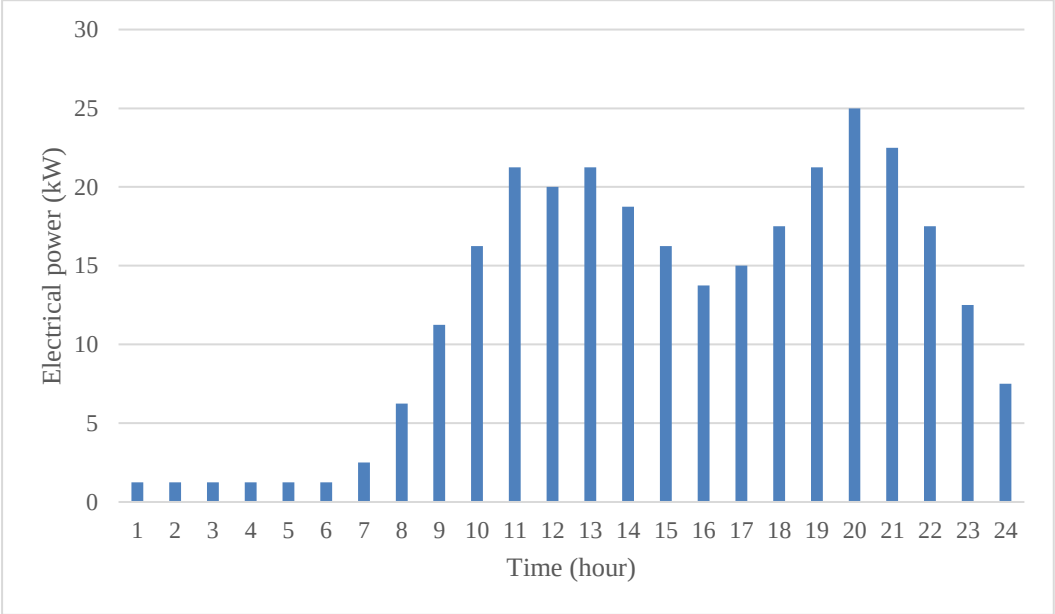

Figure 4. Daily load profile for Load 3 [2].

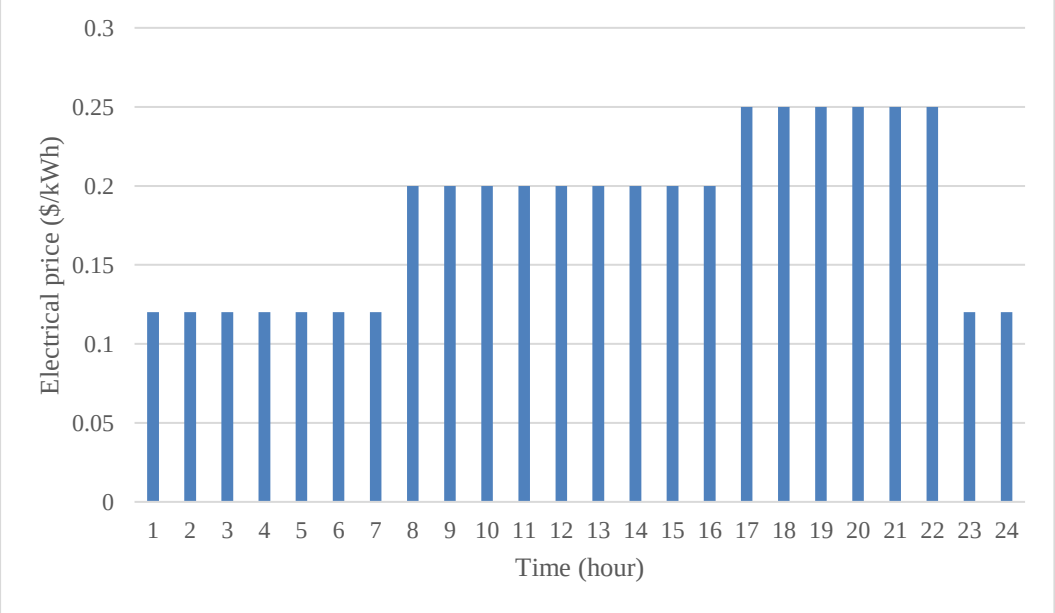

Figure 5. Daily electrical price [20].

5. Numerical Results

The introduced model is simulated on the given residential building by using hybrid sine cosine shuffled frog leaping algorithm (HSC-SFLA) based on hybrid shuffled frog leaping algorithm (HSFLA) [8] and sine cosine algorithm (SCA) [22]. In the first step, Table 1 presents the energy cost of residential buildings with and without renewable resources. The use of the WT system and the PV system reduces the energy cost from 98,687 ($ / day) to 7,607 ($ / day), which is a reduction of 91.08 ($ / day). The proposed model can correctly exploit all the possible energy of the WT and PV systems and manage the energy via the given load control program. Such an operation reduces the energy costs specified below by 92.29%.

The electrical energy exchanged between the building and the network is illustrated in Figure 6 for two cases with and without renewable resources. The building receives total energy from the grid when renewable resources are not installed. On the other hand, when the renewable resources are connected, the profile of the electrical energy is considerably changed. The plan exploits all the energy of the WT and PV systems to minimize energy costs. In addition, planning sends energy to the grid at costly times, such as 8 to 18 hours, reducing the building's energy costs. The results verify that energy is received from the grid for low-cost periods and that surplus energy is sent to the distribution grid at high-cost periods.

The results of the load control program are listed in Table 2. The optimal programming of the distribution of the five loads is obtained and listed below. Load 1 is an interruptible load and there are some interruptions in the operation. Planning runs the load in low-cost hours to minimize operational costs. The load 2 is the constant energy load and its operation is optimized, while the required energy (50 kWh) is reached. Load 3 is a constant power load and follows its defined pattern. Charging 4 to 6 hours of consecutive operation and is powered by scheduling in the low-cost hours. Load 5 is the specified percentage of each load type, as explained in Section 4. Planning optimizes the distribution of all loads to minimize the total energy cost of the building and to optimize the use of energy resources renewable.

Table 1. Energy cost for residential building with and without renewable resources.

	With WT-PV	Without WT-PV
Total daily cost ($)	98.687	7.607

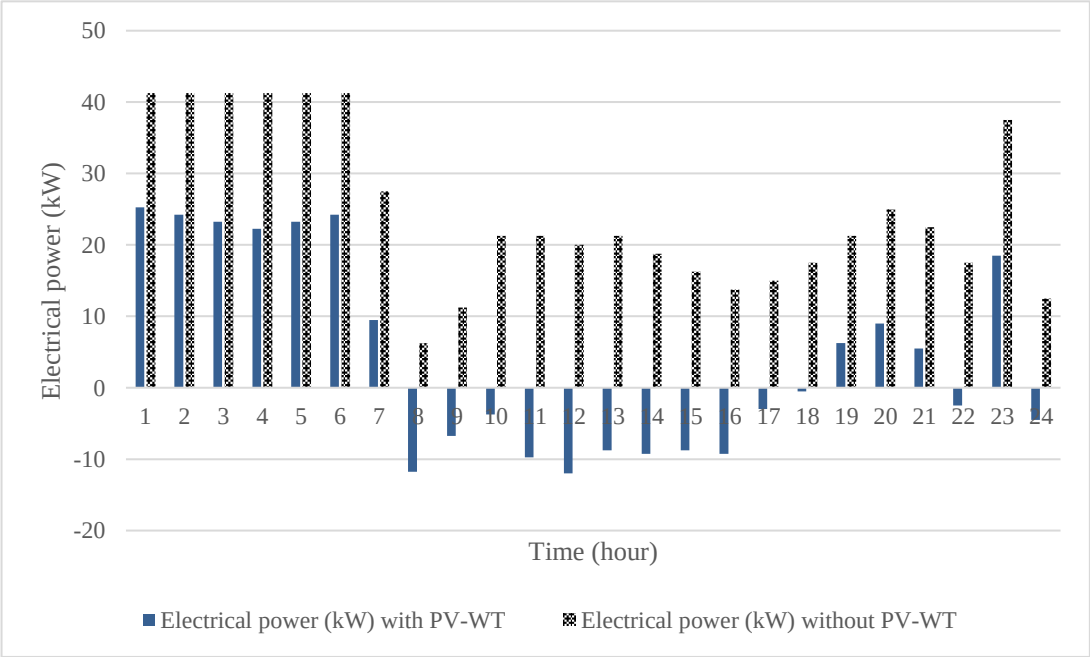

Figure 6. Exchanged electrical power between building and utility network with and without renewable resources.

Table 2. Optimal daily load control.

Time (hour)	Load 1 (kW)	Load 2 (kW)	Load 3 (kW)	Load 4 (kW)	Load 5 (kW)
1	20	5	1.250	15	37.125
2	20	5	1.250	15	37.125
3	20	5	1.250	15	37.125
4	20	5	1.250	15	37.125
5	20	5	1.250	15	37.125
6	20	5	1.250	15	37.125
7	20	5	2.500	0	24.75
8	0	0	6.250	0	5.625
9	0	0	11.25	0	10.125
10	0	5	16.25	0	19.125
11	0	0	21.25	0	19.125
12	0	0	20.00	0	18
13	0	0	21.25	0	19.125
14	0	0	18.75	0	16.875
15	0	0	16.25	0	14.625
16	0	0	13.75	0	12.375
17	0	0	15.00	0	13.5
18	0	0	17.50	0	15.75
19	0	0	21.25	0	19.125
20	0	0	25.00	0	22.5
21	0	0	22.50	0	20.25
22	0	0	17.50	0	15.75
23	20	5	12.50	0	33.75
24	0	5	7.500	0	11.25

5.1. Line Capacity Analysis

The line capacity between the distribution network and the building plays a significant role. To analyze this role, two cases with a line capacity of 42 kW as case A and a line capacity of 32 kW as case B are simulated and discussed. The results for these two cases are shown in Table 3. It shows that the decrease in line capacity increases the total energy cost by 51.68%. The electrical energy exchanged between the building and the distribution network is illustrated in Figure 7 in two cases. Comparing Figures 6 and 7, the decreasing line capacity forces the building to receive power from the utility network at expensive times such as periods 8, 9, 10, 15, 16, 18, resulting in an increase in energy costs of the building. On the other hand, a larger line capacity allows the building to provide its energy at low-cost times. Not only does the building not receive grid energy at the costly times mentioned, but it also sends energy to the upstream grid and generates profits. Table 4 summarizes the optimal load distribution in case B. The interruptible operation of the load 1 is optimized. The energy required for the load 2 is also satisfied while its operation is optimized. The load 3 follows its constant pattern and the load 4 displays 6 consecutive hours of operation. The charge 5 is offsets that

can be shifted. It should be noted that the optimal load distribution in Case A is presented earlier in Table 2.

Table 3. Energy cost under different line capacities.

	Case A	Case B
Total daily cost ($)	7.607	15.743

Table 4. Optimal daily load control for Case B.

Time(hour)	Load 1 (kW)	Load 2(kW)	Load 3(kW)	Load 4 (kW)	Load 5(kW)
1	0	5	1.25	15	19.125
2	0	5	1.25	15	19.125
3	0	5	1.25	15	19.125
4	0	5	1.25	15	19.125
5	0	5	1.25	15	19.125
6	0	5	1.25	15	19.125
7	20	5	2.5	0	24.75
8	20	5	6.25	0	28.125
9	20	0.95	11.25	0	28.98
10	20	0.75	16.25	0	33.3
11	0	0	21.25	0	19.125
12	0	0	20	0	18
13	0	0	21.25	0	19.125
14	0	0	18.75	0	16.875
15	20	0	16.25	0	32.625
16	20	0	13.75	0	30.375
17	0	0	15	0	13.5
18	0	0	17.5	0	15.75
19	0	0	21.25	0	19.125
20	0	0	25	0	22.5
21	0	0	22.5	0	20.25
22	0	0	17.5	0	15.75
23	20	3.3	12.5	0	32.22
24	20	5	7.5	0	29.25

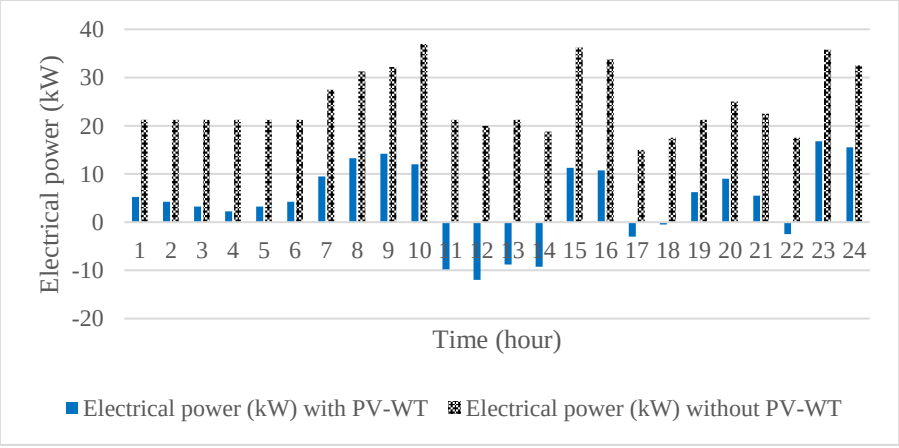

Figure 7. Exchanged electrical power between building and utility network under different line capacities.

5.2. Uncertainty Analysis and Island Operation

During planning, the uncertainties associated with the WT and PV systems are managed by the proposed load control program. The charges are correctly adjusted by the program to deal with such uncertainty. The results of the simulation show that the total cost of energy is $ 7,607 and $ 3,295 per day, with and without uncertainty about renewable energy, respectively.

The grid with renewable energy uncertainty has to manage this uncertainty through a load control program, which increases the energy cost. On the other hand, when renewable energy uncertainty is not included, the charges are not adjusted to manage the uncertainty of renewable energies, but they are to minimize the total cost of energy. As a result, the energy cost is reduced beyond the level reached by the case, including the uncertainty related to renewable energies.

The island operation of the building requires more WT and PV systems. Thus, the WT and PV systems have gone from 20 kW to 24 kW and 25 kW, respectively. Figure 8 shows the energy of the building in connected and island operations. In connected mode, most of the energy is provided by the WT and PV systems and a small part comes from the distribution network. In island mode, WT and PV respectively provide 70% and 30% of the charges. It should be noted that the total daily operating cost of an island is increased by 62%.

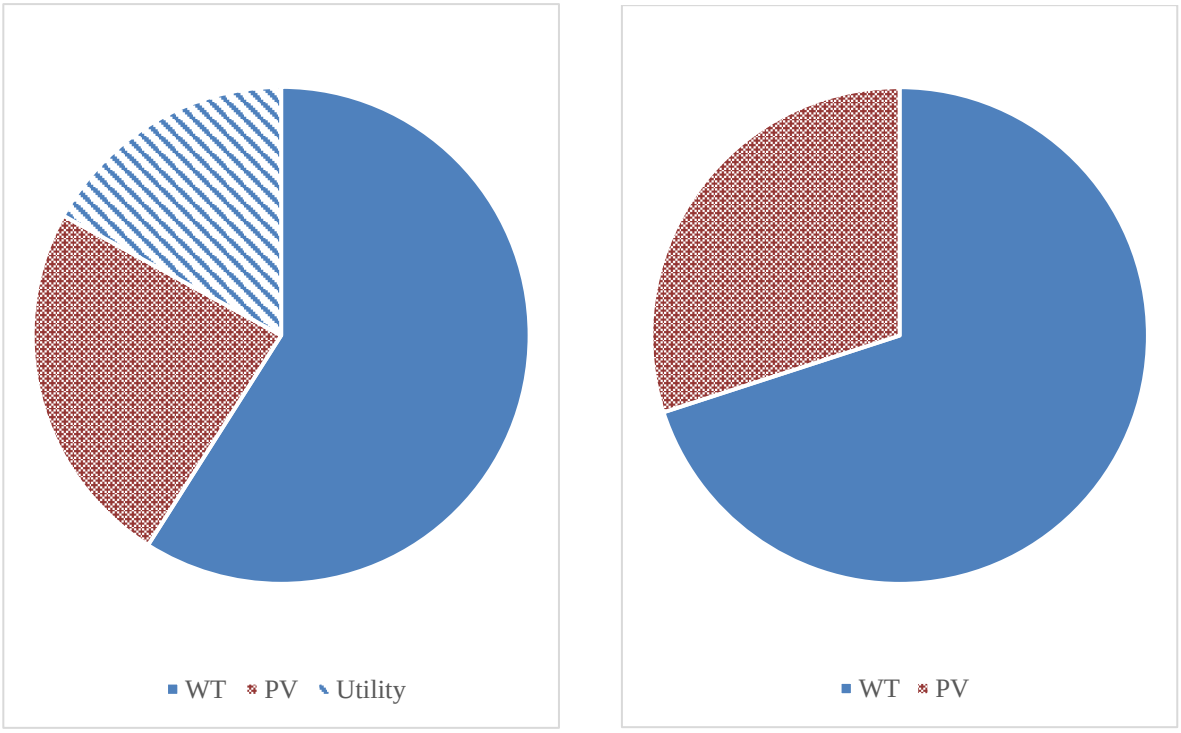

A: Connected operation **B**: Island operation

Figure 8. Energy of building under connected and island operations.

6. Conclusions

This document presents optimal energy management in the residential building, including different types of loads. Five types of loads, including interruptible, constant energy, constant power, uninterruptible and switchable loads, are modeled. The building is also equipped with renewable energy sources, including WT and PV systems. The building is connected to the distribution network and the electrical energy is exchanged between the building and the distribution network.

The simulation results show that the renewable energy assembly reduces the energy cost from 98.687 ($ / day) to 7.607 ($ / day), which represents a reduction of about 92.29%. The building without renewable energy must receive its energy from the grid, while the building with renewable resources uses all the energy of the WT and PV systems and even sends energy to the utility network at expensive hours such as hours. 8-18. The load control program successfully adjusts all building loads to minimize the total daily cost of energy, as well as the uncertainties associated with the management of renewable energy resources.

The results show that the reduction of the capacity of the line between network and building from 42 kW to 32 kW increases the cost by 51.68%. Under such conditions (limited line capacity), the building must be supplied with power by the utility network at expensive times, such as time periods 8,9,10,15,16,18, resulting in an increase in the building's daily energy costs to meet the costs.

The impact of renewable energy uncertainty on the cost of energy is also studied and it is shown that neglecting this uncertainty reduces the cost by about 56%, because the charges are adjusted only to minimize the total cost of energy. energy. Finally, it is shown that building island operation requires more WT and PV systems to meet the loads, and that connected operation reduces the total energy cost by 62% compared to island operation. For future work, it is recommended to use different types of renewable and non-renewable energy resources.

References

[1] R. Hemmati, H. Saboori, and M. A. Jirdehi, "Multistage Generation Expansion Planning Incorporating Large Scale Energy Storage Systems and Environmental Pollution," *Renewable Energy*, vol. 97, pp. 636-645, 2016.

[2] R. Hemmati, "Optimal Cogeneration and Scheduling of Hybrid Hydro-Thermal-Wind-Solar System Incorporating Energy Storage Systems," *Journal of Renewable and Sustainable Energy*, vol. 10, no. 1, pp. 014102, 2018.

[3] Z. Liu, Z. Zhang, R. Zhuo, and X. Wang, "Optimal Operation of Independent Regional Power Grid with Multiple Wind-Solar-Hydro-Battery Power," *Applied Energy*, vol. 235, pp. 1541-1550, 2019.

[4] H. Mehrjerdi, M. Bornapour, R. Hemmati, and S. M. S. Ghiasi, "Unified Energy Management and Load Control in Building Equipped with Wind-Solar-Battery Incorporating Electric and Hydrogen Vehicles Under Both Connected to the Grid and Islanding Modes," *Energy*, vol. 168, pp. 919-930, 2019.

[5] S. R. Salkuti, "Day-Ahead Thermal and Renewable Power Generation Scheduling Considering Uncertainty," *Renewable Energy*, vol. 131, pp. 956-965, 2019.

[6] B. Arandian, and M. M. Ardehali, "Effects of Environmental Emissions on Optimal Combination and Allocation of Renewable and Non-Renewable CHP Technologies in Heat and Electricity Distribution Networks Based on Improved Particle Swarm Optimization Algorithm," *Energy*, vol. 140, pp. 466-480, 2017.

[7] M. Jafari, and Z. Malekjamshidi, "Optimal Energy Management of a Residential-Based Hybrid Renewable Energy System Using Rule-Based Real-Time Control and 2D Dynamic Programming Optimization Method," *Renewable Energy*, vol. 146, pp. 254-266, 2020.

[8] B. Arandian, and M. M. Ardehali, "Renewable Photovoltaic-Thermal Combined Heat and Power Allocation Optimization in Radial and Meshed Integrated Heat and Electricity Distribution Networks with Storages Based on Newly Developed Hybrid Shuffled Frog Leaping Algorithm," *Journal of Renewable and Sustainable Energy*, vol. 9, 033503, 2017.

[9] R. Hemmati, "Optimal Design and Operation of Energy Storage Systems and Generators in the Network Installed with Wind Turbines Considering Practical Characteristics of Storage Units as Design Variable," *Journal of Cleaner Production*, vol. 185, pp. 680-693, 2018.

[10] N. Ghadimi, M. Sedaghat, et al., "An Innovative Technique for Optimization and Sensitivity Analysis of a PV/DG/BESS Based on Converged Henry Gas Solubility Optimizer: A Case Study," *IET Generation Transmission and Distribution*, vol. 17, pp. 4735-4749, 2023.

[11] A. Chakir, M. Tabaa, et al., "Optimal Energy Management for a Grid Connected PV-Battery System," *Energy Reports*, vol. 6, pp. 218-231, 2020.

[12] B. Zhou, W. Li, et al., "Smart Home Energy Management Systems: Concept, Configurations, and Scheduling Strategies," *Renewable and Sustainable Energy Reviews*, vol. 61, pp. 30-40, 2016.

[13] D.-M. Han, and J.-H. Lim, "Smart Home Energy Management System Using IEEE 802.15.4 and Zigbee," *IEEE Transactions on Consumer Electronics*, vol. 56, no. 3, pp. 1403-1410, 2010.

[14] M. Pipattanasomporn, M. Kuzlu, and S. Rahman, "An Algorithm for Intelligent Home Energy Management and Demand Response Analysis," *IEEE Transactions on Smart Grid*, vol. 3, no. 4, pp. 2166-2173, 2012.

[15] A. Anvari-Moghaddam, H. Monsef, and A. Rahimi-Kian, "Optimal Smart Home Energy Management Considering Energy Saving and a Comfortable Lifestyle," *IEEE Transactions on Smart Grid*, vol. 6, no. 1, pp. 324-332, 2014.

[16] A. M. Fallah, E. Ghafourian, et al., "Novel Neural Network Optimized by Electrostatic Discharge Algorithm for Modification of Buildings Energy Performance," *Sustainability*, vol. 15, 2884, 2023.

[17] C. Shao, Y. Ding, P. Siano, and Z. Lin, "A Framework for Incorporating Load Control of Smart Buildings into the Integrated Heat and Electricity Energy System," *IEEE Transactions on Industrial Electronics*, vol. 66, no. 2, pp. 1465-1475, 2019.

[18] M. Farrokhifar, F. H. Aghdam, A. Alahyari, A. Monavari, and A. Safari, "Optimal Energy Management and Sizing of Renewable Energy and Battery Systems in Residential Sectors via a Stochastic MILP Model," *Electric Power Systems Research*, vol. 187, 106483, 2020.

[19] P. Sheikhahmadi, S. Bahramara, et al., "Multi-Microgrids Operation with Interruptible Loads in Local Energy and Reserve Markets," *IEEE Systems Journal*, vol. 17, no. 1, pp. 1292-1303, 2023.

[20] B. Arandian, R.A. Hooshmand, and E. Gholipour, "Decreasing Activity Cost of a Distribution Company by Reconfiguration and Power Generation Control of DGs Based on Shuffled Frog Leaping Algorithm," *International Journal of Electrical Power & Energy Systems*, vol. 61, pp. 48-55, 2014.

[21] S. Nan, M. Zhou, and G. Li, " Optimal residential community demand response scheduling in smart grid," *Applied Energy*, vol. 210, pp. 1280-1289, 2018.

[22] S. Mirjalili, "SCA: A Sine Cosine Algorithm for Solving Optimization Problems," *Knowledge-Based Systems*, vol. 96, pp. 120-133, 2016.

Declaration of Competing Interest

The authors declare that they have no known competing financial interests or personal relationships that could have appeared to influence the work reported in this paper. The ethical issues, including plagiarism, informed consent, misconduct, data fabrication and/or falsification, double publication and/or submission, redundancy, have been completely observed by the authors.

Credit Authorship Contribution Statement

Behdad Arandian: Conceptualization, Formal analysis, Project administration, Supervision, Validation, Roles/Writing - original draft, Investigation, Methodology, Resources, Visualization, Writing - review & editing.

Bibliography

Behdad Arandian received the Ph.D. degree in electrical engineering from the Amirkabir University of Technology, Tehran, Iran, in 2017. He is currently an Associate Professor with the Electrical Engineering Department, Islamic Azad University, Isfahan, Iran. His current research interests include the energy planning (renewable and non-renewable resources), optimization methods, and power system planning.